Dissertation for a Ph. D. Degree

Estimation of Hyporheic Zone Depth Based on Advective Heat Transfer and Characterization of the Surface Water – Groundwater Mixing Zone

열전달을 통한 지표수- 지하수 혼합구역의 깊이 추산 및 특성에 관한 연구

Heejung Kim

AUGUST 2015

School of Earth and Environmental Sciences

Graduate School

Seoul National University

Abstract

Estimation of Hyporheic Zone Depth Based on Advective Heat Transfer and Characterization of the Surface Water – Groundwater Mixing Zone

Heejung Kim

School of Earth and Environmental Sciences

The Graduate School

Seoul National University

Surface water and groundwater can affect each other if they share a hyporheic zone, to either degrade or improve the water quality. The hyporheic zone is a region where the mixing and exchange of surface water and groundwater occur actively due to the large chemical, biological, and

hydraulic gradients. Therefore, various processes such as contaminant transport, degradation and transformation occur in the hyporheic zone. Due to the complexity and diversity of the underground medium, the delineation of the hyporheic zone is of vital importance for an integrated management of groundwater and surface water resources.

Hyporheic zone is the region where mixing if surface water and groundwater occurs. In this study, it is defined as the section from streambed to the depth where the vertical component of fluid flux becomes zero. The depth of hyporheic zone was determined with numerical analysis using time series of temperatures below the streambed. This study introduced a new concept of streambed hyporheic zone velocity models. Based on this concept, this study delineated the hyporheic zone depth more quantitative than the existing research results.

The methods of this study and the obtained results are sequentially focused on hydrological, biological, and chemical approaches to verify the proposed method.

1. Though the tracer test is somewhat challenging to determine the hyporheic zone depth using this best-fit, the hyporheic zone depth can be thought to be in the range of 2 and 30 cm, which is fairly comparable with the range (9-15 cm) of hyporheic zone depth from the proposed method using temperature analysis. The proposed method gives more precise range of the hyporheic zone depth.
2. The hyporheic zone was verified through biological approach. The effect of the flow direction of hyporheic flux determined from the proposed method on the bacterial community is examined.
3. Influence of hyporheic exchange patterns within the delineated hyporheic zone on bacterial diversity was estimated. Quantitative changes and characteristics of the hyporheic zone were analyzed to have an effect on the resident bacterial communities.
4. The hyporheic zone was verified through chemical approach. The chemical compositions of groundwater, stream water, paddy water

and hyporheic water are examined. The chemical compositions of the hyporheic water reflect the history related to the recharge and discharge of the waters.

Keywords : Surface water - groundwater interactions
(Hyporheic zones)
Delineation of hyporheic zone
Numerical analysis
Water chemistry
Microbial community

Student Number : 2010-30942

TABLE OF CONTENTS

CHAPTER 2. PROPOSED METHOD FOR DELINEATION OF HYPORHEIC ZONES

CHAPTER 3. VERIFICATION OF PROPOSED METHOD USING HYDROLOGICAL APPROACH

CHAPTER 4. VERIFICATION OF PROPOSED METHOD USING BIOLOGICAL APPROACH

CHAPTER 5. VERIFICATION OF PROPOSED METHOD USING CHEMICAL APPROACH

This page intentionally left blank

LIST OF FUGURES

CHAPTER 1.

CHAPTER 2.

CHAPTER 3.

CHAPTER 4.

CHAPTER 5.

CHAPTER 6.

This page intentionally left blank

LIST OF TABLES

CHAPTER 2.

CHAPTER 3.

CHAPTER 4.

Supplementary Table

CHAPTER 5.

CHAPTER 6.

This page intentionally left blank

This page intentionally left blank

CHAPTER 1. INTRODUCTION

1.1 Backgrounds

Surface water and groundwater have traditionally been treated as distinct entities in the most hydrological research, and have been investigated individually. In many cases, however, surface water and groundwater are hydraulically connected, and a continuous exchange of water and solute occurs across the hyporheic zone leading to the change in water quantity and

quality. Surface water and groundwater interaction area is the volume of saturated sediment beneath and beside streams and rivers where surface water and groundwater mix. Orghidan (1959) used this terminology and described the interface as a new groundwater environment called hyporheic zone.

New groundwater environment is a link among the riparian forest and the stream channel and hotspot of biological diversity contains intense physical and chemical variations. There is a typical flow pattern, in other words, surface water enters the hyporheic zone in a down-welling zone and groundwater returns to the stream in an up-welling zone. Distinctive patterns of down-welling and up-welling condition in the hyporheic zone make more complex environment, and can induce active biogeochemical processes and develop important habitat for numerous benthic micro-organisms.

Hyporheic exchanges are of great interest because they make the hyporheic zone highly productive and complex environments. When contaminants or polluted water pass through hyporheic zone, in particular, the

exchanges patterns plays important role in removing contaminants or attenuating contamination under certain conditions; however, only a few researches about hydrological and other fields (physical, chemical, biological) correlation with the hyporheic zones were found in the literature. Surprisingly, there is relatively little information about the effect of vertical flow exchange on biogeochemical processes in hyporheic zone. Also, climate change induces the change of groundwater and surface water flux. The hyporheic zone depths are one of the extraordinarily sensitive indicators for the climate change. Therefore, delineating the hyporheic zone is of vital importance for an integrated management of groundwater and surface water resources and a mitigation of the impacts by the climate change.

1.2 Objectives and Scope of this Study

Hyporheic zone is the region where mixing if surface water and groundwater occurs. In this study, it is defined as the section from streambed to the depth where the vertical component of fluid flux becomes zero.

This study proposes an easy way to delineate the hyporheic zone depth using time series data of temperature. Proposed method is verified from different approach. Firstly, the result from the proposed method is compared with that from a traditional method using tracer. Secondly, the effect of the flow direction of hyporheic flux determined from the proposed method on the bacterial community is examined. And finally, the chemical compositions of groundwater, stream water, paddy water and hyporheic water are examined.

The methods of this study and the obtained results are described in the following chapters arranged sequentially focused on hydrological, physical, biological, and chemical approaches to verify the proposed method.

In chapter 2, a method to estimate the depth of the hyporheic zone

using heat transfer analysis for a streambed was proposed. The depth of hyporheic zone has been unclear from the existing hydrological approach. In order to overcome the limitation of the hydrological approach alone, the depth of hyporheic zone was determined with numerical analysis using time series of temperatures below the streambed. The hyporheic zone was investigated through physical approach of thermal analysis.

In order to assess the adequacy of the proposed method, the sensitivity of the results of heat transfer analyses to the hyporheic flux was evaluated. Due to the high sensitivity to the hyporheic zone depth, the heat transfer analysis was determined to be appropriate to delineate the hyporheic zone depth. The depth estimated from the heat transfer analysis was comparable with that from a conventional tracer test. The proposed method has an advantage over existing methods of determining the hyporheic zone depth due to the fact that it only requires field temperature measurements.

In chapter 3, the hyporheic zone was verified through hydrological

approach (tracer test). The field temperature data was collected and the hyporheic zone depth was estimated by CAD analyses, and then the result was compared with that from the conventional tracer test. The hyporheic zone depth estimated from the proposed method was compared with that from the traditional method of tracer test. The two estimated depths were in a good agreement but the depth from the temperature analysis was relatively in a narrow range. The proposed method of estimating the hyporheic zone depth in this study has an advantage over traditional methods, in that the temperature distribution is the sole data required, and this is relatively easy to measure in the field.

In chapter 4, the hyporheic zone was verified through biological approach. The effect of the flow direction of hyporheic flux determined from the proposed method on the bacterial community is examined. Influence of hyporheic exchange patterns within the delineated hyporheic zone on bacterial diversity was estimated. The effect of quantitative changes in the

hyporheic zone on the diversity of bacterial communities was evaluated. Vertical velocity component change of the hyporheic zone was examined by installing a piezometer on the site, and a total of 20,242 reads were analyzed using a pyrosequencing assay to investigate the diversity of bacterial communities. Proteobacteria (55.1%) were overall dominant in the hyporheic zone, and Bacteroidetes (16.5%), Actinobacteria (7.1%) and other bacteria phylum (Firmicutes, Cyanobacteria, Chloroflexi, Planctomycetesm and unclassified phylum OD1) were identified. Also, the hyporheic zone was divided into 3 points – down welling point, mixed welling point and up welling point – through vertical hydraulic gradient, and the bacterial communities were compared and analyzed. When the species diversity index was additionally analyzed based on the pyrosequencing data, richness and diversity of species were observed to be highest in the order of mixed welling point >down welling point >up welling point. Hence, quantitative changes and characteristics of the hyporheic zone were analyzed to have an effect on

the resident bacterial communities.

In chapter 5, the hyporheic zone was verified through chemical approach. The chemical compositions of groundwater, stream water, paddy water and hyporheic water are examined. Surface water - groundwater exchange and mixing in a hyporheic zone were examined using the water chemistry data and multivariate statistical analyses. The chemical compositions of hyporheic water were controlled by those of the groundwater and stream water. The factor analysis identified two main factors that explain 71.8% of total variance of the water chemistry data and also revealed that the parameters responsible for water quality variances were mainly related to hyporheic exchange patterns and anthropogenic activities. The cluster analysis produced three different groups, respectively, which showed that the water quality parameters of the three groundwater, stream and paddy fields water bodies were very different and the hyporheic water showed a different mixing of the stream water and groundwater at each monitoring points.

In chapter 6, the proposed method was applied to a set of temperature data collected from a streambed across the stream. The horizontal delineation of the hyporheic zone depth was presented for different hyporheic flux shapes.

In the last chapter 7 includes concluding remarks.

1.3 Literature Review

The hyporheic zone (Orghidan, 1959; Schwoerbel, 1961; Smith, 2004) is a part of the groundwater interface in streams where a mixture of surface water and groundwater can be found (Fig. 1-1). The word of hyporheic derived from Greek roots for flow (*rheo*) and under (*hypo*). This area is saturated sediments within groundwater and associated with streams and rivers in which surface water and groundwater mix. Also, this zone has plentiful micro-organism. The hyporheic zone can be found beneath the stream channel and riparian zone. The zone is composed of permeable gravels, sands and silts and allows significant mixing of surface water with groundwater at the zone. The area is a complicated region whose boundaries are not always easy to define. The general definition is given by White(1993). White commented this zone: “Hydrologically, this zone is established by channel water advection and may be defined as a middle zone between the channel waters above and the groundwaters blow.” (Stephen et al., 2005)

There are studies of this region as a dynamic and distinguishable interface between surface water and groundwater. (Winter et al.,1998; Vought, 1994; Peter, 2002; Hill et al., 1998; Gilliam, 1994; Findlay, 1995; Brunke and Gonser, 1997; Battin, 2003; Baxter, 2000; Boulton, 2000; Andrew, 1998) Hydrologists and surface water hydrologists have approached this region with their particular perspective. There are various literatures to identify and quantify hyporheic exchange flow. (Harvey, 1993; Baxter, 2003; Becker, 2004) This water exchange is important to the hyporheic zone health because of its connection with living organisms in the zone (Giest et al., 2002). The Advance of hydrodynamicmodeling has improved research of hydrological exchange processes at the hyporheic zone (Bencala, 1983; Battin et al., 2003).

Traditionally, geochemists dealt with the hyporheic zone chemistry patterns using isotope and contaminant concentrations (Hill, 1983; Holmes et al.,1996; Kendall., 1998). Isotopic studies of nitrate of groundwater are frequently undertaken because of the information concerning sources of

nitrogen contamination and processes such as mixing and denitrification. Stable isotopes of NO_3-N in theory can be used to discrimination between sources of nitrate, as nitrate originating from different sources has characteristic isotope ratios. The stable isotopes of $\delta^{15}N$-NO_3compositions of origin were classified from different nitrogen contamination sources. The NO_3 originating from different sources has characteristic isotope ratio. The nitrogen isotope composition of chemical fertilizer ranged -4~+3‰, the chemical fertilizer and organic nitrogen mixing fertilizer ranged +3~+3‰, the organic nitrogen in soil ranged +4~+8‰, the organic nitrogen and septic waste mixing ranged +8~+10‰, and the manure and septic waste ranged +10~+20‰.

Some stream ecologists stressed the hyporheic zone as an important habitat for numerous benthic organisms (Martin, 1996), others emphasized the importance of biological processes for balance of nutrients in the zone. (Triska et al., 1989; Hill et al., 1998) Benthic microbial organism is an

important factor in understanding the hyporheic zone (Randall et al, 2006). The hyporheic zone is ecologically diverse region like hotspot. This region could potentially have vast capabilities for being a biogeochemical filter for rivers.

Fields, such as hydrology, geochemistry and ecology have treated the hyporheic zone. Therefore, there are many studies for the zone separate entities, but nowadays the area researches intend to bring these different perspectives and approaches together in order to study the surface water–groundwater system as a whole. To date, discussion of the hyporheic zone flow has focused on groundwater quality. In general, recharge and discharge to the groundwater in the hyporheic zone have been dealt as an option. However, the hyporheic zone flow is a major factor to groundwater quality. In short, study of the hyporheic zone characteristics is urgent to predict and keep vulnerable groundwater quality.

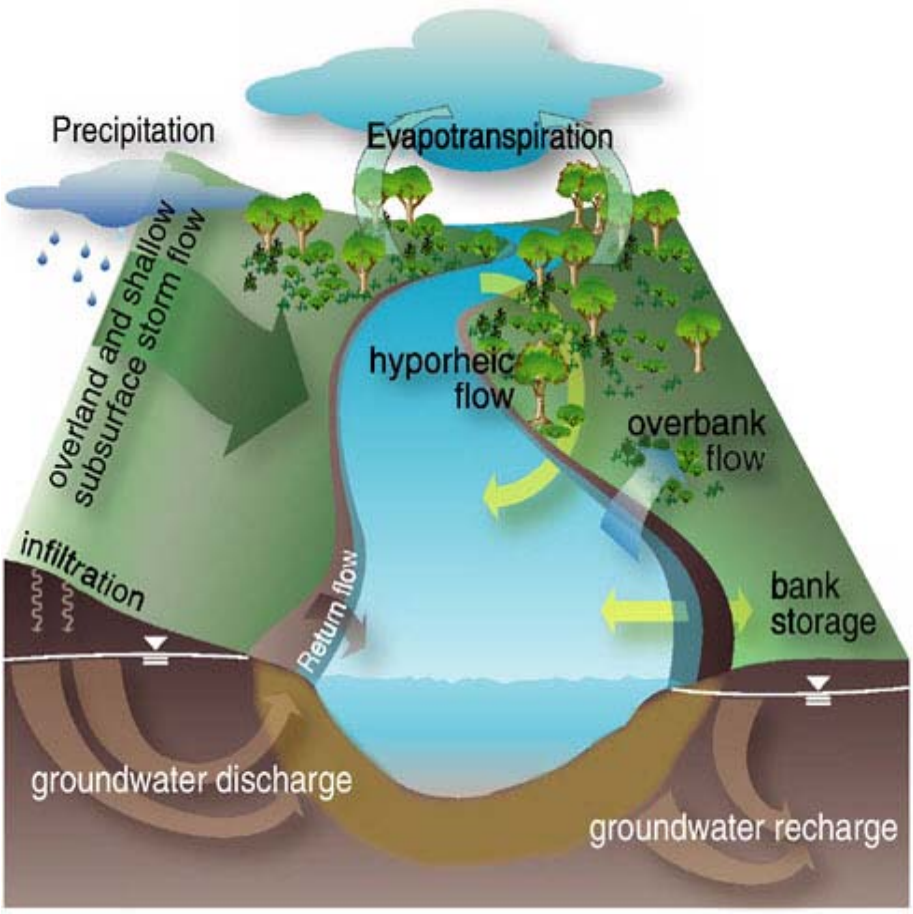

Fig. 1-1 Conceptual model of the groundwater recharge and discharge with hyporheic flow along a single stream (Source: http://books.nap.edu)

1.4 Study Site

The Haean basin is located in Gangwon province, Korea (Fig. 1-1a). The size of the basin is estimated 64 km^2. The east-west length is 11.95 km and the north-south length is 6.6 km. Geology of the study area is characterized by Jurassic igneous rocks intruding into the composite metamorphic rocks (Kwon et al. 1990). It has peculiar and interesting topographic feature like a bowl. The features of the area have been formed through prolonged differential erosion and the depressed bottom is made up of granite only (Kim and Park 1967). The geological section and profile of the basin are shown in Fig.1b. The extreme region is mainly made up of alternating meta-sedimentary rocks of mica schist, biotite-feldspar gneiss and quartzite. The basin is surrounded by mountain of Daeam, Deawoo, Dosol and Gachilbong. This area has a bowl shaped mountainous basin and a range in altitude from 339 to 1320 m above sea level (a.s.l.) (Fig.1-1 (b)) with an average slope of 28% and maximum slope of 84% (Kettering et al., 2012).

The study area has three main streams (Seonghwang, Dosol, Mandae) with several branches. These streams leave the basin at the eastern border of the study area, where it eventually converges with Soyang River. The drainage system specifically shows a dendritic pattern. The total length of streams is about 63 km and the streams flow down to the depression of the basin but only one stream flows out in the east of the basin. Therefore, the hydrographic system of the area is relatively simple when it compares with other areas (Choi and Lee 2010; Lee et al. 2009). The streambed sediments at the basin range from fine sand to coarse gravel. Generally, sediments found upstream are composed mainly of coarse gravel while fine sand is found downstream.

Groundwater levels (depth to water) on the topographic elevation from 400 to 450 m (the lowest elevation) ranged from 1 to 3 m, while that on the elevation from 500 to 600 m, ranged from 5 to 10 m, measured during April-October 2008. The groundwater levels in the study area largely depends

on the topographic elevation and groundwater use (Yun et al. 2009) and the pattern of groundwater flow is toward streams at the centre of the basin.

There are 111 groundwater wells officially reported in the study area (Lee 2009), which corresponds to 1.93 wells/km^2 of the total land area but approximately 10 wells/km^2 of the agricultural area only. Actually, there are many wells much more than reported and most of them are illegally installed in the agricultural area. Also, most illegally installed wells were poor managed and neglected. Among the reported wells, most (91%) are for agricultural water supply and groundwater pumping in the basin mainly occurs from May to August. Some deep groundwater wells have a pumping rate of over 150 m^3/day, although the exact pumping amount of others is unknown (Lee et al. 2012).

The high altitude areas above 650-700 m are mainly covered by forests (58.0%), while the moderate and lower areas (<650 m) are mostly used for agriculture, including crop farm (27.6%), rice paddy fields (11.4%) and

fruit farm (0.5%) in 2011 (Lee et al. 2012) (Fig.1-2). The climate is characterized by distinct wet and dry seasons. From 2002 to 2011, the maximum and minimum of annual mean air temperatures of the basin were 25.3ºC and -11.5ºC, respectively and their mean was 10.1ºC. The average annual precipitation for the period was 1,501 mm. The maximum and minimum of annual precipitations were 1,867.5 mm in 2010 and 1,249.6 mm in 2004, respectively (Fig. 1-3). In addition, the precipitation has generally increased with year. Based on the precipitations for the decade, the wet and dry seasons were considered to be from July to September and from October to February, respectively. More than 60-70% of total annual precipitations occur in the wet season due to the monsoon weather, which is a characteristic of the climate of Korean Peninsula (Lee and Lee 2000).

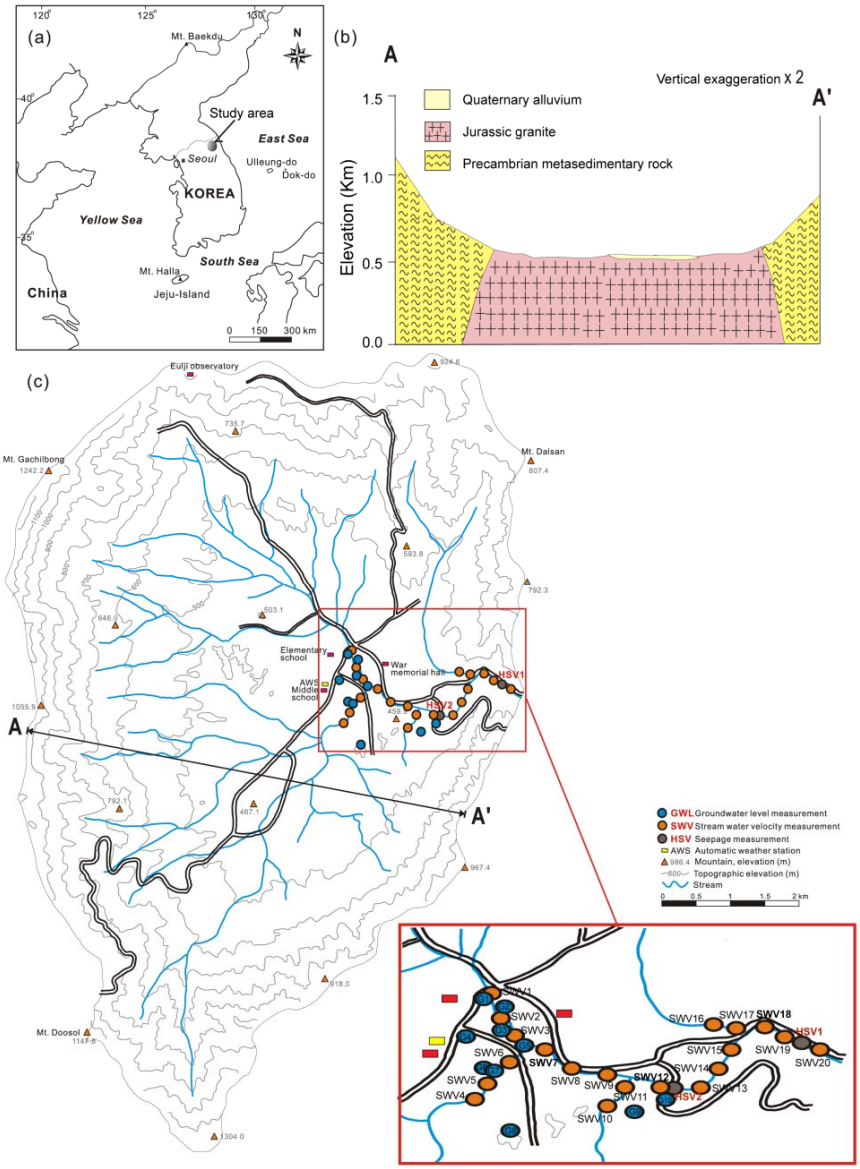

Fig.1-2 (a) Location of the study area, (b) a geologic section of the study area, and (c) locations of the groundwater level monitoring wells, stream water velocity measurement points and seepage measurement points

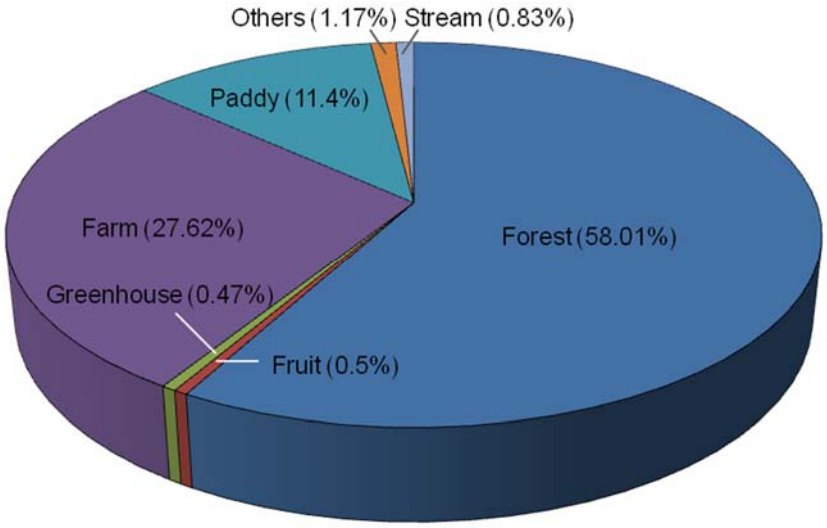

Fig. 1-3 Land use in the study area as of 2011

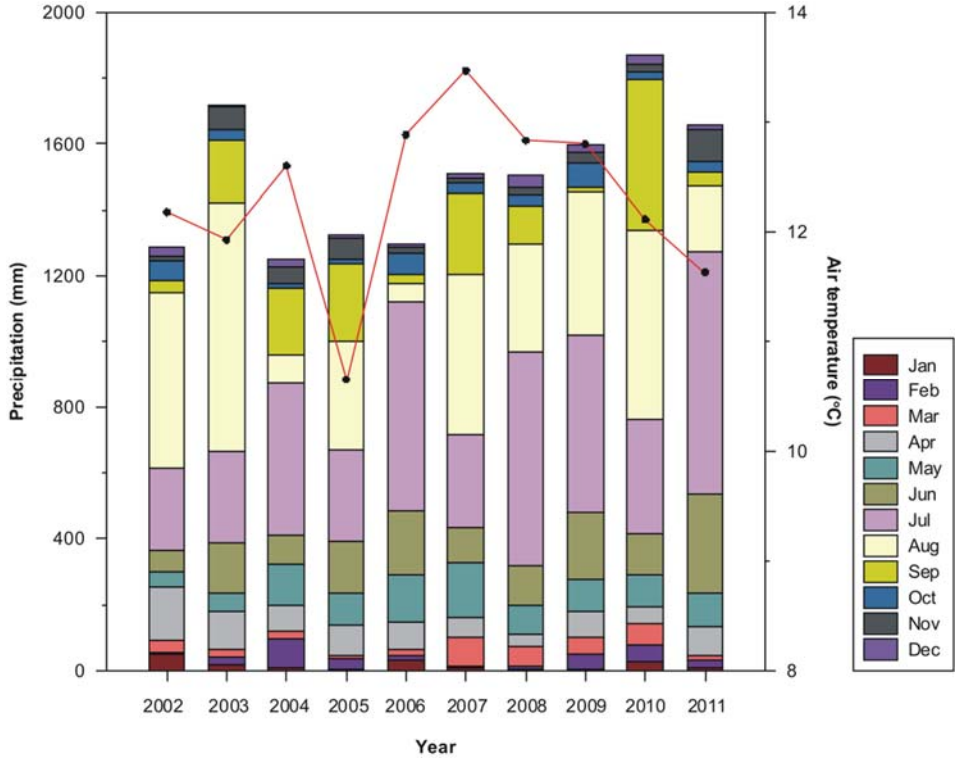

Fig.1-4 Annual precipitation and annual mean air temperature for 2002-2011 in the study area

1.5 Land Use and Agricultural Activity

Land use of the study site is dominated by rice paddy fields and vegetable fields, which accounts for approximately 40% of the total area. Another 58% are forest fields while the rest is mainly residential area (Kim et al., 2013). The agricultural area soils can be mainly characterized as terric Cambisols or as Anthrosols (Kettering et al., 2012). The estimated total amount of nitrogen fertilizer applied in the Haean basin is 101 to 179 $kgNha^{-1}yr^{-1}$ (Yanggu Country Office, 2010). Since 2010, the chemical fertilizer funding has been reduced from Korea government. The government supports an organic fertilizer using. Therefore, the usage of chemical fertilizers is decreasing year after year. On the other hand, the organic fertilizer usage is on the rise in the Haean basin. The recent quantity of organic fertilizer consumed in Haean basin shown in Table 1. The supported fertilizer from government was composed of animal waste fertilizer and organic fertilizer. The estimated total amount of organic fertilizer applied in the area is 95

$kgNha^{-1}$ in 2011 and 134 $kgNha^{-1}$ in 2012, respectively (Yanggu Country Office, 2013).

The main crops of vegetable fields were Chinese cabbage, radish, potato and soybean (Yanggu Country Office, 2012). The Chinese cabbage, one of the main crops in vegetable fields, has 2 fertilizing times at the rate of 238 $kgNha^{-1}yr^{-1}$ in crops cultivation season. Growing season of the cabbage is started in mid of May and cultivation of cabbage is ended in end of July. Growth days of the cabbage take 75~90 days. The radish has 3 fertilizing times at the rate of 225 $kgNha^{-1}$ yr^{-1}. The growing season of the radish is started in early June and cultivation is ended in end August. The growth days of the radish have 70~80 days. The crops of potato have 1 fertilizing time at the rate of 137 $kgNha^{-1}yr^{-1}$ in crops cultivation season. The potatoes are normally grown 90~120 days and the growing season is started in end April and cultivation of potatoes are ended in end August. The soybeans have 1 fertilizing time at the rate of 30 $kgNha^{-1}yr^{-1}$ in crops cultivation season.

Growing season of the soybean is started in end of May and cultivation of soybean is ended in end of October. Generally, the growth days of soybean take 120~150 days. Lastly, the rice crops have 2 fertilizing times at the rate of 90 $kgNha^{-1}yr^{-1}$. These crops in the vegetable fields are not required irrigation water but rice in the rice paddy fields need irrigation water from groundwater and stream water.

CHAPTER 2. PROPOSED METHOD FOR DELINEATION OF HYPORHEIC ZONES

2.1 Introduction

Stream water and groundwater can affect each other by sharing a hyporheic zone to degrade or improve the water quality (Findlay, 1995; Brunke and Gonser, 1997; Greenberg et al., 2002; Conant, 2004; Soulsby et al., 2005). The hyporheic zone is the area where mixing and exchange of surface and groundwater occurs and often exhibits large chemical and

hydraulic gradients (Smith, 2004; Kim et al., 2009). For the remediation of contaminated groundwater, natural attenuation by controlling environmental factors has recently received much attention (Fustec et al., 1991; Harman et al., 1996; Mengis et al., 1999; Babiker et al., 2004; Beller et al., 2004; Wakida and Nerner, 2005; Shomar et al., 2008; Hyun et al., 2011; Kim et al., 2013).

Due to the widespread contamination of surface water, overloading groundwater with organic matter and nutritive substances is a frequent occurrence (Schiff et al., 1990; Boyer et al., 2000; Sebestyen et al., 2008). It takes a lot of energy and enormous cost to remediate contaminated groundwater (Hynes, 1960; Johnson et al., 1997; Townsend et al., 1997; Parker et al., 2000), and thus, attention is being placed on measures for the efficient and cost-effective restoration of contaminated groundwater. Due to the complexity and diversity of the underground medium, the remediation of groundwater is very inefficient both in terms of economy and efficacy. Therefore a fundamental and logical assessment of the problem at hand was

required.

Existing methods to estimate the mixing zone of surface water and groundwater include the installation of seepage meters (Taniguchi and Fukou, 1993; Langhoff et al., 2001; Murdoch and Kelly, 2003; Rosenberry and Morin, 2004; Rosenberry, 2008) or piezometers (Calver, 2001; Surridge et al., 2005; Hatch et al., 2006; Kim et al., 2009; Kim et al., 2013), gauging differential discharge (Lowry et al., 2007; Essaid et al., 2008), and trace injection tests (Bencala et al., 1990; Castro and Hornberger, 1991; Triska et al., 1993; Hoehn and Cirpka, 2006). With regard to the seepage meter installation, errors can be introduced by improper installation/deployment (Rosenberry and Pitlick; 2009). The piezometer installation requires intensive labor and has a limitation of point measurement (Hatch et al., 2006; Rosenberry et al., 2012). Differential discharge gauging is also labor-intensive and difficult when flows are low or turbulent. Lastly, tracer injection tests cannot distinguish subsurface flow from loss and may be affected by tracer adsorption

(Constantz et al., 2003; Isiorho et al., 2005; Ruehl et al., 2006; Chen et al., 2007; Kim et al., 2013). Nevertheless, the tracer injection tests are widely used for hyporheic zone delineation (Triska et al., 1993).

Compared with such physical methods, which require higher cost, or chemical methods which inject further chemicals, usually causing a secondary contamination, estimating the depth of the contaminated region based on temperature change of the mixing zone of surface water and groundwater should be much more cost-effective (Stonestrom and Constantz, 2003; Anderson, 2005; Keery et al., 2007). Having focused on the fact that the temperature of a streambed is influenced by the hyporheic flux, we propose a method for estimating the depth of the hyporheic zone based on the analysis of heat transfer through the streambed (Lapham, 1989; Constantz et al., 1994; Constantz and Thomas, 1996; Taniguchi et al., 2003; Stonestrom and Constantz, 2004; Constantz, 2008; Hyun et al., 2011; Kim et al., 2011). The heat transfer analysis includes the heat transfer mode of conduction,

advection and dispersion (Stallman, 1963; Silliman and Boorh, 1993; Anderson, 2005; Constantz, 2008).

The main concept of the method is that the calculated temperature distribution which shows the best fit to the measured temperature distribution is determined from the heat transfer analysis by changing the hyporheic flux. The procedure obviously has an advantage over the previous methods of estimating the mixing zone because the proposed method simply requires the measurement of the temperature distribution in the field, as a single parameter upon which determinations are directly made.

The present paper focuses on the assessment of the adequacy of the proposed method, which estimates the depth of the hyporheic zone by gathering field temperature and performing conduction-advection-dispersion analysis (CAD analysis). The adequacy is assessed by evaluating the difference between the real field temperature distribution over time and its corresponding values from CAD analyses. The sensitivity of the sum of

squared differences (SSD) to the two factors of hyporheic flux, which are the hyporheic zone depth and the hyporheic flux magnitude, was evaluated. The SSDs for different hyporheic flux shapes are all proven to be more sensitive to the hyporheic zone depth than its magnitude. This result demonstrates the appropriateness of the proposed method. Lastly, field temperature data was collected and the hyporheic zone depth was estimated by CAD analyses, and then the result was compared with that from the conventional tracer test.

2.2 Proposed Method for Estimating the Hyporheic Zone Depth

This study arises from the fact that the temperature distribution of the streambed is influenced by the hyporheic flux, and intends to estimate the depth of the hyporheic zone. Hence, the temperature distribution of the streambed can be calculated by CAD analyses. The heat transfer in the streambed is described by the following differential equation of one-dimensional conduction-advection-dispersion equation (Carslaw and Jaeger, 1959; Stallman, 1965; Goto et al., 2005).

$$\rho c\frac{\partial T}{\partial t}=\lambda_e\frac{\partial^2 T}{\partial z^2}-n\rho_f c_f v_f\frac{\partial T}{\partial z} \tag{1}$$

where ρ = density of grain (kg/m^3)

c = specific heat capacity of soil (J/k℃)

T = temperature (℃)

λ_e = $\lambda_o+\rho c\beta|v_f|$ = effective thermal conductivity

(W/m℃)

λ_0 = $\lambda_f^n \lambda_g^{(1-n)}$ = baseline thermal conductivity (in the absence of fluid flow) (W/m℃)

λ_f = thermal conductivity of fluid (W/m℃)

λ_g = thermal conductivity of grain (W/m℃)

β = thermal dispersivity (m)

n = porosity (-)

ρ_f = density of fluid (kg/m3)

c_f = specific heat capacity of fluid (J/kg℃)

v_f = vertical fluid velocity (positive for downward direction) (m/s)

z = depth (m)

t = time (s)

For CAD analyses, as shown in Fig. 2-1, the initial and boundary conditions are indispensable. These conditions are obtained from the field temperature distribution collected over several depths and time periods. The temperature distribution over depths and times from field measurement is compared with its corresponding values from CAD analyses, and the hyporheic flux that minimize the SSD between the calculated and the measured temperatures is determined.

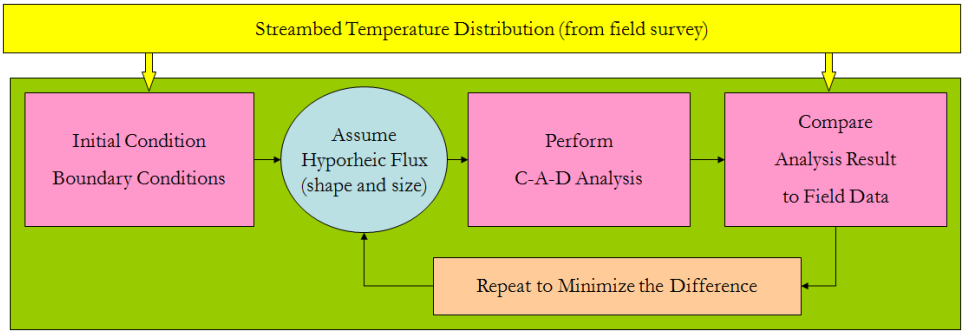

Fig. 2-1 Procedure for the determination of hyporheic flux

Hyporheic flux consists of two parameters: hyporheic flux shape and size. A set of hyporheic zone depths and the magnitude in vertical direction forms the size of hyporheic flux. Firstly, the shape of hyporheic zone is seldom reported in the literature. However, it is reasonable for a hyporheic flux to have such a shape that its magnitude is decreasing with increasing depth (Fig. 2-2). In this study, as listed in Table 2-1, the assumed shape of the hyporheic flux includes the spandrel shape, triangle shape, cosine shape, and a quarter of an ellipse. Secondly, the magnitude of hyporheic flux is comprised of the maximum flux velocity at the streambed level, $V_{f,max}$, and the hyporheic zone depth, D_H.

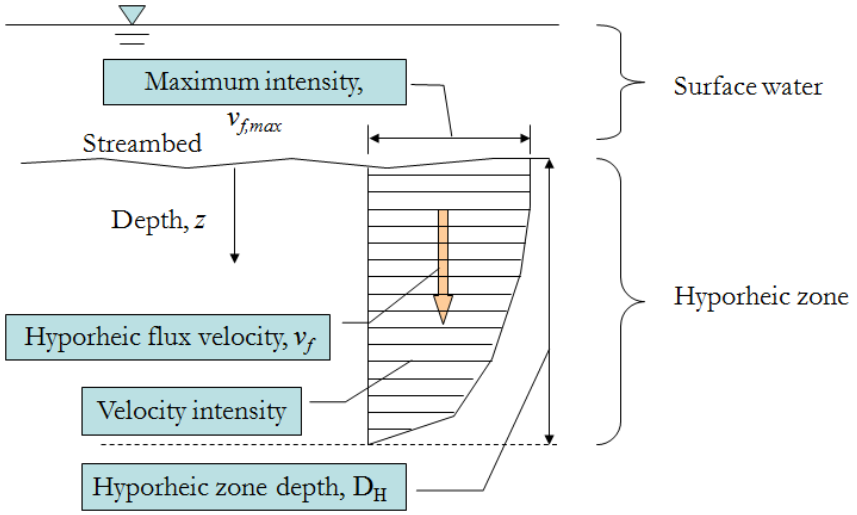

Fig. 2-2 Schematic diagram of the hyporheic flux for heat transfer analysis

Table 2-1 Different types of the hyporheic flux shape and their mathematical expressions

Type	Shape	Expression
Spandrel	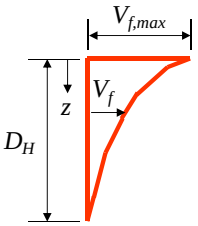	$\frac{V_f}{V_{f,\max}} = \left(\frac{D_H - z}{D_H}\right)^{1.5}$
Triangle	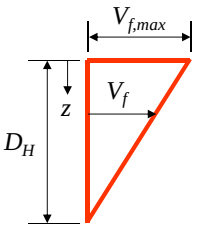	$\frac{V_f}{V_{f,\max}} = \left(\frac{D_H - z}{D_H}\right)$
Cosine curve	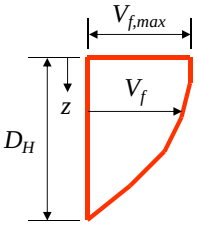	$\frac{V_f}{V_{f,\max}} = \cos\left(\frac{\pi}{2} \cdot \frac{z}{D_H}\right)$
A quarter of an ellipse	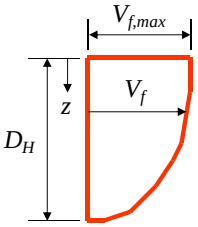	$\frac{V_f}{V_{f,\max}} = \sqrt{1 - \left(\frac{z}{D_H}\right)^2}$

2.3 Adequacy of the Proposed Method

Numerical verification to assess the adequacy of the proposed method was considered in this section. To this purpose, firstly, CAD analysis was performed one time for a hypothetical field, i.e., an initial condition (Fig. 2-3(a)) and two boundary conditions (Fig. 2-3(b)), and temperature results were set as a reference for comparison with subsequent CAD analyses (Fig. 2-4). The next stage is storing SSDs by repeating the CAD analyses while it altering the two factors of hyporheic flux, i.e., the magnitude and depth of the hyporheic zone.

The candidates for the hyporheic flux shape are listed in Table 1, and the hyporheic flux size for the reference analysis was chosen as $V_{f.max}$ = 0.005 m/min and D_H= 0.10 m. The hypothetical initial and boundary conditions are shown in Fig.2-3(a) and Fig. 2-3(b), respectively, and the parameters for CAD analyses are listed in Table 2-2. Some parameters in Table 2-2 are adopted from the literature and the others are measured values from the field where

the present study was applied. The baseline thermal conductivity calculated using the conductivities of the fluid and the grain, and the porosity in Table 2-2 equals 1.927 W/m℃, which is in good agreement with the saturated sediments reported in literature (Carslaw and Jaeger, 1959; Harlan, 1973; Kelly and Reinhard, 1985; Tarara and Ham, 1997; Anderson, 2005; Molina-Giraldo et al., 2011).

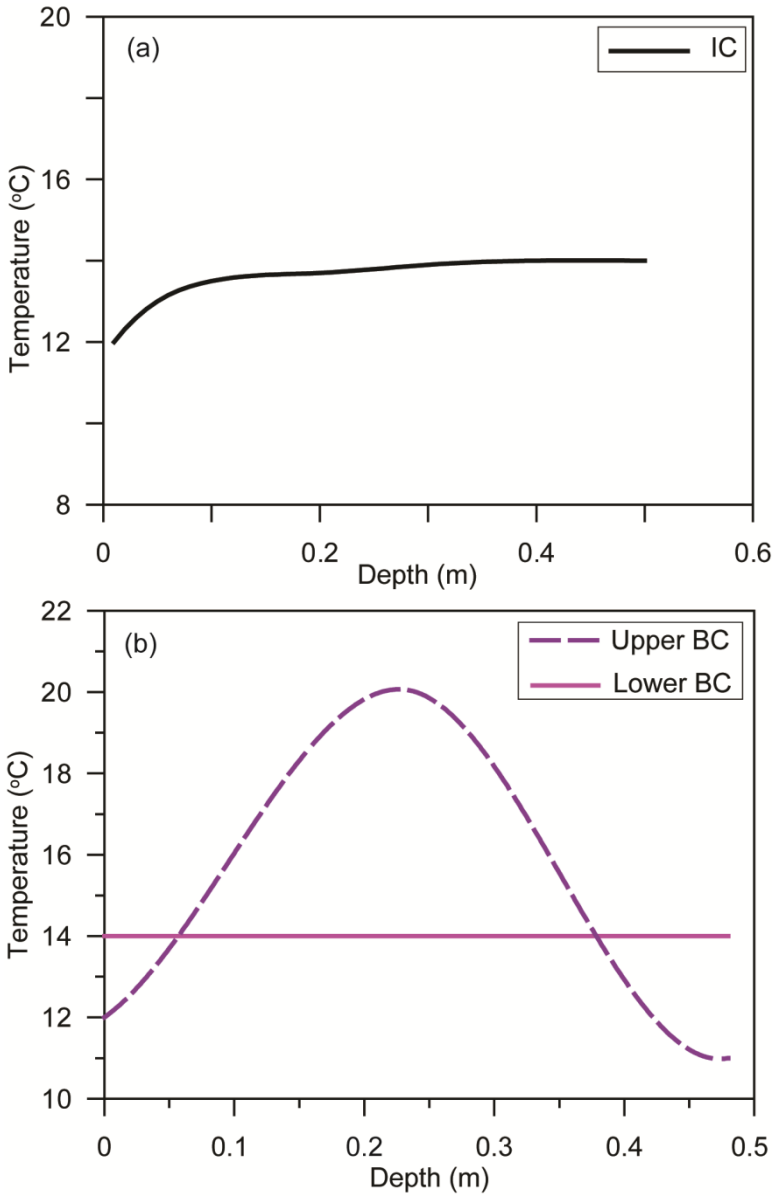

Fig. 2-3 (a) Hypothetical initial condition (IC) and (b) Hypothetical boundary conditions (BC) for an adequacy test of the proposed method

Table 2-2 Parameters used for heat transfer analysis

Parameter	Unit	Value	Reference
density of grain, ρ	kg/m^3	2156	Kelly and Reinhard (1985)
specific heat capacity of soil, c	J/kg ^{o}C	840	Tarara and Ham (1997)
thermal conductivity of fluid, λ_f	W/m ^{o}C	0.6	Harlan (1973)
thermal conductivity of grain, λ_g	W/m ^{o}C	3.337	Anderson (2005)
thermal dispersivity, β	m	0.004	Molina-Giraldo et al. (2011)
porosity, n	–	0.32	Measured from field soil
density of fluid, ρ_f	kg/m^3	1000	Domenico and Schwartz (1998)
specific heat capacity of fluid, c_f	J/kg ^{o}C	4200	Carslaw and Jaeger (1959)

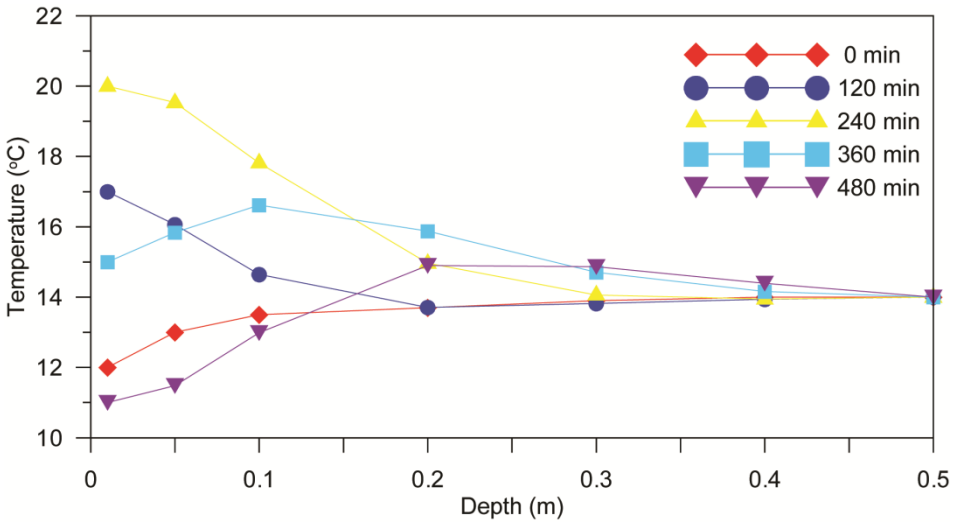

Fig. 2-4 Calculated streambed temperature distribution from the hypothetical initial and boundary conditions and the triangle-shaped hyporheic flux with $V_{f,max}$ = 0.005 m/min and D_H = 0.10 m (solid dots represent the selected value for the calculation of SSDs)

SSD is dependent on the size of hyporheic flux. The results from CAD analyses for a triangle-shaped hyporheic flux are shown in Table 2-3 and Fig. 2-5, and the hyporheic flux size, which minimizes the SSD can be determined. From Figs. 2-6 (a) and 2-6 (b), it is obvious that the sensitivity of SSD to the hyporheic zone depth is larger than that to the hyporheic flux velocity magnitude, regardless of the assumed hyporheic shape. This result shows the advantage of the proposed method to delineate the hyporheic zone, rather than to determine the hyporheic flux velocity.

Table 2-3 SSDs for the triangle-shaped hyporheic flux with different size ($^oC^2$)

D_H	$V_{f,max}$ (m/min)									
(m)	0.001	0.002	0.003	0.004	0.005	0.006	0.007	0.008	0.009	0.010
0.01	6.954	6.954	6.954	6.954	6.954	6.954	6.954	6.954	6.954	6.954
0.02	6.851	6.748	6.640	6.551	6.446	6.358	6.268	6.184	6.106	6.040
0.03	6.615	6.282	5.994	5.723	5.473	5.275	5.084	4.930	4.767	4.607
0.04	6.272	5.664	5.144	4.689	4.322	3.986	3.720	3.462	3.225	3.026
0.05	5.841	4.927	4.175	3.587	3.092	2.696	2.342	2.055	1.808	1.601
0.06	5.389	4.175	3.252	2.537	2.007	1.573	1.248	0.990	0.790	0.638
0.07	4.942	3.468	2.417	1.663	1.139	0.760	0.509	0.338	0.237	0.184
0.08	4.514	2.820	1.696	0.979	0.515	0.245	0.114	0.074	0.099	0.167
0.09	4.107	2.241	1.106	0.461	0.132	0.021	0.053	0.179	0.357	0.576
0.10	3.725	1.736	0.648	0.139	**0.000**	0.099	0.349	0.677	1.059	1.455
0.11	3.375	1.316	0.331	0.021	0.132	0.496	1.009	1.585	2.200	2.817
0.12	3.066	0.986	0.160	0.103	0.511	1.176	1.975	2.829	3.663	4.535
0.13	2.797	0.743	0.119	0.360	1.097	2.083	3.161	4.280	5.353	6.421
0.14	2.568	0.580	0.197	0.760	1.837	3.139	4.508	5.866	7.165	8.384
0.15	2.375	0.488	0.373	1.281	2.697	4.310	5.957	7.530	9.025	10.380
0.16	2.215	0.456	0.635	1.901	3.658	5.586	7.489	9.284	10.940	12.464
0.17	2.083	0.478	0.972	2.609	4.723	6.954	9.141	11.136	12.994	14.638
0.18	1.976	0.548	1.380	3.404	5.881	8.438	10.907	13.149	15.178	17.029
0.19	1.892	0.679	1.856	4.294	7.163	10.076	12.810	15.347	17.604	19.625
0.20	1.829	0.828	2.405	5.280	8.583	11.881	14.940	17.790	20.341	22.610

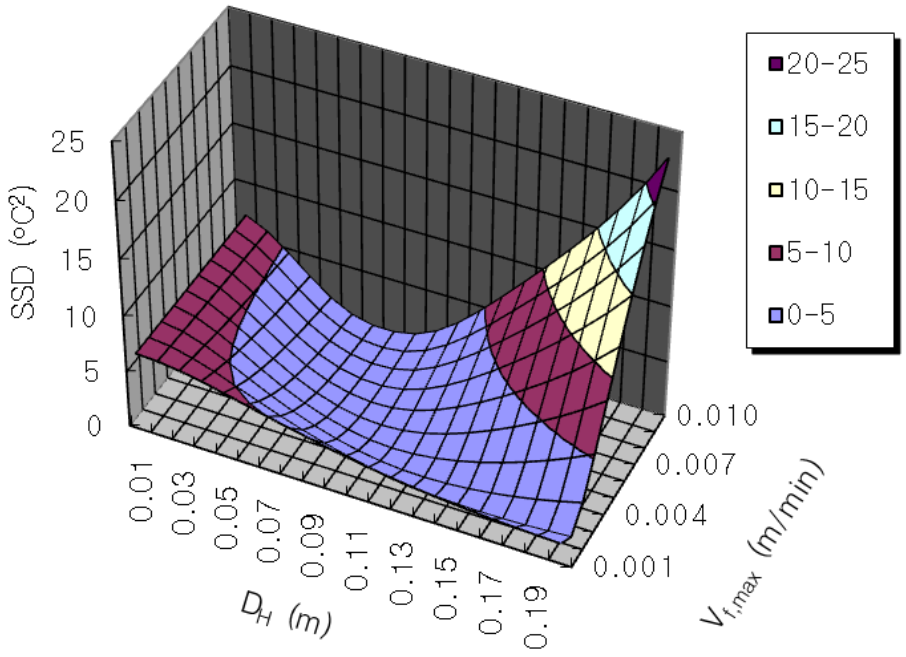

Fig. 2-5 Three-dimensional representation of SSDs for the triangle-shaped hyporheic flux with different size

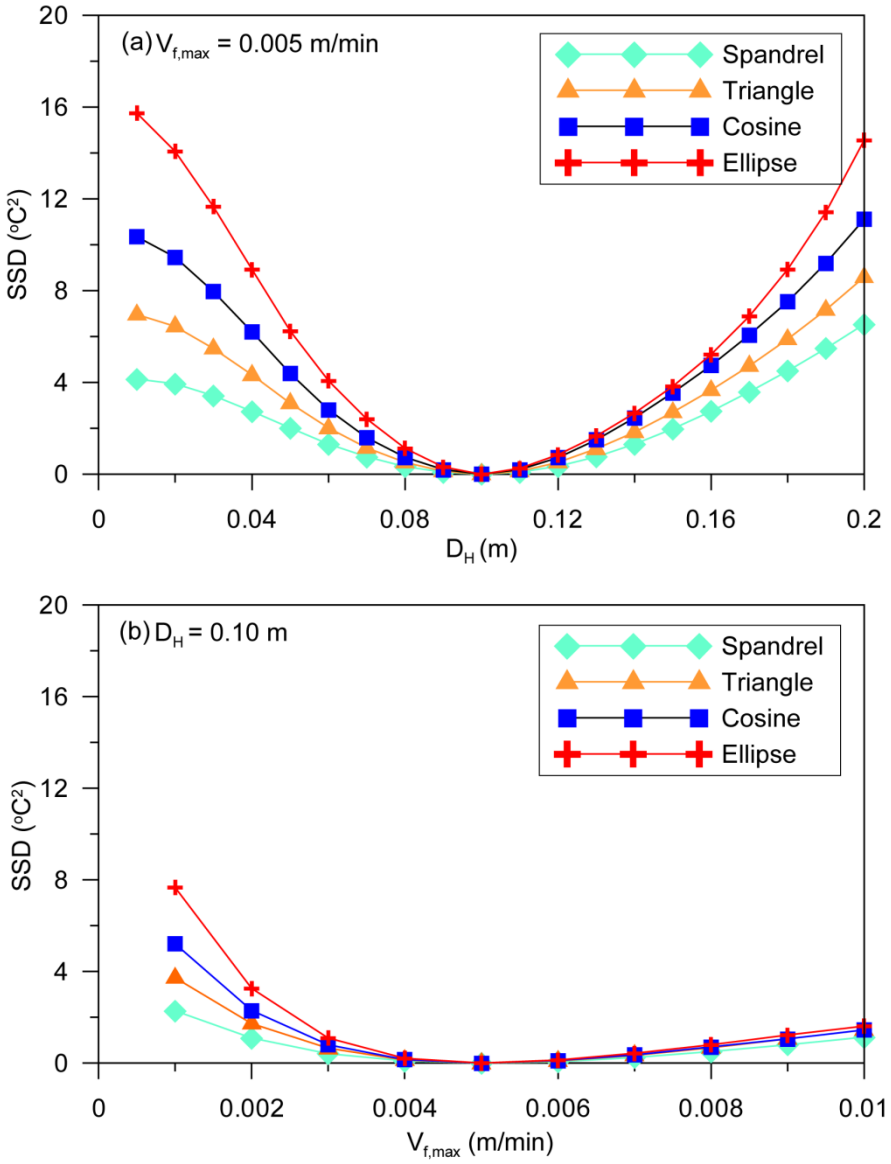

Fig. 2-6 (a) Influence of the hyporheic flux depth and shape on SSD and (b) Influence of the hyporheic velocity magnitude and shape on SSD

2.4 Effect of Hyporheic Flux Shape

The shape of the hyporheic flux in a field is dependent on many factors, and its precise shape would be hardly known. In this respect, the effect of the hyporheic flux shape on its depth was evaluated. To this purpose, the temperature distribution from a CAD analysis for a triangle-shaped hyporheic flux with its size of $V_{f.max}$ = 0.005 m/min and D_H = 0.10 m is considered as a field temperature distribution, and is set as a reference for the comparison with temperature distributions with different hyporheic flux shapes.

The optimal hyporheic zone depths are estimated for the spandrel-, cosine-, and ellipse-shaped hyporheic flux (Fig. 2-7), and the results are listed in Table 2-4. The average intensity of the hyporheic flux velocity increases as the hyporheic flux shape changes in the order of spandrel, triangle, cosine and ellipse, and accordingly the resulting depth and velocity magnitude of the hyporheic flux gets smaller.

Table 2-4 Sensitivity of the hyporheic flux depth with different hyporheic flux shapes

Optimal values	Shape of hyporheic flux			
	Spandrel	Triangle (reference)	Cosine	Ellipse
D_H (cm)	11.3 (+13%)	10	9.7 (-3%)	8.6 (-14%)
$V_{f,max}$ (mm/min)	5.8 (+16%)	5	3.8 (-24%)	3.4 (-32%)
SSD ($^oC^2$)	1.6751E-4	0	1.6583E-4	11.2543E-4

(Values in parenthesis are relative errors compared with the reference case)

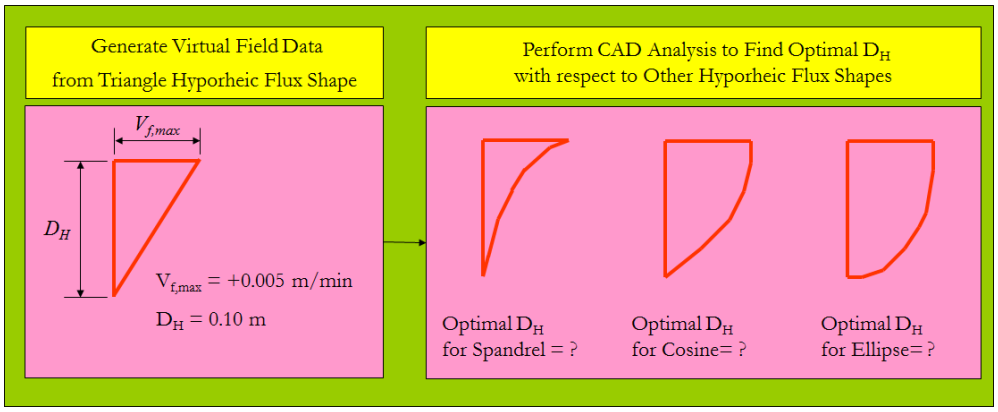

Fig. 2-7 Process to investigate the influence of the hyporheic flux shape on the optimal hyporheic flux depth

It is noteworthy that the relative error in the estimated depth is smaller than that in the velocity magnitude, meaning that the hyporheic zone depth can be determined with more precision for different hyporheic shapes than the velocity magnitude. The CAD analysis results for different hyporheic flux shapes show that the effect of the hyporheic flux shape on the hyporheic zone depth is not so large. This is an advantage of the proposed method because the exact hyporheic flux shape for a specific field is usually not known. Thus, we can determine the hyporheic zone depth within a reasonable range, regardless of the hyporheic flux shape.

2.5 Conclusions

A method for estimating the depth of the hyporheic zone using measured temperature and heat transfer analysis was proposed in this study. For different shapes of the hyporheic flux, the sensitivity of SSD to the hyporheic zone depth was larger than that to the hyporheic flux velocity magnitude. The result indicates that the hyporheic zone depth can be estimated by the proposed method.

The hyporheic zone depth was revealed to be largely independent of the hyporheic flux shapes. The result showed that the hyporheic zone depth can be estimated within a reasonable range with a rough assumption of the hyporheic flux shape; even if the real hyporheic flux shape is hardly known. The proposed method was also applied to a set of temperature data at a field site to estimate the hyporheic zone depth. For the study site, the proposed method estimated an acceptable range of the hyporheic zone depth with all the hyporheic flux shapes.

This page intentionally left blank

CHAPTER 3. VERIFICATION USING HYDROLOGICAL APPROACH

3.1 Introduction

The quantification of groundwater-stream water interactions is pivotally important to evaluate water budget in rural region where a large amount of groundwater and stream water are consumed for agricultural uses. Also, it is essential to manage the stream benthic ecology and to obtain a continuous stability of water resource in a climate change era. Water budgets

in rural region are extraordinarily sensitive to climate change (Vörösmarty et al. 2000; Christensen et al. 2004; Chiyuan et al. 2010). The global climate change will affect the balance of water demand and supply immediately and will have a significant influence over rural regions. Therefore, it is important to study the interactions between groundwater and stream water in such areas.

Over the past decades, there exist various methods for estimating the seepage between groundwater and stream water (Taniguchi and Fukuo 1993; Cable et al. 1997; Corbett et al. 1999; Rosenberry 2012). These methods include the seepage estimation by installing the seepage meters and the piezometers (Lee and Cherry 1978; Woessner and Sullivan 1984; Taniguchi and Fukuo 1993; Hatch et al. 2006), measuring streambed temperature (Constantz et al. 1994; Constanz and Thomas 1996; Constanz et al. 2002; Lowry et al. 2007), injecting tracer (Isiorho et al. 2005; Ruehl et al. 2006; Chen et al. 2007), using differential stream discharge gauging (Oberdorfer 2003; Vogt et al. 2010), water balance calculations (LaBaugh et al. 1997) and

numerical modeling (Sophocleous et al. 1999; Cardenas et al. 2008).

A recent research (Kim et al. 2014) has begun to quantify actual groundwater and stream water contributions in a mixing area through the use of tracer test. The tracer test have been widely used and it is the only way to quantify the delineation of hyporheic zone depth (Lee 1985; Lee and Cherry 1978; Krupa et al. 1998; Rosenberry and Morin 2004; Rosenberry and Meheer 2006; Brodie et al. 2009). The objective of this study was to examine spatial and temporal variation of tracer test resulting from sandbed streams with the goal of quantifying groundwater-stream water exchange in the agricultural area, the Haean basin of Korea. Specific objectives include comparing proposed method with measure depths of tracer test across the stream.

3.2 Study site and Data Acquisition

The temperature data were collected in the Haean basin, Yanggu County, Gangwon province, Korea with an area of 57.5 km^2 (Fig.3-1). The streambed sediments at the basin range from fine sand to coarse gravel. Generally, sediments found upstream are composed mainly of coarse gravel while fine sand is found downstream. Temperature probes were installed in the study site, and temperatures of stream water and sediments below the streambed were measured with EcoScan Temp 6 (a 3-wire RTD PT100 temperature probe) (Eutech Instruments). Probes were manually inserted into the streambeds at multiple depths (0, 0.1, 0.2, 0.3, 0.4, 0.5, 0.6 m), at selected point. The point consisted of 82% sand, 0.3% silt and 7.7% clay. The soil texture of the point was sand, and the bulk density and porosity were 1.43 g/cm^3 and 0.32, respectively.

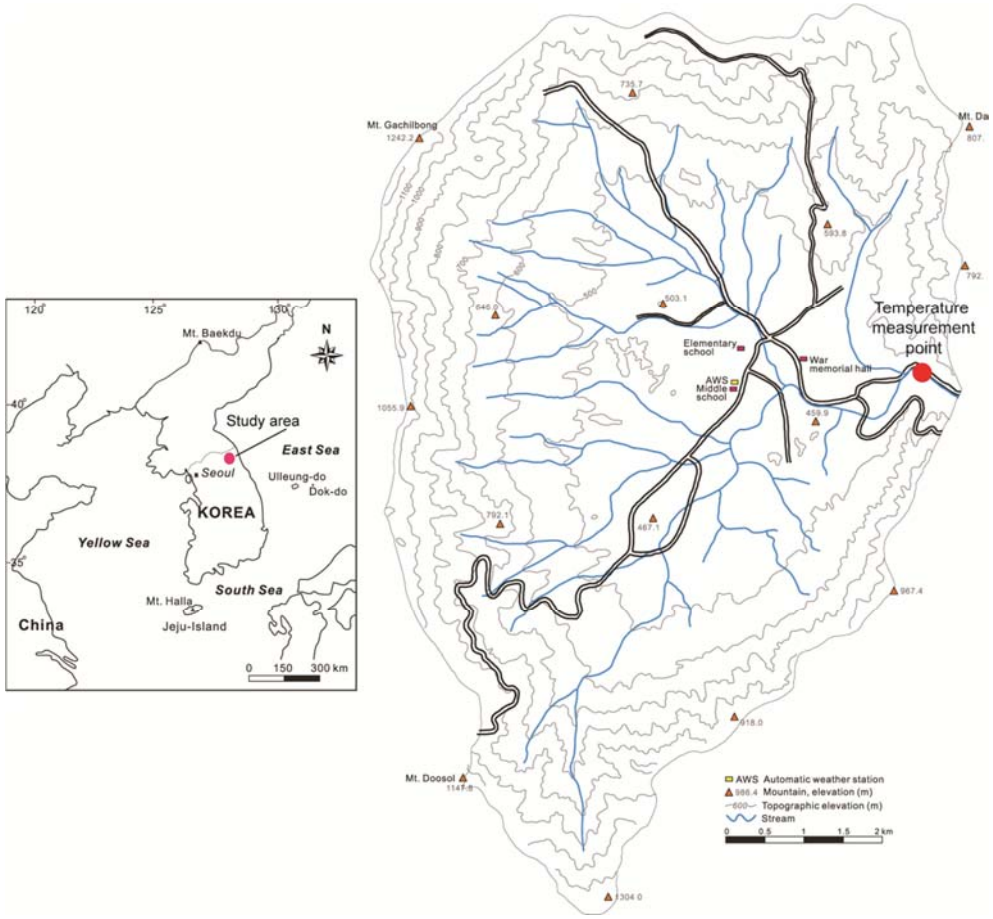

Fig. 3-1 Map of the location of study site

The tracer test was performed for the calibration of the proposed model in this study. Sodium chloride (13 kg) was melted in 60 L of distilled water. The solution was released at 50 m upper stream from the temperature measurement point with a rate of 2 L/min for 30 minutes using the peristaltic pump. The EC was measured at the temperature measurement point at an interval of 1 minute for 40 minutes using a potable meter (YSI556. YSI, USA). Water samples for analysis of chloride were also collected every minute and the chloride concentration was analyzed by ion chromatography (761 Compact IC, Metrohm AG, Switzerland) at Central Laboratory in Kangwon National University. During the tracer test, stream water velocity was measured using a field meter (FP-111, Global Water) at both of the tracer releasing point and temperature measuring point.

3.3 Application of the Proposed Method to Field Data

The proposed method was applied to field data and the hyporheic zone depth was calculated. The location of the field site is shown in Fig. 3-1 and the measured temperature distribution of the field site is shown in Fig.3-2. Temperatures were recorded for the selected depths in the streambed at intervals of 2 hours from 9 am. During the time of measurement, the surface temperature gradually rose by about 12 degrees Celsius and then dropped slightly. The heat of the surface was transported down below the streambed, which caused the temperature below to increase. Initial and boundary conditions are constructed by spline interpolation from the discrete temperature sets extracted from the measured temperatures (Figs. 3-3(a) and (b))

The optimal hyporheic zone depths for different hyporheic flux shapes are estimated as in Table 3-1, and the result of the CAD analysis for the triangle-shaped hyporheic flux is shown in Fig. 2-6. The SSDs for the

optimal size for each hyporheic flux shape are nearly the same for the study site. Though the optimal hyporheic zone depths show some variation, the estimated hyporheic zone depths are within a reasonable range for the study site. Higher hyporheic zone depth for the spandrel shapes may be due to the fact that the average hyporheic flux is smaller for the spandrel-shape than for the other hyporheic flux shapes.

Table 3-1 Estimated hyporheic flux depth of the study site with different hyporheic flux shapes

Optimal values	Shape of hyporheic flux			
	Spandrel	Triangle	Cosine	Ellipse
D_H(cm)	14.9	11.6	11.4	9.2
$V_{f,max}$(mm/min)	-0.4	-0.4	-0.3	-0.3
SSD ($^oC^2$)	7.517	7.520	7.517	7.522

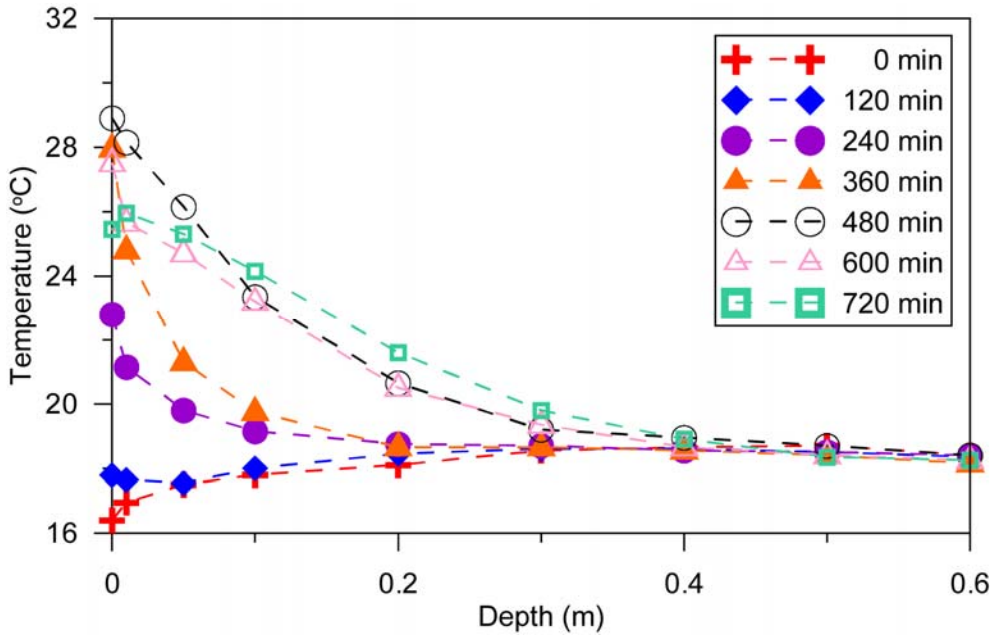

Fig. 3-2 Measured temperature distribution of the study site

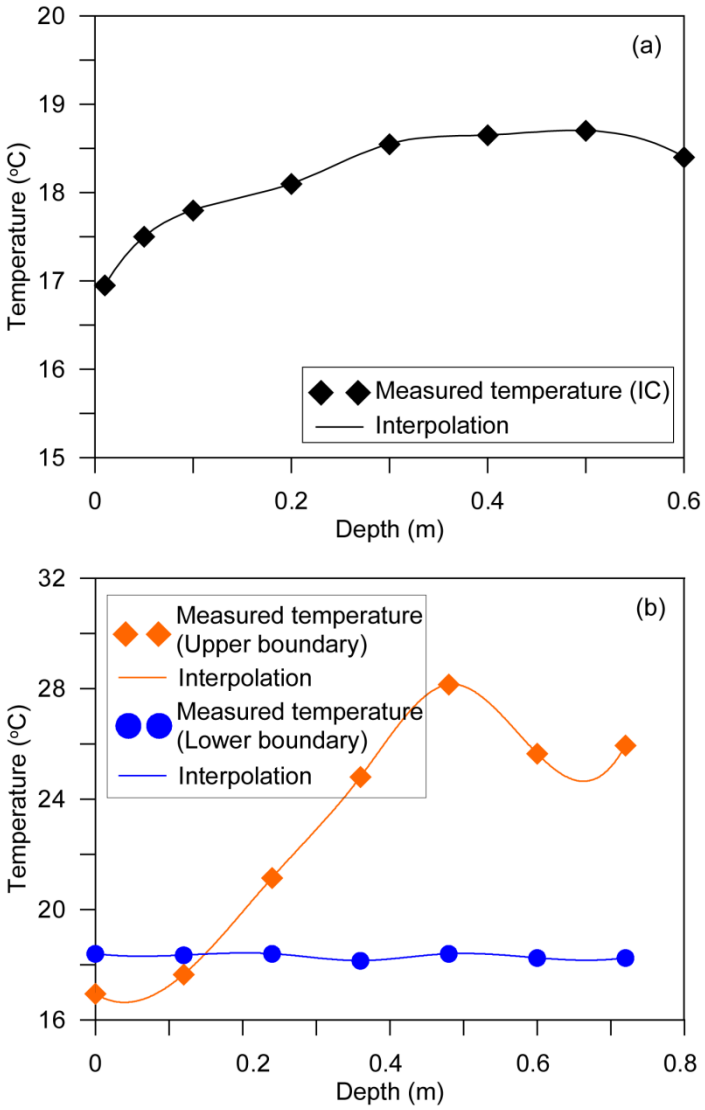

Fig. 3-3 (a) Initial condition interpolated using the measured temperature and (b) Boundary conditions interpolated using the measured temperature of the study site

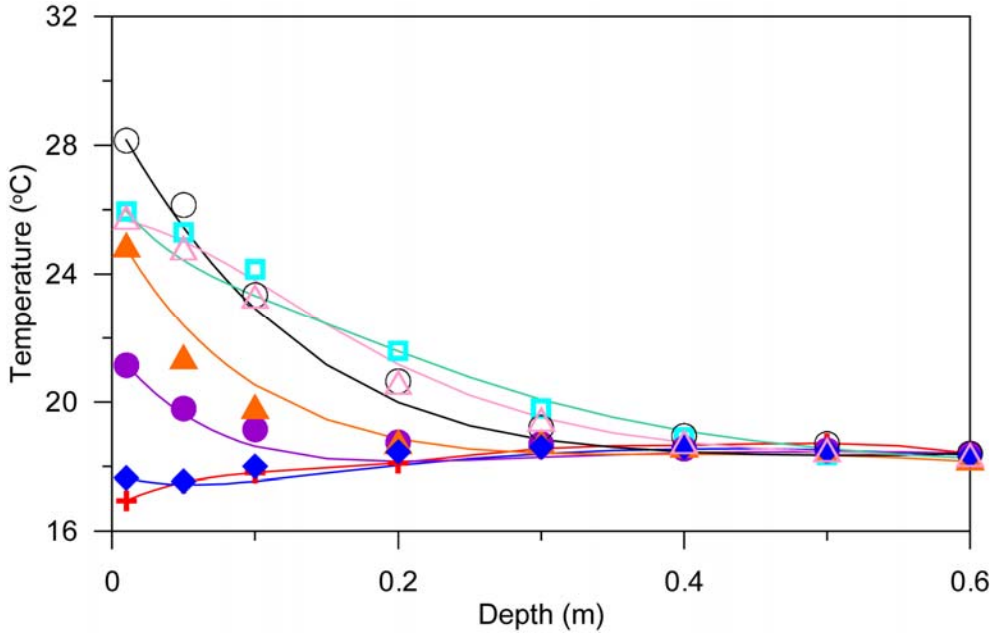

Fig. 3-4 Optimal temperature distribution of the study site for the triangle-shaped hyporheic flux with its size of $V_{f,max}$= -0.4 mm/min and D_H = 0.116 m

3.4 Comparison of the Result from the Proposed Method with Conventional Method

The results from the proposed method and a tracer test are compared in this section. The tracer test is one of the conventional methods for estimating the hyporheic zone depth (Triska et al., 1993; Bertin and Bourg, 1994; Harvey and Fuller, 1998; Hill and Lymburner, 1998). The commonly used equations to model one-dimensional transport in streams with groundwater exchange and storage are

$$\frac{\partial C}{\partial t} = -\frac{Q}{A}\frac{\partial C}{\partial x} + \frac{1}{\mathrm{A}}\frac{\partial}{\partial x}\left(AD\frac{\partial C}{\partial x}\right) + \frac{q_L^{in}}{A}\left(C_L - C\right) + \alpha\left(C_s - C\right) - \lambda C \qquad (2)$$

$$\frac{\partial C_s}{\partial t} = \alpha\frac{A}{A_s}\left(C - C_s\right) - \lambda_s C_s \qquad (3)$$

where t = time(s)

x = direction along the stream (m)

C = concentrations in the stream (mg/L)

C_s = concentrations in the storage zone (mg/L)

C_L = concentration in the groundwater (mg/L)

Q = in-stream volumetric flow rate (m^3/s)

q_L^{in} = reach-averaged groundwater influx per meter of stream ($m^3/s/m$)

D = longitudinal dispersion coefficient in the stream (m^2/s)

A = stream area (m^2)

A_s = storage zone cross-section area (m^2)

α = storage-exchange coefficient (s^{-1})

λ = first order rate constant describing net uptake of a reactive solute by a biological process in stream flow (s^{-1})

λ_s = first order rate constant describing net uptake of a

reactive solute by a geochemical process in the storage zone (s^{-1})

A nonreactive solute tracer such as chloride is injected into a stream. The interaction of the stream water with groundwater is assumed to not exist because the water flux measured near the hyporheic zone is small and the distance between tracer injection point and chloride concentration monitoring point is short. Then with the assumptions made above, the equations are simplified as

$$\frac{\partial C}{\partial t} = -\frac{Q}{A}\frac{\partial C}{\partial x} + \frac{1}{\mathrm{A}}\frac{\partial}{\partial x}\left(AD\frac{\partial C}{\partial x}\right) + \alpha\left(C_s - C\right) \tag{4}$$

$$\frac{\partial C_s}{\partial t} = \alpha\frac{A}{A_s}\left(C - C_s\right) \tag{5}$$

A rate constant α defines the rate at which stream water is exchanged for water in storage zones. According to Harvey et al. (1996), the

parameters of the storage zone model in Eqs. (4) and (5) can be related to the hyporheic fluxes defined by

$$q_s = \alpha A \tag{6}$$

where q_s = storage-exchange flux, i.e., the average flux of water through storage zones per unit length of stream (m3/s/m)

Mathematically, the storage-exchange flux is identical with the hyporheic-exchange flux, and the rate constant α is determined by using a measured storage-exchange flux. Storage-zone cross-sectional area A_s can be determined by solving Eqs. (4) and (5) simultaneously and comparing its results with that from the tracer test. Harvey and Wagner (2000) recommended a simple way in which the hyporheic zone depth d_s can be calculated from the storage-zone cross-sectional area A_s . As shown in Fig. 3-

1, a stream channel in which the storage-zone cross-sectional area is considerably smaller than the cross-sectional area of the stream ($A_s < A$), and where stream width w is much greater than the stream depth ($w/d > 20$), the hyporheic zone depth is simply approximated by

$$d_s = \frac{A_s}{wn} \tag{7}$$

where d_s = hyporheic zone depth (m)

w = stream width (m)

n = channel sediment porosity (-)

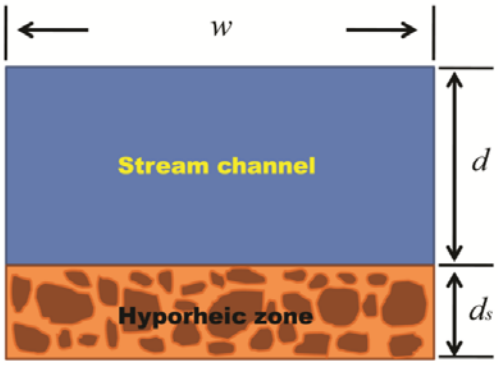

Fig. 3-5 Simple characterizations of the spatial dimension of the

hyporheic zone

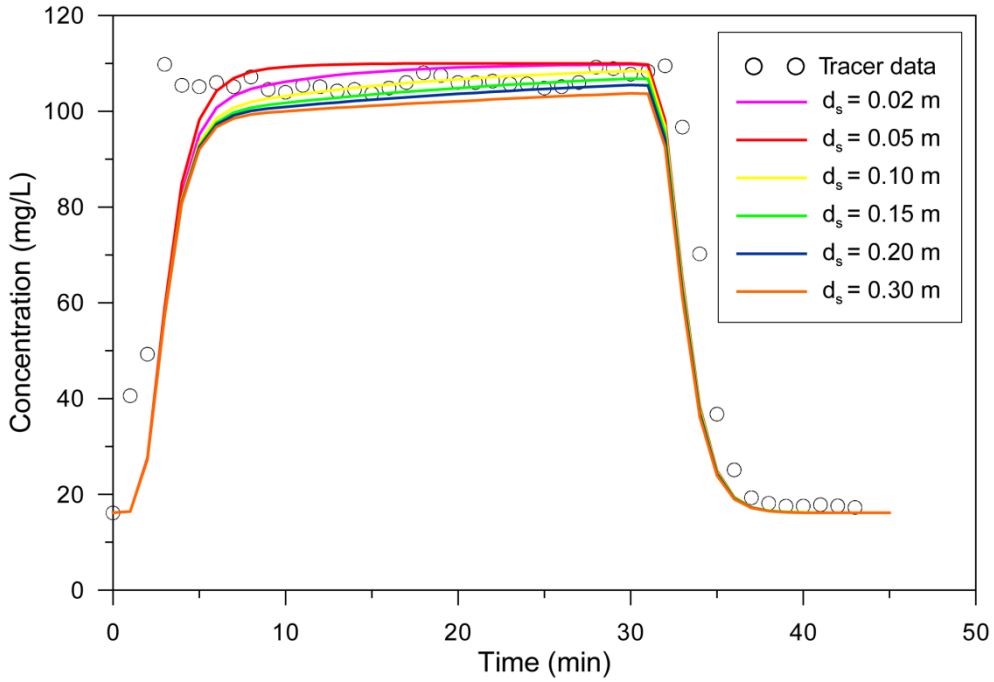

Fig. 3-6 Chloride concentrations over time at monitoring point from the tracer test and the numerical analyses for various depths of hyporheic zone

The chloride concentration obtained from the stream tracer test is shown in Fig. 3-6. The numerical analysis results for various hyporheic zone depths are also presented. Though it is somewhat challenging to determine the hyporheic zone depth using this best-fit, the hyporheic zone depth can be

thought to be in the range of 2 and 30 cm, which is fairly comparable with the range (9-15 cm) of hyporheic zone depth from the proposed method using temperature analysis. As shown in Fig. 3-7, the proposed method gives more precise range of the hyporheic zone depth.

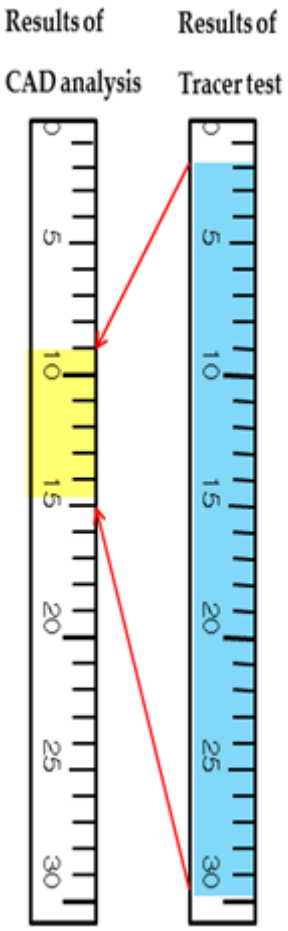

Fig. 3-7 Comparison of the results from the proposed method and the tracer test

3.5 Conclusions

The hyporheic zone depth estimated from the proposed method was compared with that from the traditional method of tracer test. The two estimated depths were in a good agreement but the depth from the temperature analysis was relatively in a narrow range.

The proposed method of estimating the hyporheic zone depth in this study has an advantage over traditional method because the temperature distribution is the sole data required and this is relatively easy to measure in the field.

In order to evaluate the calculated hyporheic depth, sampled hyporheic water which was obtained from the proposed method was estimated with biological and chemical approach, respectively in the following two chapters.

CHAPTER 4. VERIFICATION USING BIOLOGICAL APPROACH

4.1 Introduction

The hyporheic zone constituents a dynamic hotspot (Ecotone) where groundwater and surface water mix (Orghidan, 1992). This area constitutes a flow path along which surface water down wells into the streambed sediment and groundwater up wells in the stream, travels for some distance before

eventually mixing with groundwater returns to the stream channel (Hancock et al., 2005). Surface water enters the hyporheic zone when the vertical hydraulic head of surface water is greater than the groundwater (down welling). On the other hand, surface water with groundwater influence emerges from hyporheic zone where upward direction pressure of subsurface water is greater than that of the stream channel (up welling) (White, 1993).

The exchange of stream water and groundwater in the hyporheic zone is dynamic in space (the space is calculated in the chapter 3) and creates a unique community of the endemic bacteria. The exchange and mixing of groundwater and stream water plays an important role in determining the structure of hyporheic bacteria diversity by influencing hydraulic and chemical condition (Boulton, 2000). However, there have been only a few data researches reporting on the influence of hydrologic exchange on composition and spatial distribution of the hyporheos (Boulton and Stanley, 1995). This chapter represents the influence of hyporheic exchange patterns

on biological characteristics of the hyporheic zone. The effect of the flow direction of hyporheic flux determined from the proposed method on the bacterial community is examined.

4.2 Materials and Methods

4.2.1 Vertical hydraulic gradient of the hyporheic zone

Hyporheic zone, which is the mixed zone of surface water and groundwater, is where quantitative changes occur dynamically. It was divided into 3 points for analysis through vertical hydraulic gradient in the hyporheic zone: Up welling point where the effect of groundwater is greater, down welling point where the effect of surface water is greater, and mixed welling point where quantitative changes of the groundwater and surface water were evenly observed.

4.2.2 Analysis of pyrosequencing reads

The samples were filtered through 0.2 μm filter and returned to the laboratory and stored in a -70^{o}C refrigerator until DNA extraction and pyrosequencing of 16S rRNA analysis. The DNA of sampled groundwater was extracted using a FastDNA Spin Kit (Qbiogene, USA) as specified by the

manufacturer. The quality of extracted DNA was checked by standard agarose gel electrophoresis and stored at -20ºC. The DNA concentration was determined using a UV-VIS Spectrophotometer (Mechasys Co. Ltd., Korea). 16S rRNA genes were amplified using forward and inverse primers to distinguish each sample prior to sequencing at Chun Laboratory (Kaown et al., 2014). Amplification condition for PCR was i) an initial denaturation step of 94°C or 5 min, ii) 30cycles of denaturation, and annealing (94°C for 30 sec followed by 55°C for 45 sec), and iii) an extension step at 72°C for 90 sec. Pyrosequencing was conducted using 454 Genome Sequence FLX Titanium Junior (Roche, NJ, USA) by Chun Laboratory (Seoul, South Korea). Distinct sequences have been deposited in the Sequence Read Archive (Chun Lab). The full sequences were analysed and compared with other known sequences that were available in the NCBI(National Center for Biotechnology Information) database. The NCBI web site can help to access to genomic information. The tools in the NCBI allow users to perform a BLAST (Basic

Local Alignment Search Tool) search for similar sequences in the GenBank.A search for sequence similarities with known genes was performed using a BLAST analysis. Identification of the conserved region and protein translations and analysis of amino acids were performed using BioEdit Sequence Alignment Editor (Ibis Biosciences, USA).

Bacterial communities of down welling point (PDHS4, ground water< surface water), mixed welling point(PMHS8, groundwater≒ surface water) and up welling point(PUHS20, groundwater> surface water) in the hyporheic zone were analyzed using a pyrosequencing assay. Total of 37,511 reads were analyzed in the three regions based on bacterial 16S rRNA partial gene (approximately 490 bp). Excluding reads where primer mismatch, non target, low quality, short length, chimera, matching or similarity of 80% or below with eukaryotes were observed, total of 20,242 reads (PMHS8 6,065 reads, PDHS4 7,603 reads and PUHS20 6,574 reads)were analyzed (Table 4-1).

4.2.3 Total bacterial communities

When the bacterial communities inhabiting the hyporheic zone were analyzed at the phylum-level, Proteobacteria phylum was dominant with 11,067 reads (55.1%), and Bacteroidetes phylum had 3,238 reads (16.5%), Actinobacteria phylum had 1,516 reads (7.1%), Acidobacteria phylum had 885 reads (3.9%), Firmicutes phylum had 685 reads (3.5%), Cyanobacteria phylum had 490 reads (2.3%), Chloroflexi phylum had 464 reads (2.2%), Planctomycetes phylum had 435 reads (2.1%), and unclassified phylum OD1 had 240 reads (1.2%). Other phylum [Gemmatimonadetes, Armatimonadetes, Verrucomicrobia, Nitrospirae, Elusimicrobia, Chlorobi, Fibrobacteres, Lentisphaerae, Fusobacteria, Deinococcus-Thermus and unclassified (TM7, GN02, TM6, OP11, OP3, MATCR, WS3, WS5, AD3 and SR1)] were identified to be lower than 1~0.05% (data below 0.05% not shown) (Table 4-1).

4.3 Results and Discussion

4.3.1 Down welling point(PDHS4)

In the down welling point which is largely affected by the surface water among the hyporheic zone, Proteobacteria phylum was dominant with 44.38%, followed by Actinobacteria (14.14%), Acidobacteria (10.75%), Chloroflexi (6.04%), Bacteroidetes (5.95%), Planctomycetes (5.55%), Firmicutes (1.93%), Gemmatimonadetes (1.82%), unclassified TM7 (1.33%), Armatimonadetes (1.18%) and Nitrospirae (1.09%). α-Proteobacteria class, δ-Proteobacteria class, Actinobacteria phylum and Acidobacteria phylum were observed to be relatively high in the down welling point distinctively compared to mixed welling point and up welling point(Table 4-1 and Fig. 4-1).

Table 4-1 Analysis of bacterial diversity in the hyporheic zone (phylum-level)

Phylum	% (number of reads)			Total reads	Ratio (%)
	PDHS4	PMHS8	PUHS20		
Proteobacteria*					
α-Proteobacteria	20.79 (1,581)	7.75 (470)	1.17 (77)	2,128	10.51
β-Proteobacteria	13.80 (1,049)	28.54 (1,731)	50.27 (3,305)	6,085	30.06
γ-Proteobacteria	6.62 (503)	12.91 (783)	14.25 (937)	2,223	10.98
δ-Proteobacteria	3.09 (235)	2.11 (128)	0.53 (35)	398	1.97
ε-Proteobacteria	0.08 (6)	3.12 (189)	0.58 (38)	233	1.15
Bacteroidetes	5.95 (452)	16.72 (1,020)	26.86 (1,766)	3,238	16.00
Actinobacteria	14.14 (1,075)	6.56 (400)	0.62 (41)	1,516	7.49
Acidobacteria	10.75 (817)	0.69 (42)	0.40 (26)	885	4.37
Firmicutes	1.93 (147)	6.29 (384)	2.34 (154)	685	3.38
Chloroflexi	6.04 (459)	0.36 (22)	0.14 (9)	490	2.42
Planctomycetes	5.55 (422)	0.49 (30)	0.18 (12)	464	2.29
Cyanobacteria	0.83 (63)	5.85 (357)	0.23 (15)	435	2.15
OD1†	0.83 (63)	2.18 (133)	0.67 (44)	240	1.19
TM7†	1.33 (101)	1.20 (73)	0.30 (20)	194	0.96
Gemmatimonadetes	1.82 (138)	0.15 (9)	0.08 (5)	152	0.75
Armatimonadetes	1.18 (90)	0.34 (21)	0.06 (4)	115	0.57

Nitrospirae	1.09 (83)	0.21 (13)	0.03 (2)	98	0.48
Verrucomicrobia	0.70 (53)	0.54 (33)	0.14 (9)	95	0.47
GN02†	0.33 (25)	0.49 (30)	0.26 (17)	72	0.36
TM6†	0.66 (50)	0.21 (13)	0.02 (1)	64	0.32
OP11†	0.54 (41)	0.16 (10)	0.05 (3)	54	0.27
OP3†	0.17 (13)	0.36 (22)	0.09 (6)	41	0.20
Elusimicrobia	0.11 (8)	0.38 (23)	0.18 (12)	43	0.21
Chlorobi	0.32 (24)	0.21 (13)	0.08 (5)	42	0.21
MATCR†	0.16 (12)	0.28 (17)	0.05 (3)	32	0.16
WS3†	0.34 (26)	0.03 (2)	0.00 (0)	28	0.14
Fibrobacteres	0.05 (4)	0.25 (15)	0.09 (6)	25	0.12
WS5†	0.08 (6)	0.18 (11)	0.06 (4)	21	0.10
Lentisphaerae	0.05 (6)	0.20 (12)	0.03 (2)	18	0.09
Fusobacteria	0.00 (0)	0.21 (13)	0.05 (3)	16	0.08
Deinococcus-Thermus	0.05 (4)	0.11 (7)	0.03 (2)	13	0.06
AD3†	0.16 (12)	0.00 (0)	0.00 (0)	12	0.06
SR1†	0.00 (0)	0.10 (6)	0.06 (4)	10	0.05
Synergistetes	0.00 (0)	0.11 (7)	0.00 (0)	7	0.03
Tenericutes	0.00 (0)	0.07 (4)	0.03 (2)	6	0.03
NKB19†	0.04 (3)	0.02 (1)	0.02 (1)	5	0.02

TDNP†	0.00 (0)	0.03 (2)	0.03 (2)	4	0.02
BRC1†	0.04 (3)	0.00 (0)	0.00 (0)	3	0.01
WS1†	0.03 (2)	0.00 (0)	0.00 (0)	2	0.01
GN04†	0.01 (1)	0.00 (0)	0.02 (1)	2	0.01
Spirochaetes	0.03 (2)	0.00 (0)	0.00 (0)	2	0.01
OMAN†	0.01 (1)	0.00 (0)	0.00 (0)	1	<0.01
10BAV†	0.01 (1)	0.00 (0)	0.00 (0)	1	<0.01
Unidentified	0.31 (24)	0.31 (19)	0.02 (1)	44	0.22
Total	7,603	6,065	6,574	20,242	100.00

*Total 11,067 reads (55.10%) were analyzed. Details are as follows; PDHS4 (44.38%, 3,374 reads), PMHS8 (54.11%, 3,301 reads) and PUHS20 (66.81%, 4,392 reads).

†Unclassified phylum.

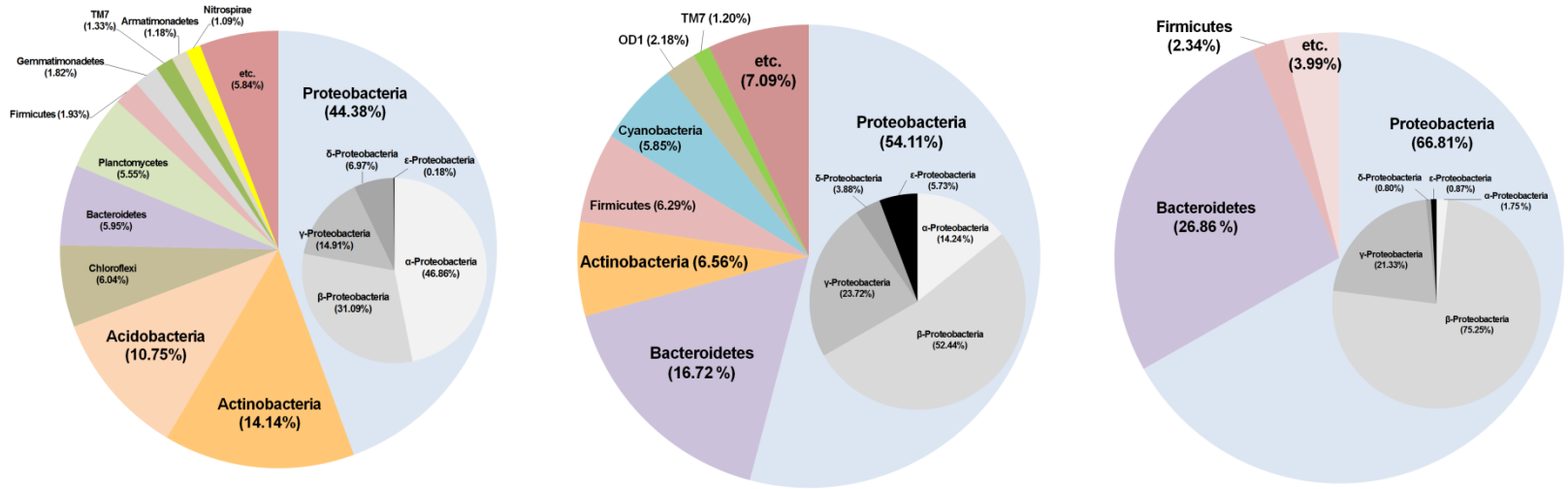

PDHS4 **PMHS8** **PUHS20**

Fig. 4-1 Regional bacterial diversity in the hyporheic zone (phylum-level)

4.3.2 Mixed welling point(PMHS8)

In the mixed welling point which is equally affected by groundwater and surface water, Proteobacteria phylum was dominant with 54.11%, followed by Bacteroidetes (16.72%), Bacteroidetes (6.56%), Firmicutes (6.29%), Cyanobacteria (5.85%), unclassified OD1 (2.18%), unclassified TM7 (1.2%) and others (7.09%). Mixed welling point showed dominance and percentage that are between those of down welling and up welling points, but Firmicutes phylum, Cyanobacteria phylum, and ε-Proteobacteria class were observed at relatively higher percentage compared to down welling and up welling points (Table 4- 1 and Fig. 4-1).

4.3.3 Up welling point(PUHS20)

In the up welling point, Proteobacteria phylum was dominant with 66.81%, followed by Bacteroidetes (26.86%), Firmicutes (2.34%) and others (3.99%). Sum of Proteobacteria and Bacteroidetes phylum accounted for

93.67% of the total in the up welling point, showing a characteristic of increasing dominance compared to down welling point and mixed welling pointwhile percentages of other phyla were observed to be low. Especially, Proteobacteria phylum (specifically β-Proteobacteria class) and Bacteroidetes phylum were observed to be high at 22.43% and 20.91%, respectively, compared to the down welling point while percentages of Actinobacteria, Acidobacteria, Chloroflexi, Planctomycetes, Gemmatimonadetes, Armatimonadetes, Verrucomicrobia, Nitrospirae, Chlorobi and unidentified phylum (TM7, TM6, OP11 and WS3) were observed to be low (Table 4-1 and Fig. 4-1).

4.3.4 Analysis of bacterial species diversity index

In order to analyze bacterial species diversity in the down welling point, mixed welling point and up welling point, operational taxonomic unit (OUTs)and biotic diversity index (ACE, Chao1, JackKnife, NPShannon and

Shannon)were analyzed. In the mixed welling point, only JackKnife index was low and the rest of the diversity indices were observed to be high. In the up welling point, all indices including OTUs were observed to be low. Thereby, its species richness and diversity were evaluated as low compared to the mixed welling point and down welling point. Therefore, bacterial species richness and diversity of the three regions were the highest in the order of mixed welling point > down welling point > up welling point (Table 4-2).

Table 4-2 Analysis of regional bacterial diversity in the hyporheic zone

Diversity index	**PDHS4**	**PMHS8**	**PUHS20**
OTUs*	3018	3126	2307
ACE	7938.0	8491.8	5676.6
Chao1	5886.3	5991.2	4151.7
JackKnife	9431.4	8771.2	5385.6
NPShannon	7.08	7.18	6.69
Shannon	6.901	7.019	6.524

*OTUs were defined as groups of sequences sharing 00%.

4.3.5 Detailed analysis of dominant bacteria in the down welling point

Actinobacteria phylum, Acidobacteria phylum, α-Proteobacteria class and δ-Proteobacteria class, which showed high percentage in the down welling point compared to up welling point were subjected to detailed analysis. Actinobacteria phylum was identified with higher percentage in the down welling point (1,075 reads, 14.14%) than the up welling point (41 reads, 0.62%). Detailed analysis of the down welling point (1,075 reads) showed that *Arthrobacter* genus was dominant with 367 reads (34.14%), and high percentage of *Gaiella* genus, *Streptomyces* genus and *Cryobacterium* genus were observed in the down welling point compared to the up welling point (Supplementary Table S1). Acidobacteria phylum was identified with relatively high percentage in the down welling point (817 reads, 10.75%) compared to the up welling point (26 reads, 0.40%). Detailed analysis of the down welling point (817 reads)showed that *Blastocatella* genus (132 reads)and *Koribacter* genus (86 reads) were dominant, and its difference with

the up welling point was analyzed (Supplementary Table S2). Also, α-Proteobacteria class had 1151 reads accounting for 46.86% among the Proteobacteria phylum in the down welling point, showing difference from 14.24% and 1.75% in the mixed welling point and up welling point, respectively. Among them, Rhizobiales order had 1006 reads showing dominance among α-Proteobacteria class, which was different from other regions (Supplementary Table S3). Detailed analysis of δ-Proteobacteria class showed 235 reads, which was relatively higher than those of the mixed welling point(128 reads)and up welling point(35 reads).Among them, Myxococcales order was dominant with 70 reads, showing difference with other regions (Supplementary Table S4).

4.3.6 Detailed analysis of dominant bacteria in the mixed welling point

Relatively high bacterial diversity was observed in the mixed welling point compared to the up welling and down welling points (Table 4-2).

Analysis of the bacteria phylum (or class)-level in the mixed welling points showed high percentages of Firmicutes, Cyanobacteria, ε-Proteobacteria, Elusimicrobia, Lentisphaerae, Fusobacteria, Deinococcus-Thermus, Synergistetes, Tenericutes and unclassified (OD1, GN02, OP3, MATCR and WS5)compared to the up welling point and down welling point (Table 1). Particularly, Firmicutes (6.29%), Cyanobacteria (5.85%), ε-Proteobacteria (3.12%) and unclassified OD1 (2.18%)showed higher percentages than the means of the down welling point and up welling point, which were 2.34%, 0.23%, 0.58% and 0.75%, respectively. Rest of the phyla showed percentages lower than 0.5% in the mixed welling point, but they were still relatively higher than those of the down welling or up welling point (Table 1).

Detailed analysis of Firmicutes phylum (384 reads) in the mixed welling point showed dominance of Firmicutes phylum with 160 reads (41.67%) of *Trichococcus* genus, and66 reads (17.19%) of *Clostridium* genus. *Clostridium*genus had 21 reads in the down welling point, but they were not

present in the up welling point. In the mixed welling point, *Acetivibrio*, *Acidaminobacter*, *Anaeromusa*, *Anaerosinus*, *Anaerosporobacter*, *Anaerostipes*, *Butyricicoccus*, *Carnobacterium*, *Coprococcus*, *Dendrosporobacter*, *Dialister*, *Fervidicella*, *Lactovum*, *Megamonas*, *Megasphaera*, *Oscillibacter*, *Phascolarctobacterium*, *Proteiniclasticum*, *Proteocatella*, *Pseudoflavonifractor*, *Ruminococcus*, *Saccharibacillus*, *Saccharofermentans*, *Sedimentibacter* and *Succinispira* genus were observed that were not present in the down welling point or up welling point. Additionally, *Bacillus*, *Virgibacillus*, *Alicyclobacillus*, *Tumebacillus*, *Anaerovorax*, *Paenisporosarcina*, *Dethiobacter*, *Sporosarcina*, *Dorea*, *Turicibacter*, *Planifilum*and *Coprococcus* genus were observed in the down welling point that were not present in the mixed welling point, and only *Arcobacter*, *Sulfurospirillum* and *Sulfuricurvum* genus were observed in the up welling point among Firmicutes phylum, showing differences with the mixed welling point (Supplementary Table S5). Detailed analysis of

Cyanobacteria phylum (357 reads) revealed 242 reads (67.79%) of *Prochlorococcus* genus, and *Limnococcus* (46 reads), *Chamaesiphon* (16 reads), *Pleurocapsa* (13 reads), *Snowella* (2 reads) and *Vampirovibrio* genus (1 read) that were not observed in the down welling point and up welling point (Supplementary Table S6). Detailed analysis of ε-Proteobacteria class (189 reads) revealed *Arcobacter* genus (128 reads, 67.72%), *Sulfurospirillum* genus (57 reads, 30.16%), *Sulfuricurvum* genus (2 reads, 1.06%) and unidentified ε-Proteobacteria (Campylobacterales order; 2 reads, 1.06%) (Supplementary Table S7).

4.3.7 Detailed analysis of dominant bacteria in the up welling point

Proteobacteria and Bacteroidetes phylum that exist at high percentage in the up welling point were analyzed in detail. Analysis of Proteobacteria phylum at the class-level revealed that α-Proteobacteria existed in the down welling point at 20.79%, which showed 19.62%

difference from 1.17% in the up welling point, and β-Proteobacteria existed in the down welling point at 13.80% and in the up welling point at 50.27%, showing 30.47% difference. Additionally, 7.63% difference was observed with γ-Proteobacteria in the down welling point (6.62%) and up welling point (14.25%), and 2.56% difference was observed with δ-Proteobacteria between the down welling point (3.09%) and up welling point (0.53%). These results showed differences in the bacterial diversity in the down welling point and up welling point within the hyporheic zone (Table 4-1). Detailed analysis of 3,305 reads of β-Proteobacteria that are dominant in the up welling point revealed 3,118 reads (94.34%) of Burkholderiales order (Supplementary Table S8). Among them, *Comamonas* genus was dramatically higher in the up welling point at 60.46% than in the down welling point (0.77% among Burkholderiales order), and the difference between *Malikia* genus [Down welling point(2.19%) and Up welling point(25.53%)] and *Acidovorax* genus [Down welling point(0.90%) and Up welling point(3.08%)] was also

observed (Supplementary Table S9).

Detailed analysis of Bacteroidetes phylum revealed the difference between the up welling point and down welling point in Flavobacteria class and Sphingobacteria class. Flavobacteria class was dominant in the up welling point at 1,645 reads among 1,766 reads of Bacteroidetes phylum, accounting for 93.15%, but it showed 52 reads (11.50%) in the down welling point among 425 reads of Bacteroidetes phylum, showing difference with the up welling point (Supplementary Table S3). Detailed analysis of 1.645 reads of Flavobacteria class showed the dominance of *Flavobacterium* genus at 1,456 reads (88.51%). Sphingobacteria class accounted for 372 reads (82.30%) among Bacteroidetes phylum in the down welling point but had only 56 reads in the up welling point, showing difference in the bacterial communities between the down welling and up welling points (Supplementary Table S10).

4.4 Conclusion

Bacterial community was evaluated in the Hyporheic zone depth calculated with the proposed method in chapter 2. Quantitative changes of the hyporheic zone were examined by installing a piezometer on the site, and a total of 20,242 reads were analyzed using a pyrosequencing assay to investigate the diversity of bacterial communities. Proteobacteria (55.1%) were overall dominant in the hyporheic zone, and Bacteroidetes (16.5%), Actinobacteria (7.1%) and other bacteria phylum (Firmicutes, Cyanobacteria, Chloroflexi, Planctomycetesm and unclassified phylum OD1) were identified. Also, the hyporheic zone was divided into 3 points – down welling point, mixed welling point and up welling point – through vertical hydraulic gradient, and the bacterial communities were compared and analyzed.

In the down welling point, α-Proteobacteria class, δ-Proteobacteria class, Actinobacteria phylum and Acidobacteria phylum were relatively high compared to mixed welling point and up welling point. *Arthrobacter* genus in

the Actinobacteria phylum, *Blastocatella* genus in the Acidobacteria class, Rhizobiales order in theα-Proteobacteria class, and Myxococcales order in the δ-Proteobacteria class were dominant, and the difference between mixed welling point and up welling point were observed. In the mixed welling point, Firmicutes phylum, Cyanobacteria phylum and ε-Proteobacteria class were identified with higher percentage compared to the down welling point and up welling point. *Trichococcus* genus in the Firmicutes phylum, *Prochlorococcus* genus in the Cyanobacteria phylum and *Arcobacter* genus in the ε-Proteobacteria class were dominant, and the difference between down welling point and up welling point was observed. In the mixed welling point, various species were identified that were not present in the up and down welling points.

In the up welling point, Proteobacteria and Bacteroidetes phylum were dominant, and the sum of two phyla was 93.67% indicating high dominance. Especially in β-Proteobacteria of Proteobacteria and

Flavobacteria class of Bacteroidetes, which showed far higher dominance compared to the down welling point and mixed welling point, *Comamonas* genus and *Flavobacterium* genus were identified with high percentage, respectively, showing differences between the down welling point and mixed welling point. When the species diversity index was additionally analyzed based on the pyrosequencing data, richness and diversity of species were observed to be highest in the order of mixed welling point >down welling point >up welling point. Hence, quantitative changes and characteristics of the hyporheic zone were analyzed to have an effect on the resident bacterial communities.

The composition of bacterial communities was influenced by the direction of the vertical component of hyporheic flux which was determined from the proposed method of delineating the hyporheic zone depth. The indexes of bacterial diversity such as OUT, ACE, Cho1, NPShannon and Shannon were low in the region where surface water or ground water were

dominant, respectively. However, the indexes were the highest for the sections influenced by both surface water and groundwater.

Supplementary Table S1 Detailed analysis of Actinobacteria genus

Genus	Number of reads		
	PDHS4	PMHS8	PUHS20
4P003540_g	2	0	0
AB021325_g	4	3	0
AB240334_g	3	0	0
AB245397_g	2	0	0
AB630582_g	17	0	0
AcI_B_g	0	1	0
Aciditerrimonas	1	0	0
Actinoallomurus	2	0	0
Actinomadura	1	0	0
Actinoplanes	4	6	0
Aeromicrobium	1	0	0
AF408985_g	1	0	0
AF498716_g	2	0	0
AJ507468_g	0	1	0
AJ863193_g	1	0	0
Alpinimonas	6	8	0
AM277063_g	1	1	0
AM991247_g	110	1	1
Amnibacterium	1	0	0
Angustibacter	2	0	0
Aquiluna	2	29	2
Arthrobacter	367	15	4
Asanoa	1	0	0
AY234624_g	0	0	1
Brooklawnia	2	0	0
Cellulomonas	0	1	0

Chryseoglobus	0	1	0
Collinsella	0	0	2
Conexibacter	7	0	0
Corynebacterium	0	1	0
Cryobacterium	25	0	0
Demequina	0	0	1
DQ125551_g	2	0	1
EF016795_g	1	0	0
EF018137_g	0	1	0
EF516392_g	1	1	0
EF516411_g	1	0	0
EF516773_g	1	0	1
EF520360_g	2	0	0
EF584530_g	0	0	1
EF632905_g	10	0	0
EU289467_g	1	0	0
EU335168_g	1	0	0
EU374107_g	0	1	0
EU801210_g	2	5	0
EU861899_g	14	0	0
EU861937_g	3	0	0
EU980607_g	2	0	0
FJ478790_g	1	0	0
FJ478799_g	25	0	2
FM209069_g	3	0	1
FM886842_g	1	0	1
FN436189_g	1	0	0
FN554394_g	5	0	0
FN687458_g	6	0	0

FN811204_g	10	0	0
Friedmanniella	1	0	0
Frigoribacterium	0	1	0
Gaiella	95	5	1
Gordonibacter	0	2	0
GQ387490_g	34	26	0
GQ396807_g	4	1	0
GQ396959_g	2	0	1
GQ487899_g	3	0	0
GU305765_g	13	0	1
Herbiconiux	0	1	0
HM445971_g	0	4	0
HM748665_g	6	0	0
HQ674860_g	1	1	0
HQ864103_g	0	1	0
HQ910322_g	1	0	0
Humibacillus	1	0	0
Ilumatobacter	6	0	0
Jatrophihabitans	8	0	0
JN588609_g	2	0	0
Kitasatospora	11	1	0
Knoellia	1	0	0
Leifsonia	0	0	2
Leucobacter	0	1	0
Longispora	1	0	0
Lysinimonas	1	0	0
Marmoricola	1	0	0
Microbacterium	9	5	0
Micrococcus	0	1	0

Microlunatus	2	0	0
Micromonospora	2	1	0
Microterricola	3	1	0
Mycobacterium	21	0	4
Nakamurella	9	0	0
Nocardia	2	0	0
Nocardioides	24	5	0
Nocardiopsis	1	0	0
Nonomuraea	2	0	0
Oryzihumus	27	1	0
Phycicoccus	20	0	0
Planktoluna	2	6	0
Planktophila	12	208	7
Propioniciclava	2	2	2
Propionicimonas	3	1	2
Rhodococcus	6	1	0
Rhodoluna	9	43	2
Saccharomonospora	1	0	0
Salinibacterium	2	1	0
Sanguibacter	0	2	0
Sinomonas	1	0	0
Streptomyces	44	0	0
Streptosporangium	1	0	0
Terrabacter	14	0	0
Tetrasphaera	5	2	1
Tropheryma	1	0	0
Total	**1,075**	**400**	**41**

Supplementary Table S2 Detailed analysis ofAcidobacteria genus

Genus	Number of reads		
	PDHS4	PMHS8	PUHS20
AB179509_g	2	0	0
AB240310_g	5	0	0
AB252946_g	5	0	0
AB355055_g	9	0	0
Acidobacterium	4	0	0
AF234701_g	3	0	0
AM180888_g	7	0	0
AY212581_g	1	0	0
AY281358_g	52	0	0
AY921986_g	1	0	0
Blastocatella	132	6	0
Bryobacter	2	0	0
DQ083303_g	0	1	0
DQ139454_g	1	0	0
DQ451510_g	5	0	0
DQ453805_g	15	0	0
DQ648914_g	8	0	0
DQ829648_g	4	0	0
DQ833485_g	4	0	0
DQ906882_g	1	0	0
Edaphobacter	2	0	0
EF492943_g	1	0	0
EF999370_g	0	1	0
EU192989_g	4	0	0
EU335275_g	15	1	0
EU373937_g	1	0	0

EU445199_g	11	0	0
EU652507_g	4	0	0
EU676413_g	1	0	0
EU686607_g	16	0	0
EU861837_g	1	0	0
EU881271_g	1	0	0
FJ416115_g	2	0	0
FJ478829_g	5	0	0
FJ478953_g	7	0	0
FJ479026_g	8	0	0
FJ479597_g	2	0	0
GQ214092_g	1	0	0
GQ302594_g	2	0	1
GQ472805_g	7	0	1
Granulicella	3	0	0
GU127807_g	1	0	0
GU187031_g	64	3	3
GU187034_g	1	0	0
GU260705_g	79	5	2
GU727715_g	1	0	0
HM061812_g	8	1	0
HM131972_g	3	0	0
HM243779_g	2	0	0
HM243842_g	2	0	0
HM445331_g	29	3	0
HM748715_g	1	0	0
Holophaga	6	6	7
HQ010775_g	3	0	0
HQ166644_g	1	0	0

HQ190378_g	2	0	0
HQ190410_g	19	5	2
HQ190481_g	6	0	0
HQ445629_g	2	0	0
HQ445649_g	3	0	0
HQ445680_g	7	4	1
HQ445759_g	0	1	1
HQ645210_g	9	0	0
HQ864177_g	8	0	0
JF429092_g	1	0	0
JF718667_g	8	0	0
Koribacter	86	0	3
Solibacter	28	0	0
Telmatobacter	2	0	0
Z95718_g	6	0	0
Z95727_g	73	5	5
Z95729_g	1	0	0
Total	**817**	**42**	**26**

Supplementary Table S3 Detailed analysis of α-Proteobacteria order

Order	% (number of reads)		
	PDHS4	**PMHS8**	**PUHS20**
AY957891_o	0.13 (2)	0.42 (2)	0 (0)
Caulobacterales	2.97 (47)	4.68 (22)	3.9 (3)
EF573150_o	0.32 (5)	0.42 (2)	0 (0)
FJ612212_o	0 (0)	0.21 (1)	0 (0)
Kordiimonadales	0 (0)	0.21 (1)	1.3 (1)
Micavibrio_o	0.13 (2)	2.13 (10)	1.3 (1)
Parvularculales	0.06 (1)	0 (0)	0 (0)
Rhizobiales	63.63 (1006)	21.49 (101)	29.87 (23)
Rhodobacterales	8.41 (133)	17.03 (80)	27.28 (21)
Rhodospirillales	10.50 (166)	10.64 (50)	6.49 (5)
Rickettsiales	1.58 (25)	12.77 (60)	9.09 (7)
Sphingomonadales	12.27 (194)	30 (141)	20.77 (16)
Total	**1,581**	**470**	**77**

Supplementary Table S4 Detailed analysis of δ-Proteobacteria order

Order	% (number of reads)		
	PDHS4	**PMHS8**	**PUHS20**
AF269002_o	1.28 (3)	0.00 (0)	0.00 (0)
AY921748_o	0.00 (0)	0.78 (1)	0.00 (0)
Bdellovibrionales	2.13 (5)	10.16 (13)	5.71 (2)
CU925466_o	15.33 (36)	6.25 (8)	8.57 (3)
Deferrisoma_o	0.42 (1)	0.00 (0)	0.00 (0)
Desulfobacca_o	0.00 (0)	0.00 (0)	2.85 (1)
Desulfobacterales	0.85 (2)	0.78 (1)	0.00 (0)
Desulfobulbaceae_o	0.00 (0)	0.78 (1)	0.00 (0)
Desulfovibrionales	0.00 (0)	3.91 (5)	2.85 (1)
Desulfuromonadales	5.11 (12)	3.91 (5)	2.85 (1)
EF574244_o	0.85 (2)	0.78 (1)	0.00 (0)
EU335163_o	0.42 (1)	0.00 (0)	0.00 (0)
EU617842_o	0.85 (2)	0.00 (0)	0.00 (0)
EU861868_o	1.28 (3)	5.47 (7)	0.00 (0)
FJ889281_o	7.66 (18)	21.09 (27)	51.45 (18)
FM253572_o	23.84 (56)	2.34 (3)	0.00 (0)
GU567808_o	0.42 (1)	2.34 (3)	0.00 (0)
HM243977_o	0.42 (1)	0.78 (1)	0.00 (0)
Myxococcales	29.79 (70)	21.88 (28)	8.57 (3)
OM27	0.42 (1)	0.78 (1)	2.85 (1)
SAR324	0.00 (0)	0.78 (1)	0.00 (0)
Spirobacillus_o	8.09 (19)	17.19 (22)	14.3 (5)
Syntrophobacterales	0.42 (1)	0.00 (0)	0.00 (0)
Syntrophorhabdaceae_o	0.42 (1)	0.00 (0)	0.00 (0)
Total	**235**	**128**	**35**

Supplementary Table S5 Detailed analysis of Firmicutes genus

Genus	Number of reads		
	PDHS4	PMHS8	PUHS20
AB237727_g	0	1	0
Acetivibrio	0	1	0
Acidaminobacter	0	3	0
AF304435_g	0	2	0
AM183112_g	0	1	0
AM406061_g	0	2	0
AM500748_g	0	3	0
Anaeromusa	0	1	0
Anaerosinus	0	1	0
Anaerosporobacter	0	2	0
Anaerostipes	0	3	0
AY532583_g	0	1	0
Blautia	3	2	0
Butyricicoccus	0	1	0
Carnobacterium	0	2	0
Clostridium	11	53	0
Clostridium_g22	0	3	0
Clostridium_g25	0	2	0
Clostridium_g4	10	6	0
Clostridium_g7	0	1	0
Clostridium_g9	0	1	0
Coprococcus_g2	0	1	0
D16279_g	0	1	0
Dendrosporobacter	0	1	0
Dialister	0	1	0
DQ071484_g	1	3	0

DQ206415_g	0	1	0
DQ777915_g	0	1	0
EF403870_g	1	1	0
EF404752_g	0	1	0
EU753611_g	0	1	0
EU845632_g	0	4	0
Eubacterium_g2	2	2	0
Exiguobacterium	5	4	0
Faecalibacterium	1	4	0
Fervidicella	0	2	0
FJ799146_g	0	1	0
FJ880290_g	0	2	0
GQ406188_g	0	3	0
GQ871709_g	1	1	0
GU112184_g	0	2	0
GU324404_g	1	1	0
GU454868_g	0	1	0
HM123979_g	0	1	0
HQ132444_g	0	1	0
HQ904156_g	0	2	0
Lactobacillus	2	6	0
Lactococcus	3	12	0
Lactovum	0	1	0
Leuconostoc	1	7	0
Megamonas	0	7	0
Megasphaera	0	1	0
Oscillibacter	0	2	0
Paenibacillus	12	2	0
Phascolarctobacterium	0	1	0

Propionispira	1	7	0
Proteiniclasticum	0	11	0
Proteocatella	0	7	0
Pseudoflavonifractor	0	1	0
Psychrobacillus	1	5	0
Psychrosinus	2	1	0
Ruminococcus	0	1	0
Ruminococcus_g2	0	3	0
Ruminococcus_g5	0	3	0
Saccharibacillus	0	1	0
Saccharofermentans	0	2	0
Sedimentibacter	0	1	0
Streptococcus	1	3	0
Subdoligranulum	1	1	0
Succinispira	0	2	0
Trichococcus	12	160	0
Ureibacillus	1	1	0
Dethiobacter	1	0	0
EF558947_g	1	0	0
GQ480002_g	1	0	0
HQ660796_g	1	0	0
AF050591_g	1	0	0
Bacillus	27	0	0
EF404788_g	1	0	0
Virgibacillus	1	0	0
Alicyclobacillus	1	0	0
Tumebacillus	3	0	0
AB239481_g	2	0	0
Anaerovorax	1	0	0

Paenisporosarcina	13	0	0
Eubacterium_g5	2	0	0
Eubacterium_g8	2	0	0
Sporosarcina	1	0	0
DQ394658_g	1	0	0
Dorea	1	0	0
Turicibacter	1	0	0
HQ716403_g	1	0	0
AB298726_g	1	0	0
DQ887956_g	1	0	0
Planifilum	1	0	0
Coprococcus	2	0	0
AM500798_g	1	0	0
AM277340_g	2	0	0
GQ897654_g	3	0	0
Sulfuricurvum	0	0	1
Arcobacter	0	0	34
Sulfurospirillum	0	0	3
Total	**147**	**384**	**38**

Supplementary Table S6 Detailed analysis of Cyanobacteria genus

Genus	Number of reads		
	PDHS4	PMHS8	PUHS20
AB240501_g	0	1	1
AB354619_g	0	1	2
AJ536844_g	0	1	0
AJ583204_g	0	1	0
AY375144_g	0	5	3
Chamaesiphon	0	16	0
Chroococcus_g2	0	1	0
DQ128639_g	1	1	2
EF032660_g	0	2	0
EF580987_g	0	1	0
EU101276_g	0	3	0
EU491779_g	0	1	0
FJ236035_g	0	1	0
FJ425638_g	0	1	0
FJ625338_g	1	1	0
GQ451200_g	0	2	2
HM124232_g	0	1	0
JF733399_g	0	2	0
Limnococcus	0	46	0
Limnothrix	0	3	1
Merismopedia	0	3	0
Microcystis	0	3	0
PCC7335_g	0	1	0
Phormidium_g6	0	1	0
Pleurocapsa	0	13	0
Prochlorococcus	28	242	3

Snowella	0	2	0
Vampirovibrio	0	1	0
FJ543055_g	1	0	0
GU444060_g	5	0	0
EU134274_g	1	0	0
AY493962_g	4	0	0
EU753634_g	5	0	0
AJ544083_g	2	0	0
JF417809_g	1	0	0
Woronichinia	2	0	0
Nostoc_g1	1	0	0
Anabaena_g2	1	0	0
EF018129_g	2	0	0
Nostoc	2	0	0
JF737898_g	4	0	0
Microcoleus	1	0	0
Cylindrospermum	1	0	0
FJ810552_g	0	0	1
Total	**63**	**357**	**15**

Supplementary Table S7 Detailed analysis of ε-Proteobacteria genus

Genus	Number of reads		
	PDHS4	**PMHS8**	**PUHS20**
Arcobacter	4	128	34
Sulfurospirillum	1	57	3
JF747790_g	0	2	0
Sulfuricurvum	1	2	1
Total	**6**	**189**	**38**

Supplementary Table S8 Detailed analysis of β-Proteobacteria genus

Genus	% (number of reads)		
	PDHS4	**PMHS8**	**PUHS20**
AB294329_o	0.09 (1)	0.00 (0)	0.00 (0)
AB308366_o	7.05 (74)	0.35 (6)	0.15 (5)
Burkholderiales	74.0 (776)	83.42 (1,444)	94.34 (3,118)
DQ009366_o	1.33 (14)	0.17 (3)	0.03 (1)
DQ395705_o	4.1 (43)	0.46 (8)	0.06 (2)
DQ469205_o	0.00 (0)	0.06 (1)	0.03 (1)
EU786132_o	4.39 (46)	0.4 (7)	0.15 (5)
Ferritrophicales	0.00 (0)	0.06 (1)	0.00 (0)
Gallionellales	1.53 (16)	0.29 (5)	0.00 (0)
Methylophilales	2.76 (29)	1.33 (23)	0.06 (2)
Neisseriales	1.04 (11)	5.03 (87)	2.23 (74)
Nitrosomonadales	0.57 (6)	0.00 (0)	0.00 (0)
Rhodocyclales	1.14 (12)	4.16 (72)	1.42 (47)
Sterolibacterium_o	1.71 (18)	1.5 (26)	0.94 (31)
Thiobacillus_o	0.00 (0)	0.06 (1)	0.00 (0)
Thiobacter_o	0.09 (1)	0.12 (2)	0.00 (0)
Zoogloea_o	0.19 (2)	2.59 (45)	0.57 (19)
Total	1,049	1,731	3,305

Supplementary Table S9 Detailed analysis of Burkholderiales order

Order	Number of reads		
	PDHS4	PMHS8	PUHS20
4P000609_g	1	1	5
4P002413_g	0	2	0
4P003243_g	0	2	0
AB076847_g	2	1	1
AB240255_g	49	0	0
AB672287_g	9	1	0
Acidovorax	7	49	96
Actimicrobium	3	3	0
AF236011_g	0	2	2
AF289156_g	0	5	0
AF418942_g	13	33	11
AJ565430_g	0	7	8
AJ575697_g	2	2	1
AJ863277_g	13	7	4
Albidiferax	11	25	28
AM777983_g	55	5	0
Aquabacterium	4	17	17
Aquincola	4	0	1
AY218568_g	6	7	19
AY234747_g	182	1	0
AY328716_g	0	2	0
Azohydromonas	1	0	0
Bordetella	0	2	0
Brachymonas	0	4	0
Burkholderia	18	0	1
Caenimonas	10	1	0

Collimonas	0	1	0
Comamonas	6	322	1885
Cupriavidus	4	1	0
Curvibacter	6	35	9
Delftia	0	1	0
Derxia	0	0	4
DQ450176_g	0	4	0
DQ469209_g	0	1	0
DQ520167_g	6	7	1
Duganella	5	43	5
EF580985_g	1	1	8
EU104128_g	0	2	4
EU636042_g	28	2	1
EU735703_g	1	1	0
EU800906_g	0	1	0
EU801607_g	5	2	0
EU937973_g	8	3	3
FJ517712_g	9	8	4
FJ624877_g	2	0	1
FJ660572_g	0	4	5
FJ755754_g	1	3	0
FM209333_g	0	6	0
FN668029_g	0	4	1
Giesbergeria	2	3	8
GU134931_g	1	11	0
Herbaspirillum	47	6	2
Herminiimonas	29	2	0
HM445266_g	2	0	0
HQ166641_g	7	0	0

HQ178927_g	6	1	0
HQ324854_g	1	2	1
HQ910358_g	1	0	0
Hydrogenophaga	7	19	20
Ideonella	9	23	4
Inhella	1	3	0
Janthinobacterium	12	30	25
JF697503_g	1	3	1
JN679217_g	4	16	1
Kinneretia	1	1	0
Leptothrix	8	24	11
Limnobacter	0	2	0
Limnohabitans	11	108	2
Malikia	17	331	796
Massilia	21	18	8
Methylibium	1	3	0
Mitsuaria	0	0	1
Oxalobacter	0	1	0
Pandoraea	0	1	0
Paucibacter	2	12	8
Pelomonas	0	5	4
Piscinibacter	2	0	1
Polaromonas	38	12	7
Polyangium_g1	1	0	0
Polynucleobacter	9	86	5
Pseudoduganella	0	0	2
Pseudorhodoferax	2	3	17
Ralstonia	2	5	0
Ramlibacter	7	1	2

Rhizobacter	9	10	2
Rhodoferax	5	10	10
Rivibacter	1	1	0
Simplicispira	4	5	2
Sphaerotilus	4	14	2
Sutterella	0	2	0
Undibacterium	5	24	45
Variovorax	5	1	2
Xenophilus	19	12	0
Z93984_g	0	2	4
Total	1,049	1,731	3,305

Supplementary Table S10 Detailed analysis of *Bacteroidetes* genus

Genus	% (number of reads)		
	PDHS4	**PMHS8**	**PUHS20**
Bacteroidia	1.33 (6)	31.96 (326)	3.4 (60)
Cytophagia	4.87 (22)	6.18 (63)	0.28 (5)
Flavobacteria	11.5 (52)	36.76 (375)	93.15 (1,645)
Sphingobacteria	82.3 (372)	25.1 (256)	3.17 (56)
Total	**452**	**1,020**	**1,766**

This page intentionally left blank

CHAPTER 5. VERIFICATION USING CHEMICAL APPROACH

5.1 Introduction

The mixing of groundwater and contaminated stream water in the hyporheic zone has been found to have a negative impact on the groundwater vulnerable to contamination (Hancock 2002). Hydrogeological properties of the hyporheic zone are affected by the nutrients, organic materials, compositions of sediments, relief of stream bed and porosity (Boulton et al.

1998). An increase in the porosity of a stream bottom causes a volumetric increase of the mixing zone (Fuss and Smock 1996). Many studies have demonstrated the importance of the direction of hydrological exchange on the chemistry of the hyporheic water (Marmonier and Dole 1986; Sterba et al. 1992; Cooling and Boulton 1993; White 1993; Boulton et al. 1998). It also has been suggested that the hyporheic water chemistry is a key factor understanding the hyporheic zone hydrology (Boulton 1993). The hyporheic water quality is largely regulated by the hydrological conditions of the stream water and groundwater interactions, and their relative contributions (Fraser and William 1997; Malcolm et al. 2003, 2004).

Studying the hydrological processes (groundwater up-welling and stream water down-welling) in the hyporheic zone is very valuable, but needs to integrate the various chemical analysis and physical measurement studies for characterization of the hyporheic zone. The chemistry of the hyporheic zone may be controlled by a combination of different processes, including the

stream water down-welling, groundwater up-welling, and mixed welling. The chemical compositions of the hyporheic water reflect the history related to the recharge and discharge of the waters. In various stages of the path and circulation history, solutes dissolve or exchange through the interactions between the groundwater and stream water. Generally, solutes are more enriched in groundwater than stream water due to the longer residence time of the groundwater. Therefore, a mixing history between groundwater and stream water can be evaluated using chemical compositions of the hyporheic water.

In this chapter, chemical compositions of groundwater, stream water, paddy water and hyporheic water identified using temperature analysis were examined, and mixing and exchange of groundwater and stream water were evaluated using their chemistries and the multivariate statistical analyses for the chemical data.

5.2 Methods and materials

5.2.1 Water sampling and analysis

Quantitative samples of hyporheic water are difficult to obtain. The pump sampler was deemed appropriate in the site since each stream had similar substrate composition and land use. This method also causes little disturbance to physical integrity of hyporheic zone and provides samples for water chemistry at the points where different hyporheic exchange occurs.

The collected samples were transferred to bottles and returned to the laboratory and analyzed for major cations and anions constituents. 100 ml water samples were transferred in acid-washed polypropylene bottles for chemical analysis of cations (Ca^{2+}, K^{+}, Mg^{2+}, Na^{+}, and Si^{4+}) and anions (Cl^{-}, NO_3^{-} and SO_4^{2-}) after filtering through 0.45 μm membrane filters. Alkalinity, expressed as bicarbonate, was quantified with a digital auto-titrator with 0.05 N HCl, and methyl orange as an indicator. Sodium, potassium, calcium, magnesium and silica concentrations were determined by inductively coupled

plasma atomic emission spectrometry (ICP-OES/ iCAP 6500 Duo; SPECTRO, USA). Anions including sulfate, chloride and nitrate were analyzed by ion chromatography (761 Compact IC, Metrohm AG, Switzerland) at the Analytical Center for Science Research (ACSR) in Korea. The reliability of chemical analyses was estimated by the calculation of charge imbalance between cations and anions, which was better than ±10% for all samples.

The $\delta^{15}N$ and $\delta^{18}O$ values of dissolved nitrate were analyzed in the Isotope Science Laboratory at the University of Calgary (Alberta, Canada) using the denitrifier method (Casciotti et al., 2002). The N and O isotope ratios were measured on the produced N_2O using a Finnigan MAT delta plus XL isotope ratio mass spectrometer. The isotope ratios were normalized using international and internal laboratory standards. $\delta^{15}N\text{-}NO_3$ values are reported in the usual delta notation as per mil relative to AIR with an analytical

precision of ±0.3‰ and $\delta^{18}O\text{-}NO_3$ values are referenced to V-SMOW (Vienna Standard Mean Oceanic Water) with an uncertainty of ±0.5‰.

5.2.2 Estimation of hydrologic exchange

The ambient vertical hydraulic gradient between groundwater and stream water was recorded using piezometer. The vertical hydraulic gradient during the seepage measurements was calculated using the data from potentiomanometer. Also, direction and magnitude of hydrologic interaction were evaluated at the two sites using piezometer transects. Each piezometer was made up of 2 inch (internal diameter) PVC (polyvinyl chloride) pipe.

At each transect, a total of 20 piezometers were inserted at 0.1 m depth (this depth is calculated in chapter 3) beneath the streambed adjacent to each seepage meter installation point with a regular interval (Fig. 5-1). The head was measured relative to the stream water surface and vertical hydraulic gradient was determined by dividing Δh by the piezometer insertion depth.

$$VHG = \frac{\Delta h}{\Delta l} \tag{8}$$

where Δh is the difference in water levels of the piezometers and stream water, Δl is the difference in depths between streambed and the point where the piezometers are installed. However, head differences were often very small in the coarse-grained streambeds and thus, three to five observations were averaged to obtain Δh at both sites. The positive and negative vertical hydraulic gradients indicate up welling and down welling conditions of the hyporheic zone, respectively.

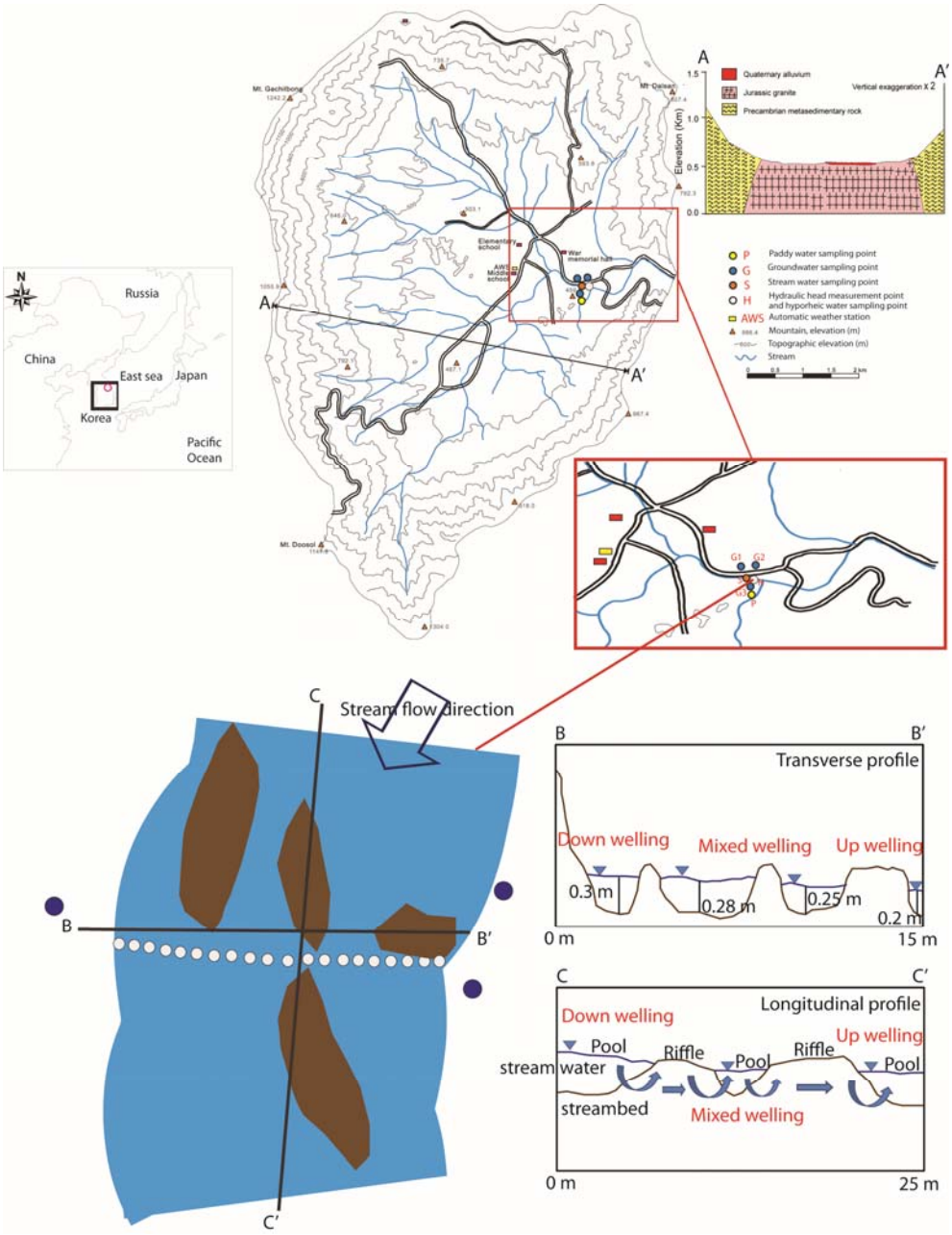

Fig. 5-1 Hyporheic water sampling points

5.2.3 Data Treatment and Multivariate Analysis

Multivariate analyses using FA and CA techniques for the groundwater, stream water, and hyporheic water data sets were performed to determine the underlying processes of the water chemistry (Lee et al., 2001, 2009; Reghunath et al., 2002; Panda et al., 2006; Kim et al., 2009, 2013b). A principal component provides information on the most meaningful parameters that describe the whole data set, allowing data reduction with minimum loss of original information. A factor analysis further reduces the contribution of less significant variables.

CA, which is an unsupervised pattern recognition technique, reveals the intrinsic structure of a data set without making a prior assumption about the data to classify objects in the system into categories or clusters based on their nearness or similarity (Daughney and Reeves, 2006). The Euclidean distance usually indicates similarities between two samples, and a distance

can be represented by the difference between analytical values from both samples.

Prior to any statistical analysis in this study, the experimental data were standardized through a z-transformation to avoid misinterpretation due to wide differences in data dimensionality (Omo-Irabor et al., 2008). First, a Pearson correlation analysis was performed between the measured chemical parameters to identify possible relationships. Then, a factor analysis of the physicochemical data was undertaken to quantify the contributions of anthropogenic inputs and natural weathering processes to the chemical composition of groundwater and stream water. The factor analysis technique extracts the Eigenvalues from the co-variance matrix of original variables. The variables for FA and CA were T, EC, ORP, DO, pH, Ca, K, Mg, Na, Si, Cl, NO_3, SO_4, and HCO_3. The calculation was performed using SPSS.18.

5.3 Results and discussion

5.3.1 Groundwater and stream water chemistry with its spatial and temporal variations

Box and whisker plots of selected field parameters (temperature, EC, ORP, DO, and pH) showing temporal and spatial trends are shown in Fig.5.2. The average stream water temperature was higher in August, June, and September than in November and April. However, the groundwater temperature was almost constant for all seasons. The EC levels of stream water varied less in August 2011 than in June 2012. However, the variation in EC levels followed an inverse pattern in groundwater. Precipitation had a large effect on the EC of stream water but a small effect on the EC of groundwater. The average ORP in stream water is higher in August 2011 and September 2012, than in June 2012. The average ORP in groundwater was constant by season. However, there was wide variation of groundwater ORP in April 2012 as compared to August and November 2011, and June and

September 2012. The DO of groundwater was constant; however, the DO of stream water followed a seasonal pattern. The inverse relationship between DO and temperature is a natural process (Knights et al., 1995). The DO of stream water was higher in November 2011 than in August 2011 and April, June, and September 2012. However, the temperature results in April 2012 were similar to those in November 2011. This similarity might have been due to a severe drought in 2012. The pH of groundwater and stream water was constant throughout the seasons. The major ions in water samples in different seasons are plotted on a piper diagram (Fig. 5-3). The water samples mainly plot in the area of the Ca-HCO3 water type and partly in the Ca-Cl type. The Ca-Cl type found in August and November 2011 was considered to indicate pollution by anthropogenic inputs, whereas the Ca-HCO3 type represented relatively clean water (Prasanna et al., 2011).

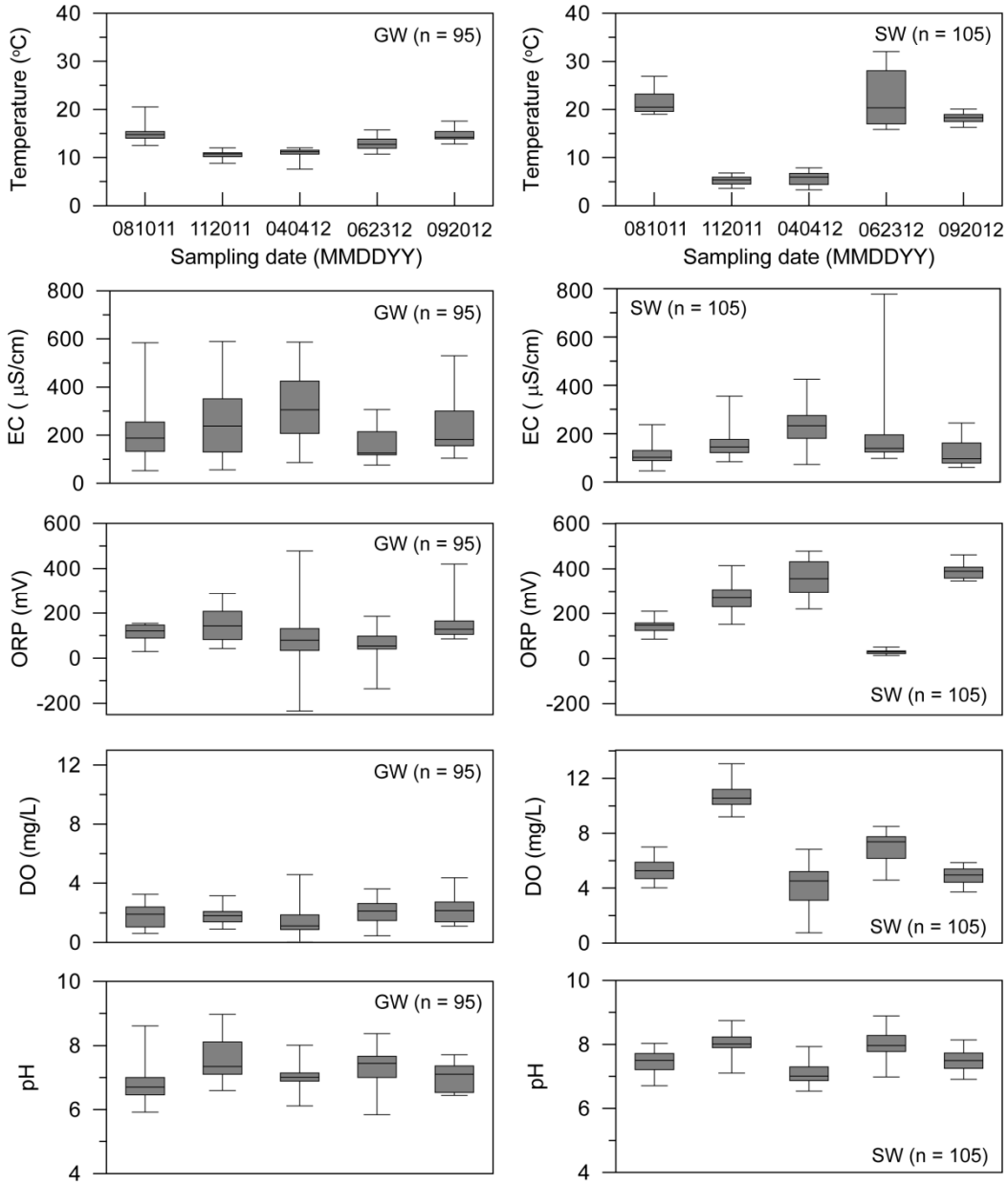

Fig. 5-2 Spatial and temporal variations in temperature, EC, ORP, DO, and pH in stream water and groundwater in the Haean basin

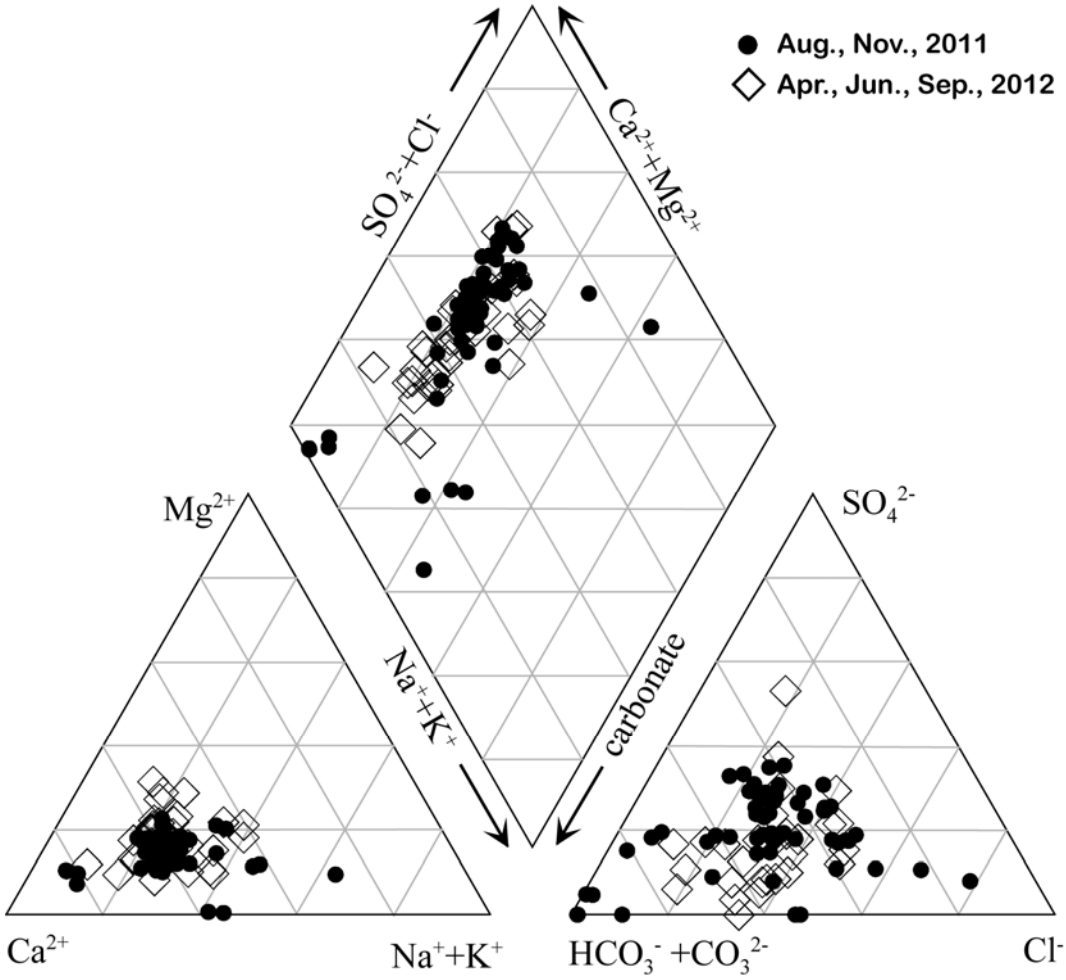

Fig. 5-3 Piper plot showing the major chemical composition of water samples

The basic statistics for all of the groundwater and stream water quality parameters measured during the 2-year sampling period at 20 groundwater sampling sites and 22 stream water sampling sites in an agricultural area of the Haean basin are summarized in Table 5-1. The groundwater was enriched in NO_3 and SO_4 as anions and Ca, K, and Mg as cations, which is typical of water contaminated by chemical fertilizers [$(NH_4)_2SO_4$, K_3PO_4, and (Ca, Mg)CO_3]. The levels of the five ions in groundwater were more variable than those in stream water (see the coefficients of variation). Ca and K ions in the groundwater were the most variable of the five ions. The mean nitrate concentrations were below the maximum acceptable level according to Korean water quality standards (44 mg/L NO3). However, 18% of all groundwater samples (HG5, HG11, HG16, HG17, and HG19 in August 2011; HG5, HG8, and HG17 in April 2012; HG3, HG5, and HG11 in June 2012; HG18 and HG19 in September 2012) exhibited concentrations exceeding the maximum acceptable level.

Furthermore, 38% of the groundwater samples contaminated by nitrate were collected during the heavy monsoon season in August 2011, 23% in the pre-monsoon season in April and June, and 15% after the monsoon season in September 2012. Soil conditions can enhance or retard nitrate leaching (Alhajjar et al., 1990). Leaching can also be enhanced by flood irrigation practices and by storm water (Domagalski and Dubrovsky, 1992). Among the stream water samples, 80% (HS8 in August 2011, HS3, HS5, HS6, and HS8 in April, and HS5 in September 2012) exceeded nitrate quality standards. Furthermore, 68% of stream water samples were contaminated in the pre-monsoon season in April 2012.

Table 5-1 Statistical summary of the measured parameters and major chemical constituents from 71 stream water and 72 groundwater samples

Parameter	Source	Minimum	Maximum	Mean	Median	S.D	C.V
T	S	3.3	28.2	13.9	16.9	7.6	0.5
	G	7.4	20.5	13.2	13.6	2.3	0.2
EC	S	45.8	425.0	150.7	130.0	74.0	0.5
	G	56.3	2999.0	291.0	182.0	398.5	1.4
ORP	S	21.0	479.0	262.0	264.0	138.3	0.5
	G	-136.1	478.0	126.5	114.0	90.4	0.7
DO	S	0.8	13.1	6.5	5.5	2.8	0.4
	G	0.1	9.1	2.2	2.0	1.5	0.7
pH	S	6.6	8.7	7.7	7.7	0.5	0.1
	G	5.8	9.0	7.1	7.1	0.6	0.1
Ca	S	3.4	42.2	14.7	13.1	7.2	0.5
	G	4.1	273.5	32.0	20.6	46.6	1.5
K	S	0.0	13.3	1.8	1.2	2.1	1.1
	G	0.0	20.2	1.8	1.1	2.6	1.5
Mg	S	0.8	10.3	2.7	2.3	1.7	0.6
	G	0.1	28.3	4.2	3.1	4.5	1.1
Na	S	2.8	44.4	6.7	5.1	6.7	1.0
	G	4.8	52.0	10.3	8.2	6.4	0.6
Si	S	1.7	10.5	6.7	6.4	1.8	0.3
	G	4.3	40.5	11.9	10.4	7.2	0.6
Cl	S	1.3	106.0	10.4	6.9	14.5	1.4
	G	0.6	59.0	10.0	8.8	9.4	0.9
NO_3	S	0.1	76.1	21.9	16.8	15.8	0.7
	G	0.0	134.9	23.9	17.6	24.5	1.0
SO_4	S	2.0	37.3	7.6	6.1	5.5	0.7
	G	0.0	52.4	6.6	5.2	7.2	1.1
HCO_3	S	4.3	35.6	14.5	12.8	6.2	0.4
	G	9.6	411.1	44.1	26.0	73.1	1.7

S, G, S.D, and C.V. are the stream water, groundwater, standard deviation, and coefficient of variation, respectively. T, EC, ORP, and DO are the temperature, electric conductivity, oxidation reduction potential, and dissolved oxygen, respectively.

5.3.2 A cumulative frequency plot of NO_3 concentrations

A cumulative frequency plot of NO3 concentrations in the water samples can be used to evaluate the influence of agricultural activities. Cumulative probability technique was taken to investigate the NO3-N background value (Sinclair, 1991; Panno et al., 2006). One of the most frequently cited studies of nitrate background values in groundwater is Madison and Brunett (1985). They suggested that the natural background concentration of NO3-N was 0.2 mg/L and that concentrations over 3 mg/L could be attributed to anthropogenic effects. Also, the background concentration of NO3-N in groundwater in Gangwon province of Korea was 2.7 mg/L (Kaown et al., 2007).

Cumulative probability graphs of NO_3-N data for the groundwater samples are shown in Fig. 7. The histogram of the log NO_3-N values showed a lognormal distribution. The inflection points on the probability graph indicate an interpretable breakdown of distribution of the logged values, as

follows: (1) above a logged value of 1.08 (NO_3-N = 12.3 mg/L), the distribution was the skewed in the left with relatively short left-hand tail; (2) between the logged values of 0.46 and 1.08 (NO_3-N = 2.92 and 12.3 mg/L, respectively), the distribution was somewhat skewed to the right; and (3) between logged values of -0.16 and 0.46 (NO_3-N = 0.69 and 2.92 mg/L, respectively), the distribution was skewed in the opposite direction, to the right.

Three thresholds (inflection points or points where the slope change) were used to identify the NO_3-N background values for data sets in Haean basin. The threshold values for the groundwater samples were 0.69, 2.92, and 12.3 mg/L, respectively. The lowest NO_3-N threshold value (0.69 mg/L) was interpreted as the natural background concentration from precipitation. The threshold value of 2.92 mg/L was regarded as the upper limit of present-day background concentration, and concentrations above this value in the site were land-based anthropogenic sources. The water samples with

concentrations exceeding 12.3 mg/L were probably dominated by septic and animal wastes. In the Haean basin, present-day background in the sampled groundwater was estimated to be 0.69 to 2.92 mg/L.

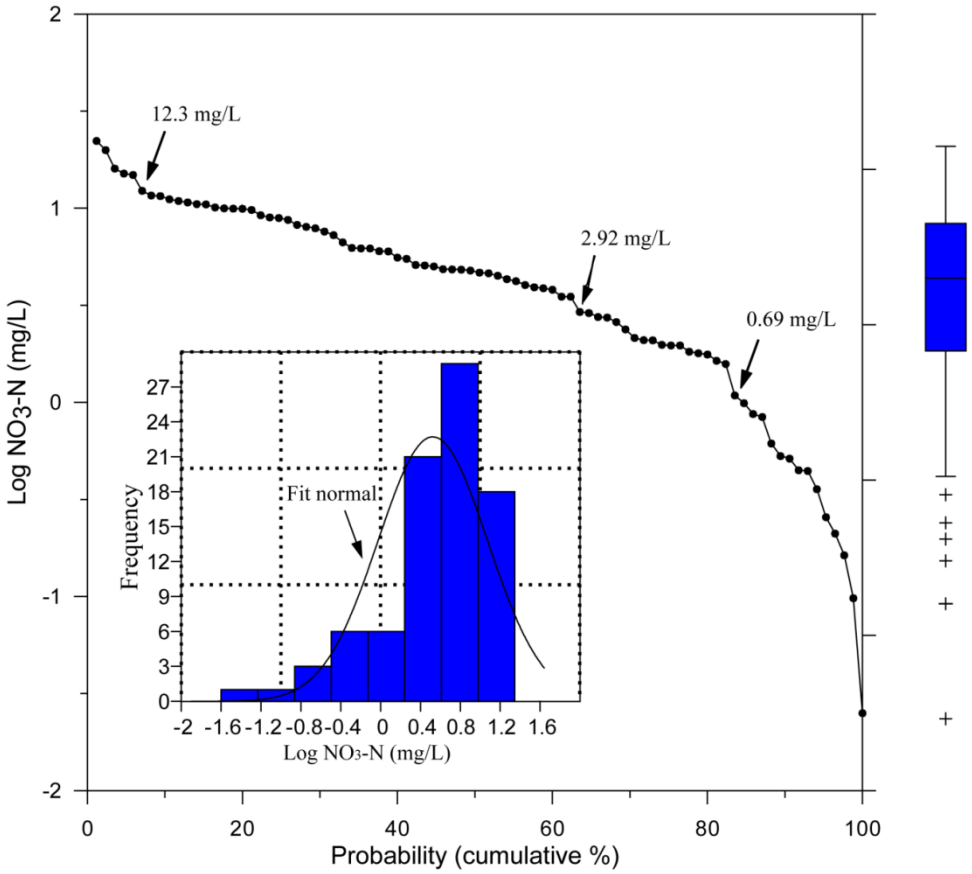

Fig. 5-4 Cumulative probability graph for groundwater samples showing threshold values. A histogram and box and whisker plot of the data are also shown

5.3.3 Environmental characteristics of hyporheic water

Table 5-2 represents the environmental conditions for up welling points (PDH2 and 4), down welling points (PUM18 and 20), mixed welling points (PMH8 and 13), stream water, three groundwater, and paddy water, respectively. The pH of hyporheic water samples were highest in down welling points (PDH2 and 4). The hyporheic water pH in down welling points were consistently higher than the stream water, whereas hyporheic water pH in up welling points (PUH18 and 20) were 7-14% lower than stream water in the site. pH was not significantly different between groundwater wells. The only significant interaction was between welling points and stream water. Temperature was significantly cooler in up welling points compared with down welling points. The mixed welling points showed intermediate values between temperatures of up welling and down welling point. Hyporheic water temperature was coolest in the up welling point (PUH18) (mean 16.4^{o}C) and highest in the mixed welling point (PMH13). Electrical conductivity was

significantly higher at up welling points and lowest at mixed welling point (PMH8). Dissolved oxygen values were significantly lower at up welling points. The concentration was similar in up welling points and mixed welling points.

Table 5-2 Environmental conditions for up welling points (PDH2 and 4), down welling points (PUM18 and 20), mixed welling points (PMH8 and 13), stream water, three groundwater, and paddy water, respectively. (DO means dissolved oxygen; Temp. means temperature; EC means electrical conductivity; SW means stream water; GW means groundwater; HW means hyporheic water, respectively)

Sample	Water type	Temp. (°C)	DO (mg/L)	pH	EC (μS/cm)
SW	SW	19.7	8.1	8.4	143
TGL-1	GW	13.6	2.9	6.8	244
TGR-1	GW	15.1	2.3	6.8	194
TGR-2	GW	13.6	3.5	6.8	275
SP21	Paddy	11.9	2.9	6.8	224
PDH2	HW	18.2	8.2	8.7	168
PDH4	HW	18.2	8.9	8.7	136
PMH8	HW	16.6	8.5	8.3	133
PMH13	HW	18.8	7.6	8.2	145
PUH18	HW	16.4	4.9	7.8	287
PUH20	HW	17.1	5.7	7.2	246

5.3.4 $\delta^{15}N$ and $\delta^{18}O$ values of nitrate

The isotopic composition of water samples nitrate may indicate the major contaminant source, since nitrate from different sources has characteristics $\delta^{15}N\text{-}NO_3^-$ and $\delta^{18}O\text{-}NO_3^-$ values (Clark and Fritz, 1997; Kendall, 1998; Kendall and Aravena, 2000; Kendall et al., 2007). Figure 5-4 shows the typical ranges of $\delta^{15}N\text{-}NO_3^-$ and $\delta^{18}O\text{-}NO_3^-$ values for major sources of nitrate that may influence hyporheic water (Kendall, 1998; Chae et al., 2009). The $\delta^{15}N\text{-}NO_3^-$ values in the up welling points (PUH13 and 18) showed higher values than those in down welling points (PDH2 and 4) and mixed welling points (PMH8 and 10). In the groundwater up welling point, high $\delta^{15}N\text{-}NO_3^-$ values was correlated with high values of $\delta^{18}O\text{-}NO_3^-$ values. These samples showed low concentrations of NO_3-N (4.7 - 6.3 mg/L) and HCO_3 (30.3 - 35.0 mg/L) showed correlation indicating evidence of denitrification. The $\delta^{15}N\text{-}NO_3^-$ values in the groundwater (TGL1) was increased while the $\delta^{15}N\text{-}NO_3^-$ values in the TGR2 and TGR3 was decreased.

Groundwater discharge occursin the groundwater TGL1 and recharge occurs in the groundwater TGR2 and 3. Therefore, the groundwater wells of water chemical signatures were reflected groundwater and stream water chemistry.

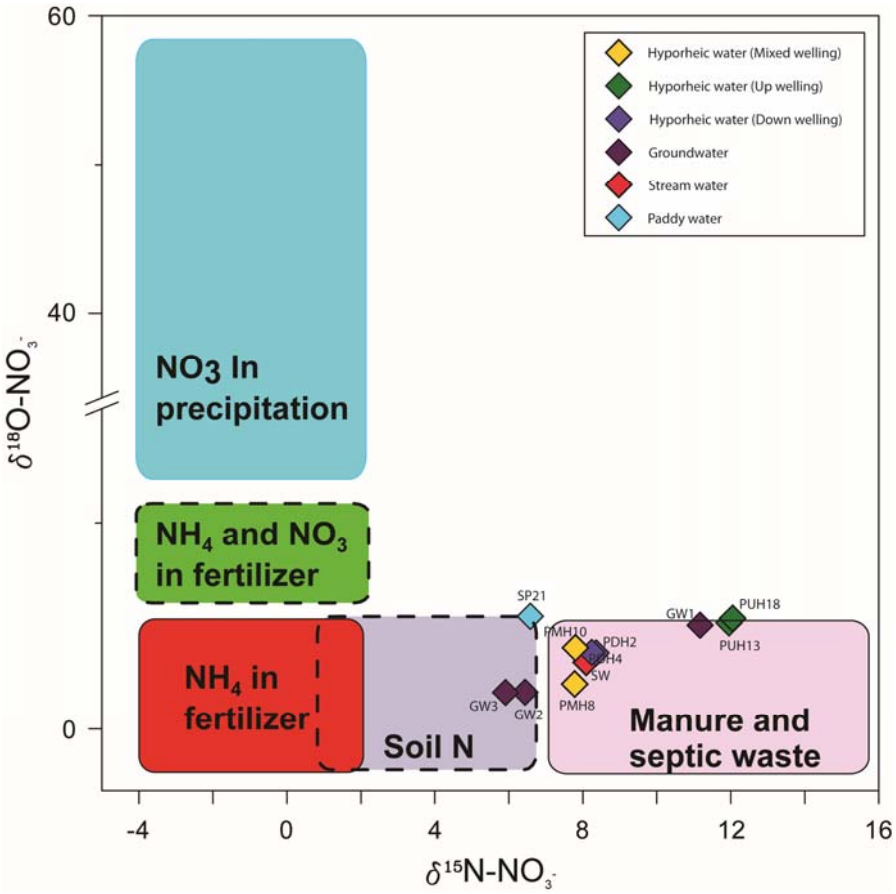

Fig. 5-5 Concentration of $\delta^{18}O$ versus concentration of $\delta^{15}N$ values for sampled waters with different hyporheic exchange patterns, groundwater, stream water, and paddy water, respectively. Typical ranges of $\delta^{15}N\text{-}NO_3^-$ and $\delta^{18}O\text{-}NO_3^-$ values for different nitrate sources were taken from Kendall (1998)

5.3.5 Factor analysis

Table 5-3 summarizes the FA results after rotation, including the loadings, the Eigenvalues, the amount of variance explained by each factor, and the cumulative variance. The results of factor analysis based on the two most significant factors indicated that these factors explain 71.8% variance for groundwater chemistry, stream water, and hyporheic water chemistry. In this analysis, factor 1 of water samples explained 55.3% of the variance and was strongly related with EC, TDS, Sal, Ca, Cl, and HCO_3.

The variables of EC, Sal, TDS and Cl have high positive loading on factor 1. The factor 1 group represent sea water intrusion into groundwater. However, sea water intrusion is less convincing because the study site is located in inland. Therefore, this factor clearly represents contamination with chemical deicer, as indicated by its strong correlation with EC, HCO_3, Na and Cl. Yanggu Country Office (2013) uses approximately 40,000 kg of sodium chloride for de-icing purposes on roads every winter. Factor 1 of groundwater

was interpreted as groundwater contaminated by anthropogenic pollutants. The factor 2 explained 16.50% of the total variance, with strong positive loading for NO_3 and SO_4. It can be inferred that the factor 2 are involved in determining the chemical fertilizer composition. The factor 2 described as affected by pollution sources related to agricultural activity. The constituents NO_3 could be derived from anthropogenic pollution. The NO_3 comes from anthropogenic pollution sources such as sanitation facilities, domestic effluents, atmospheric fallout, and agricultural fertilizer usage (Ritzi et al., 1993). The source has no known lithological source (Jeong, 2001). This factor 1 is attributed to anthropogenic influence of Ca, Cl, and Sal in sampled water. The data shows that these ions have migrated from surface. When polluted surface water is infiltrated, the HCO_3 could be derived from natural processes such as the dissolution of carbonate minerals, soil CO_2, or bacteria degradation of organic materials (Jeong, 2001).

Table 5-3 Eigenvalues of factors extracted through principal component analysis, differences between the factors and the variance explained by the factors (groundwater, stream water, hyporheic water, and paddy water), and the rotated factor pattern of extracted factors after Varimax rotation (high loading values (>0.8) are shown in bold)

Variance	PC1	PC2
Temp.	-0.76	0.33
EC	**0.90**	0.07
ORP	-0.40	0.63
DO	**-0.89**	0.03
pH	**-0.86**	0.05
TDS(g/L)	**0.98**	-0.10
Sal	**0.98**	-0.05
Ca	**0.98**	0.11
K	0.19	-0.04
Mg	0.73	0.50
Na	0.75	0.39
Si	0.26	-0.31
Cl	**0.94**	0.27
NO_3	-0.20	**0.82**
SO_4	0.13	**0.90**
HCO_3	**0.89**	-0.24
Eigenvalue	8.85	2.65
%variance	55.30	16.50
Cumulative	55.30	71.80

5.3.6 Clustering into similar compositions

As shown in Fig. 5-6, all water samples were classified into three statistically significant clusters. Cluster I included stream water, two different hyporheic waters (down welling, mixed welling), and groundwater of TGR1, respectively. These results have a close relationship with the hyporheic exchange pattern records. Cluster II included groundwater of TGR-2 and TGL and hyporheic waters (up welling and mixed welling). The cluster I and II indicted that the groundwater and stream water mixing occurred in the hyporheic zone. Furthermore, the effect on mixing in the hyporheic zone caused by stream water is greater than groundwater. Cluster III just include paddy water. The paddy water have different chemical signature between hyporheic water, stream water and groundwater.

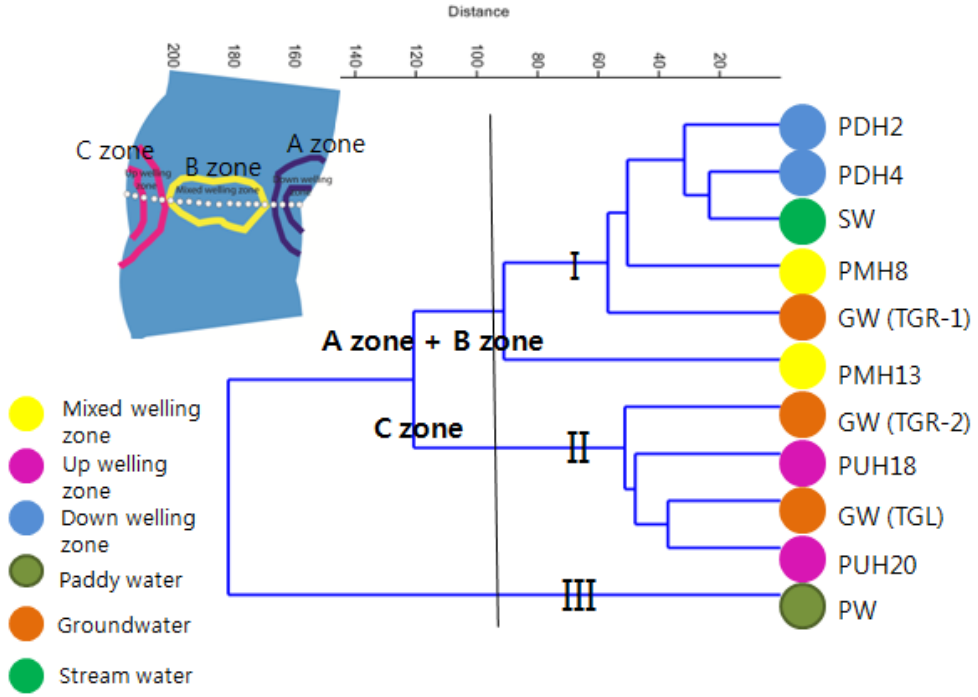

Fig.5-6 Dendrogram showing the clustering of sampling sites according to water quality characteristics of the Haean basin

5.4 Conclusions

In this study, multivariate statistical techniques and isotopic analysis were used to evaluate the groundwater, stream water, and hyporheic water quality of an intensive agricultural area in the Haean basin, Korea. The statistical analysis revealed the spatial and temporal properties of the hydrochemistry.The processes responsible for hydrochemical variations in water qualities and isotopic data are hyporheic exchanges, domestic and agricultural pollution, and geologic deposits.

First, the FA results indicated two latent factors controlling groundwater and stream water chemistry. In the water samples, 71.80% of total variance was explained by two factors. These latent factors were identified as being responsible for the anthropogenic factors. Therefore, the FA could be useful for evaluation of potential environmental contaminants in the region.

The results of CA showed three different groups according to similarity of geochemical properties. Clusters I and II indicated that groundwater and stream water mixing occurred in the hyporheic zone. These results also varied depending on the exchange patterns of the hyporheic zone.

Consequently, the results of this study showed that the hyporheic zone was sensitive to the surrounding environment. Thus, characterizing the geochemical properties of each end member (stream water and groundwater) is very important for this kind of study.

CHAPTER 6. DELINEATION OF HYPORHEIC ZONES ACROSS THE STREAM

In this chapter, the proposed method was applied to a set of temperature data collected from a streambed across the stream, and the horizontal delineation of the hyporheic zone depth was presented for different hyporheic flux shapes. Fig. 6-1 (a) shows the installed piezometer and Fig. 6-1 (b) shows the insulted temperature measuring devices across the stream. Collected data across the stream are shown in Table 6-1.

Fig. 6-1 (a) Installed piezometers and (b) insulted temperature measuring device for data collection across the stream

Table 6-1 Collected temperature data across the stream of (a) PDH2, (b) PDH4, (c) PMH8, (d) PMH13, (e) PDH18 and (f) PDH20

Depth(m)	Temperature (°C)				
	0 min	120 min	240 min	360 min	480 min
0.01	14.8	17.2	18.5	16.5	16.4
0.05	14.5	16.4	18	16	16.1
0.1	14.3	15.6	16.5	15.8	15.8
0.2	14.5	14.1	15.4	15.3	15.5
0.3	14.3	14.6	14.7	14.5	14.9
0.4	14.2	14.3	14.5	14.3	14.7
0.5	14.2	14.3	14.3	14.3	14.2

(a)

Depth(m)	Temperature (°C)				
	0 min	120 min	240 min	360 min	480 min
0.01	15	18	19	17.3	17
0.05	14.8	17	18.2	17.2	16.5
0.1	14.6	16.1	17.2	16.5	16.5
0.2	14.5	15	15.2	15.3	15.8
0.3	14.3	14.5	14.5	15.3	14.8
0.4	14.2	14.3	14.6	14.6	14.3
0.5	14.1	14.3	14.8	14.1	14

(b)

Table 6-1 (continued)

Depth(m)	Temperature (°C)				
	0 min	120 min	240 min	360 min	480 min
0.01	15.8	19.7	20.3	18.5	17.1
0.05	15	18	19.2	18.2	17
0.1	14.8	16.2	17.9	17.6	17.2
0.2	14.5	15	16	17	16.3
0.3	14.2	14.5	15	15.8	15.5
0.4	14.2	14.4	14.8	15	14.5
0.5	14.1	14.3	14.8	14.1	14

(c)

Depth(m)	Temperature (°C)				
	0 min	120 min	240 min	360 min	480 min
0.01	15.7	18.9	19.5	18.8	18
0.05	15.6	17.5	18.5	18	17.5
0.1	14.7	16.2	17	16.9	17.2
0.2	14.3	14.6	15.8	16	17
0.3	14.3	14.7	14.3	15.3	15
0.4	14.2	14.4	14.6	15	14.6
0.5	14.1	14.5	14.7	14.3	14.2

(d)

Table 6-1 (continued)

Depth(m)	Temperature (°C)				
	0 min	120 min	240 min	360 min	480 min
0.01	16	19	20.1	19.8	18.2
0.05	15.2	17.5	19	18.5	17.9
0.1	14.8	16.2	17.5	18.1	17.3
0.2	14.3	15	15.2	15.8	16.2
0.3	14.2	14.3	14.3	14.8	15.1
0.4	14.2	14.4	14.5	14.5	14.5
0.5	14.3	14.3	14.3	14.3	14.2

(e)

Depth(m)	Temperature (°C)				
	0 min	120 min	240 min	360 min	480 min
0.01	15.9	19.2	20.3	19.5	18.5
0.05	15.2	17.6	18.9	18.7	18
0.1	14.9	16.2	17.8	18	17.2
0.2	14.5	15	15.8	16.5	16.5
0.3	14.2	15	14.4	15.6	15.2
0.4	14.2	14.8	14.5	14.8	14.4
0.5	14.4	14.4	14.5	14.4	14.4

(f)

Initial and boundary conditions for each temperature collecting points are shown in Fig. 6-2.

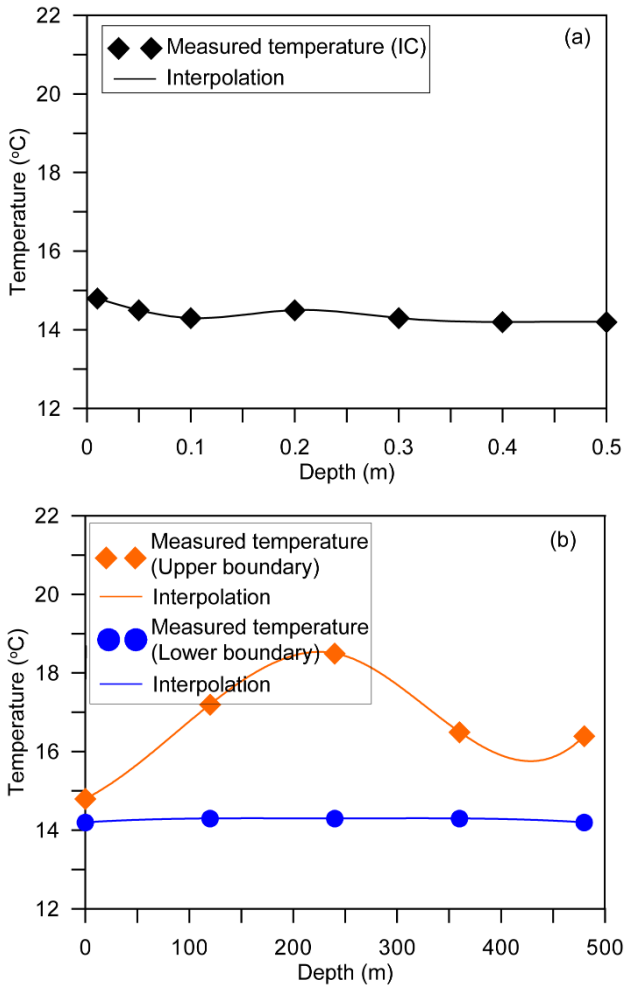

(a)

Fig. 6-2 Initial and boundary conditions of (a) PDH2, (b) PDH4, (c) PMH8, (d) PMH13, (e) PDH18 and (f) PDH20

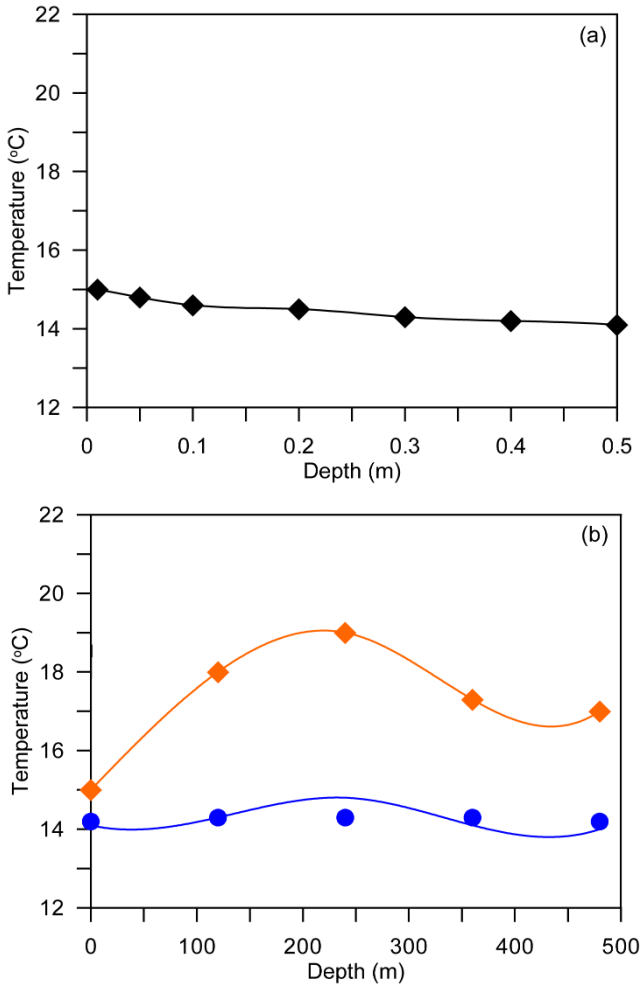

(b)

Fig. 6-2 (continued)

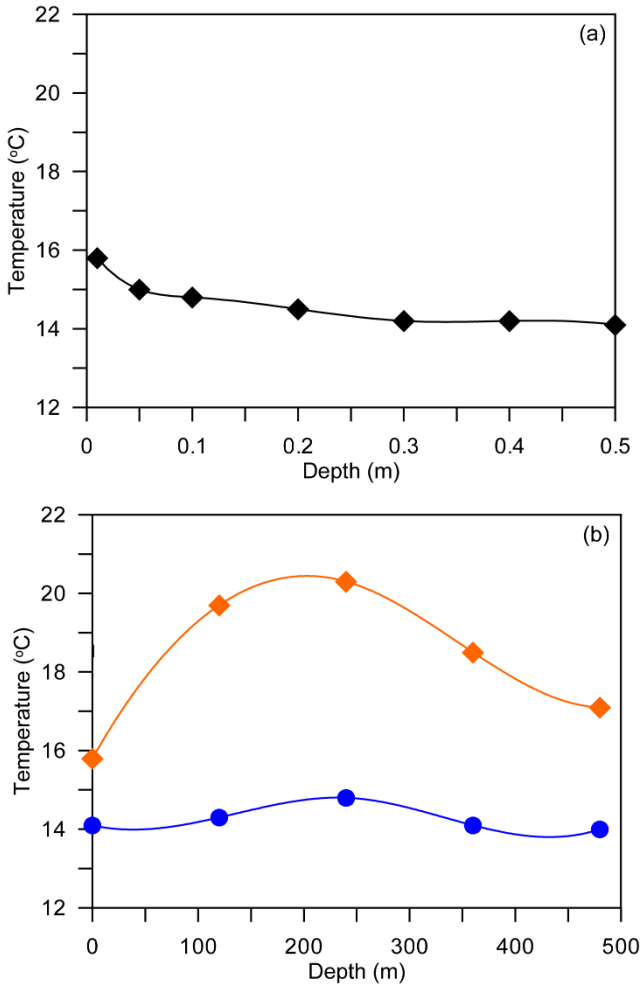

(c)

Fig. 6-2 (continued)

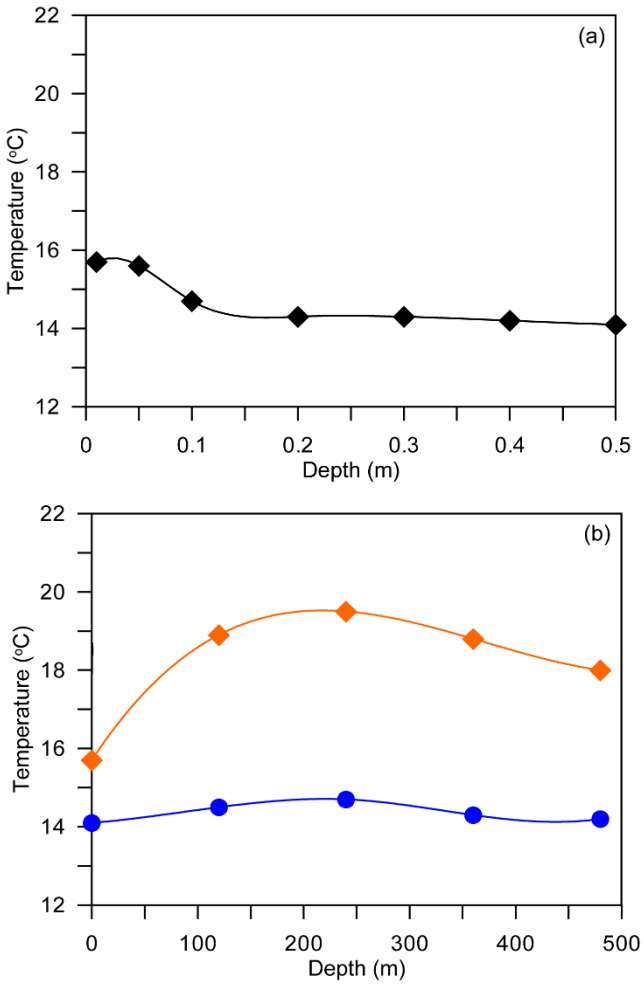

(d)

Fig. 6-2 (continued)

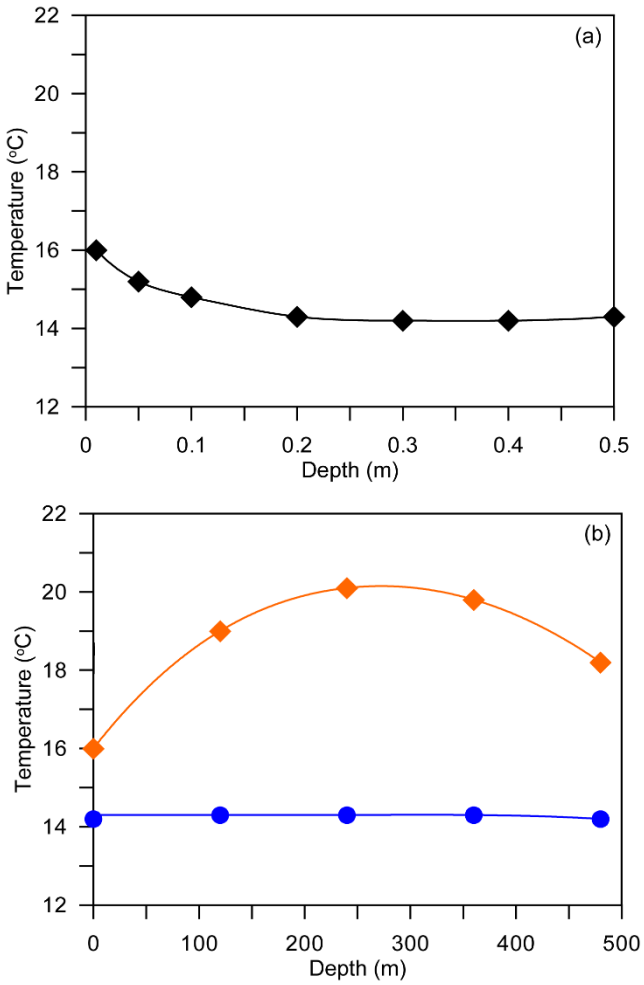

(e)

Fig. 6-2 (continued)

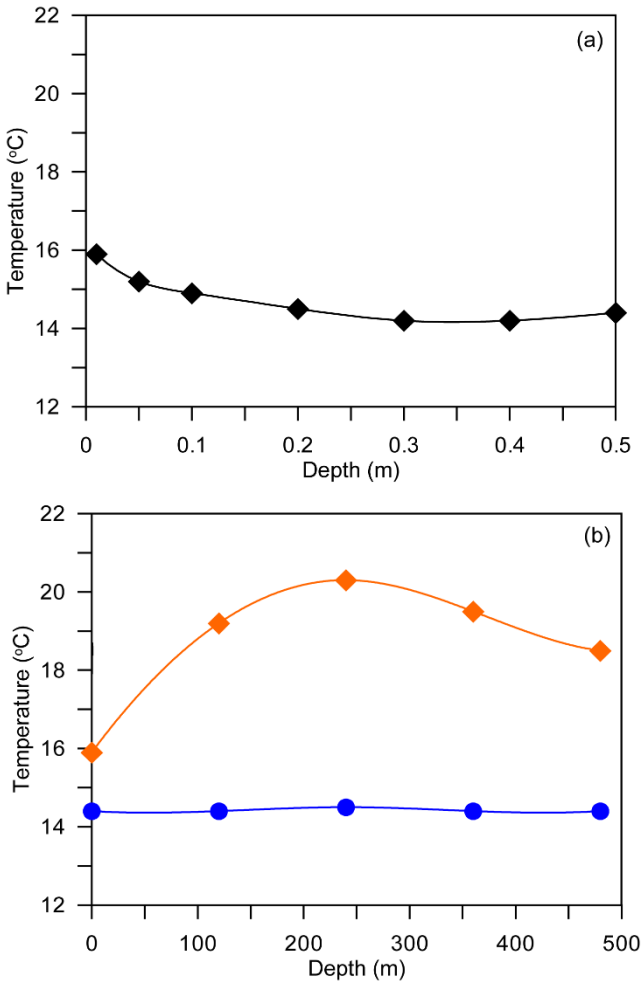

(f)

Fig. 6-2 (continued)

The proposed method of CAD analysis were performed for the six temperature collecting points. The calculated hyporheic zone depth for each hyporheic flux shape are listed in Table 6-2, the corresponding analysis results are shown in Fig. 6-3.

Table 6-2 Optimal values for the hyporheic zone depth of (a) PDH2, (b) PDH4, (c) PMH8, (d) PMH13, (e) PDH18 and (f) PDH20

Optimal values for (a)	Shape of hyporheic flux			
	Spandrel	Triangle	Cosine	Ellipse
D_H (cm)	4.8	4.5	4.3	3.6
$V_{f,max}$ (mm/min)	6.5	5.2	4	3.7
SSD ($^oC^2$)	1.9012	1.9003	1.8993	1.899

(a)

Optimal values for (b)	Shape of hyporheic flux			
	Spandrel	Triangle	Cosine	Ellipse
D_H (cm)	2.9	2.6	2.3	2.5
$V_{f,max}$ (mm/min)	29.4	26.8	29.3	36.5
SSD ($^oC^2$)	1.3692	1.3678	1.3667	1.3559

(b)

Optimal values for (c)	Shape of hyporheic flux			
	Spandrel	Triangle	Cosine	Ellipse
D_H (cm)	2	1.7	1.6	1.6
$V_{f,max}$ (mm/min)	57.5	57.6	55.9	41.6
SSD ($^oC^2$)	1.2066	1.2137	1.2139	1.2252

(c)

Table 6-2 (continued)

Optimal values for (d)	Shape of hyporheic flux			
	Spandrel	Triangle	Cosine	Ellipse
D_H (cm)	3	2.7	2.6	2.6
$V_{f,max}$ (mm/min)	-81.8	-82	-187.6	-16.5
SSD ($^oC^2$)	1.8027	1.8021	1.7978	1.804

(d)

Optimal values for (e)	Shape of hyporheic flux			
	Spandrel	Triangle	Cosine	Ellipse
D_H (cm)	3	2.7	2.7	2.6
$V_{f,max}$ (mm/min)	-174.9	-184.9	-108.4	-29.7
SSD ($^oC^2$)	1.5126	1.5112	1.512	1.5144

(e)

Optimal values for (f)	Shape of hyporheic flux			
	Spandrel	Triangle	Cosine	Ellipse
D_H (cm)	8.6	8.1	7.2	6.6
$V_{f,max}$ (mm/min)	-0. 9	-0. 7	-0.6	-0.5
SSD ($^oC^2$)	1.7971	1.7966	1.7982	1.7981

(f)

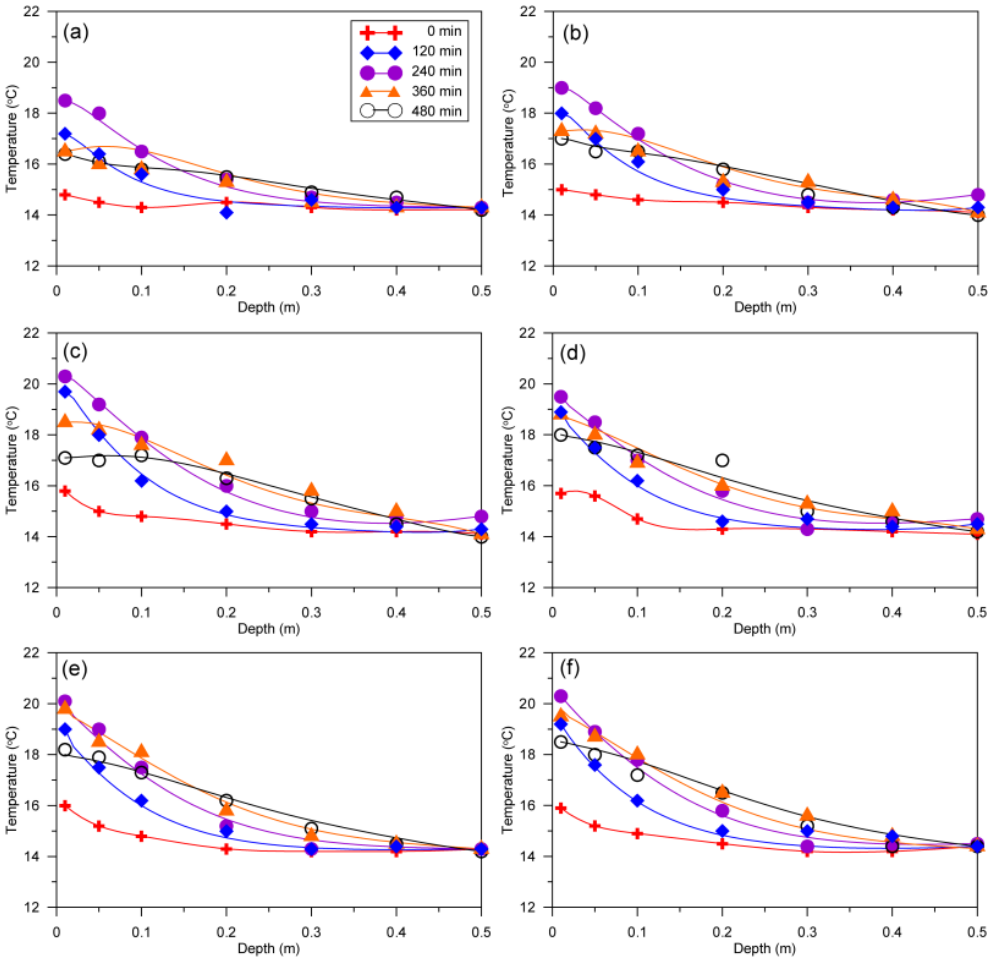

Fig. 6-3 CAD analysis results

The distributions of hyporheic zone depth delineated across the cross section of the stream are shown in Fig. 6-4.

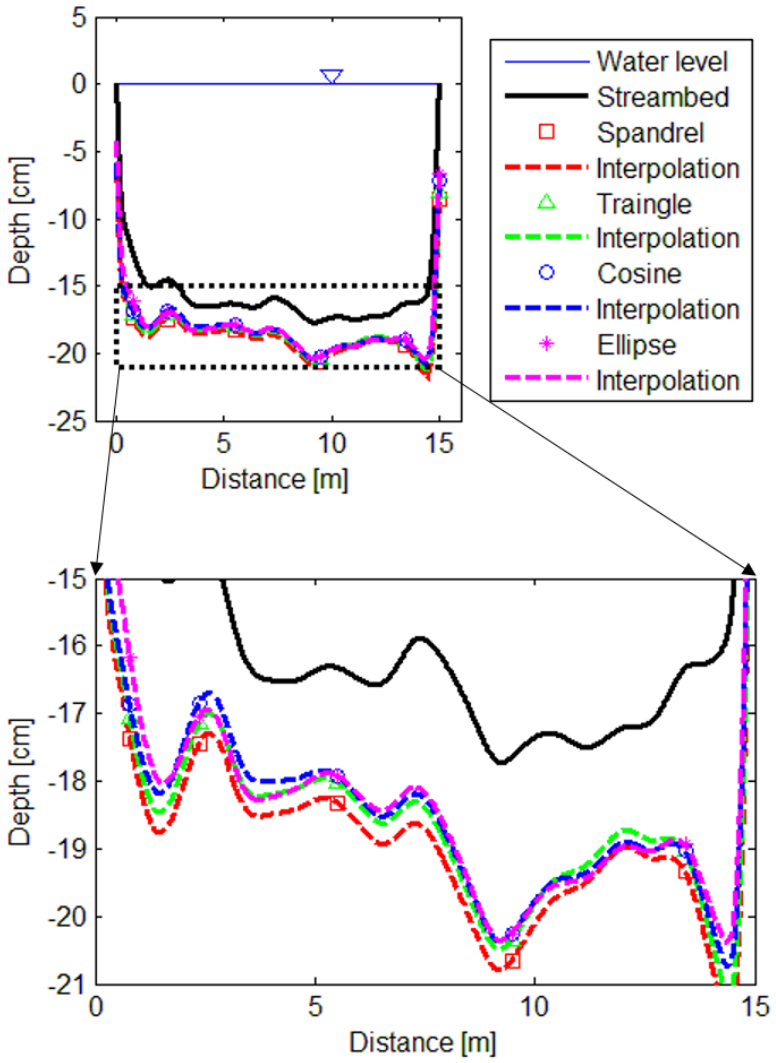

Fig. 6-4 Hyporheic zone depth delineated across the cross section

CHAPTER 7. CONCLUSION

The hyporheic zone is temporally and spatially dynamic ecotone where surface water and groundwater mix. The research on the hyporheic zone is complex and challenging because the zone is influenced by and also influences surface water and groundwater. Existing studies for the mixing zone of surface water and groundwater have been conducted separately and there were hardly integrated studies for the zone. The studies for the

biogeochemical processes at the zone are relatively abundant, but the consideration for the depth of the mixing zone is scarce.

The depth of the surface water-groundwater mixing zone was determined quantitatively by systematically combining the hydrological and the heat transfer analyses. Based on the determined depth of the zone, the effect of the change in hydraulic condition on the community variation of indigenous microorganism and the water quality was examined. To do this, molecular analysis and isotope analysis were utilized.

Hydrological approach is essential to identify the mixing and exchange of surface water and groundwater. However, hydrological approach alone lacking in careful evaluation of the hyporheic zone depth may have a fundamental problem of evaluating shallow groundwater, not the mixing and exchange zone. In order to settle this situation, the hyporheic zone depth was delineated by systematically combining the traditional hydrological approach with the thermal conduction-advection-dispersion analysis. The hyporheic

zone depth determined in this manner can be used to evaluate the interaction between surface water and groundwater more quantitatively. The calculated depth of the mixing zone of the study site varied from 9.2 to 14.9 cm below streambed. The proposed method improved the precision compared to the existing method using tracer where the depth lied in the range of 2 and 30 cm.

The community variation of indigenous microorganism and the water quality were examined in connection with the change in hydraulic condition. From the systematic connection of biological and chemical approach, it was discovered that the indigenous microorganism and the water quality were sensitively reacted with the change in the hydraulic condition. Bacterial species richness and diversity were high when the hydraulic condition of the hyporheic zone varies. Isotope analysis showed that the denitrification processes occur where the hydraulic condition of the hyporheic zone varies.

This page intentionally left blank

REFERENCES

Anderson, M. (2005) Heat as a groundwater tracer. Ground Water 43(6), 951-968

Andrew, J.B. (1998) The functional significance of the hyporheic zone in streams and rivers, Annu. Rev. Ecol. Syst., Vol. 2, pp. 59-81

Appelo C.A.J., Postma D. (2005) Geochemistry. Groundwater and Pollution (2nd ed.) A.A. Balkema Publishers, Amsterdam

Babiker, I.S., Mohamed, M.A.A., Terao, H., Kato, K., Ohta, K. (2004) Assessment of groundwater contamination by nitrate leaching from intensive vegetable cultivation using geographical information system. Environ. Int. 29, 1009-1017

Barlow P.M., Moench A.F. (1998) Analytical solutions and computer programs for hydraulic interaction of stream-aquifer system. USGS Open Field Report 98-415A

Battin, T.J. (2003) A mixing model analysis of stream solute dynamics and the contribution of a hyporheic zone to ecosystem function, Freshwater Biology., Vol. 48, pp. 995-1014

Baxter, C.V., Hauer, F.R. and Woessener, W.W. (2003) Measuring groundwater-stream water exchange: New techniques for installing minipiezometers and estimating hydraulic conductivity, Trans. Am. Fisher Society, Vol. 132, pp. 493-502

Becker, M.W., Georgian, T. and Ambrose, H. (2004) Estimating flow and flux of groundwater discharge using temperature and velocity, Journal of Hydrology, Vol. 296, pp. 221-233

Beller, H.R., Hudson, Vic M.G.B., McNab, W.W.M., Carlsen, T. (2004) Biogeochemistry and natural attenuation of nitrate in groundwater at an explosives test facility. Appl. Geochem. 19, 1483-1494

Bencala, K.E. and Walters, R.A. (1983) Simulation of solute transport in a mountain pool-and-riffle stream: a transient storage model, Water Resources Research, Vol. 19, pp. 718-724.

Bencala, K.E., MaKnight, D.M., Zellweger, G.W., 1990. Characterization of transport in an acidic and metal-rich mountain stream based on a lithium tracer injection and simulations of transient storage. Water Resour. Res. 26 (5), 989-1000

Bertin, C., Bourg, A.C.M., 1994. Radon-222 and chloride as natural tracers of the infiltration of river water into an alluvial aquifer in which there is significant river/groundwater mixing. Environ. Sci. Tech. 28, 794-798

Boulton, A.J. (1993) Stream ecology and hyporheic exchange: implications, techniques and limitations. Marine and Freshwater Res 44:553-564

Boulton, A.J., Findlay, S., Marmonier, P, Stanley, E.H., Valett, H.M. (1998) The functional significance of the hyporheic zone in streams and rivers. Annu Review Ecol Syst 29:59-81

Boulton, A. J., Stanley, E. H. (1995) Hyporheic processes during flooding and drying in a Sonoran Desert stream. II: Faunal dynamics. Archiv f?r

Hydrobiologie, 134(1), 27-52

Boulton, A.J. (2000) River ecosystem health down under: assessing ecological condition in riverine groundwater zones in Australia, Ecosystem Health., 6, 108-118

Boulton, A.J. (2000) River ecosystem health down under: assessing ecological condition in riverine groundwater zones in Australia, Ecosystem Health., Vol. 6, pp. 108-118

Boyer, E.W., Hornberger, G.M., Bencala, K.E., McKnight, D.M. (2000) Effects of asynchronous snowmelt on flushing of dissolved organic carbon: A mixing model approach. Hydrol. Proc. 14 (18), 3291-3308

Brodie, R.S., Baskaran, S., Ransley, T., Spring, J. (2009) Seepage meter: progressing a simple method of directly measuring water flow between surface water and groundwater systems. Australian J Earth Sci 56: 3-11

Brunke, M. and Gonser, T. (1997) The ecological significance of exchange processes between rivers and groundwater, Freshwater Biology., Vol. 37, pp. 1-33

Brunke, M., Gonse, T. (1997)The ecological significance of exchange processes between rivers and groundwater. Freshwater Biol. 37, 1-33

Cable, J.E., Burnett, W.C., Chanton, J.P. (1997) Magnitude and variations of groundwater seepage along a Florida marine shoreline. Biogeochem 38: 189-205

Cardenas, M.B., Wilson, J.L., Haggerty, R. (2008) Residence time of

heterogeneity, bed forms, and stream curvature on subchannel hyporheic exchange. Water Resour Res 40: W08307

Carslaw, H.S., Jaeger, J.C. (1656) Conduction of heat in solids, Clarendon, Oxford, U.K., 510 pp

Carver, A. (2001) Riverbed permeabilities: information from pooled data. Ground Water 39 (4), 546-553

Castro, N.M., Hornberger, G.M. (1991) Surface-subsurface water interactions in an alluviated mountain stream channel. Water Resour. Res. 27 (7), 1613-1621

Chen, J., Chen, C., Chen, C.Y. (2007) Analysis of solute transport in a divergent flow tracer test with scale-dependent dispersion. Hydrol Process 21: 2526-2536

Chiyuan, M., Junren, N., Alistair, G.L.B. (2010) Recent changes of water discharge and sediment load in the yellow river basin, China. Progress Physic Geol 34: 541-561

Choi, H.M., Lee, J.Y. (2010) Groundwater level distribution and rainfall response characteristics in Haean basin of Yangu. J Soil Groundwater Environ 15: 1-8 (in Korean)

Christensen, N.S., Wood, A.W., Voisin, N., Lettenmaier, D.P., Palmer, R.N. (2004) The effects of climate change on the hydrology and water resources of the Colorado river basin. Clim Change 62: 337-363

Conant Jr., B. (2004) Delineating and quantifying groundwater discharge

zones using streambed temperatures. Ground Water 41 (2), 243-257

Constantz, J., Stewart, A.E., Niswonger, R., Sarma, L. (2002) Analysis of temperature profiles for investigating steam losses beneath ephemeral channels. Water Resour Res 38: 1316

Constantz, J., Thomas, C.L. (1996) The use of streambed temperature profiles to estimate the depth, duration, and rate of percolation beneath arroyos. Water Resour Res 32: 3597-3602

Constantz, J., Thomas, C.L., Zwllweger, G. (1994) Influence of diurnal variations in stream temperature on streamflow loss and groundwater recharge. Water Resour Res 30: 3253-3264

Constantz, J. (2008) Heat as a tracer to determine streambed water exchanges. Water Resour. Res. 44 (4), DOI: 10.1029/2008WR006996

Constantz, J., Cox, M., Su, G.W. (2003) Comparison of heat and bromide as groundwater tracers near streams. Ground Water 41 (5), 647-656

Constantz, J., Thomas, C.L. (1996)The use of streambed temperature profiles to estimate the depth, duration, and rate of percolation beneath arroyos. Water Resour. Res. 32 (12), 3597-3602

Constantz, J., Thomas, C.L., Zellweger, G. (1994) Influence of diurnal variations in stream temperature on streamflow loss and groundwater recharge. Water Resour. Res. 30 (12), 3253-3264

Cooling, M.P., Boulton, A.J. (1993) Aspects of the hyporheic zone below the terminus of a South Australian arid-zone stream. Marine Freshwater Res

44:411-426

Corbett, R.D., Chanton, J.P., Burnett, W.C., Dillon, K., Rutkowski, C., Fourqurean, J.W. (1999) Patterns of groundwater discharge into Florida bay. Am Soc Limnol Oceanol 44: 1045-1055

Domenical, P.A., Schwartz, W. (1998) Physical and chemical hydrology. 2nd edition, John Wiley & Sons, Inc. New York

Essaid, H., Zamora, C., McCarthy, K., Vogel, J., Wilson, J. (2008) Using heat to characterize streambed water flux variability in four stream reaches. J. Environ. Qual. 37, 1010

Findlay, S. (1995) The importance of surface-subsurface exchange in stream ecosystems: the hyporheic zone, Limnology and Oceanography., Vol. 40, pp. 159-164

Findlay, S. (1995)The importance of surface-subsurface exchange in stream ecosystems: the hyporheic zone. Limnol. Oceanogra. 40, 159-164

Fraser, B.G., Williams, D.D. (1997) Accuracy and precision in sampling hyporheic fauna. Can J Fish Aquat Sci 54:1135-1141

Fuss, C. and Smocke, L. (1996) Spatial and temporal variation in microbial respiration rates in blackwater stream. Freshwater Biol 36:339-349

Fustec, E., Mariotti, A., Grillo, X., Sajus, J. (1991) Nitrate removal by denitrification in alluvial groundwater: Role of a former channel. J. Hydrol. 123, 337-354

Geist, D.R. (1998) A method for installing piezometers in large cobble bed

rivers, Groundwater Monitoring and Remediation, Winter. pp. 78-82

Gilliam, J.W. (1994) Riparian wetlands and water quality, Journal of Environmental quality, Vol. 23, pp. 896-900

Gooseff, M.N., Mcknight, D.M., Lyons, W.B., Blum, A.E. (2002) Weathering reactions and hyporheic exchange controls on stream water chemistry in a glacial meltwater stream in the McMurdo Dry Valleys. Water Resour Res 38:1279Weathering reactions and hyporheic exchange controls on stream water chemistry in a glacial meltwater stream in the McMurdo Dry Valleys

Goto, S., Yamano, M., Kinoshita, M. (2005) Thermal response of sediment with vertical fluid flow to periodic temperature variation at the surface. J. Geophys. Res. 110 (B1), DOI: 10.1029/2004JB003419

Greenberg, M.S., Burton Jr., G.A., Rowland, C.D. (2002) Optimizing interpretation of in situ effects of riverine pollutants: impact of upwelling and downwelling. Environ. Toxicol. Chem. 21 (2), 289-297

Hancock, P.J. (2002) Human impacts on the stream-groundwater exchange zone. Environ Manage 6:763-781

Hancock, P.J., Boulton, A.J., Humphreys, W.F. (2005) Aquifers and hyporheic zones: towards an ecological understanding of groundwater. Hydrogeology Journal, 13(1), 98-111

Hantush, M.S. (1965) Wells near streams with semipervious beds. J Geophys Res 12: 2829-2838

Harlan, R.L. (1973) Analysis of coupled heat-fluid transport in partially

frozen soil. Water Resour. Res. 9 (5), 1314-1323

Harman, J., Robertson, W.D., Cherry, J.A., Zanini, L. (1996) Impacts on a sand aquifer from old septic system: Nitrate and phosphate. Ground Water 34 (6), 1105-1114

Harvery, J.W., Wagner, B.J., 2000. Quantifying Hydrologic Interactions between Streams and Their Subsurface Hyporheic Zones. Streams and Ground Waters 3-44,?doi:10.1016/b978-012389845-6/50002-8??Key: citeulike:8512185

Harvery, J.W., Wagner, B.J., Bencala, K.E. (1996) Evaluating the reliability of the stream tracer approach to characterize stream-subsurface water exchange. Water Resour. Res 32(8), 2441-2451

Harvey, J.W. and Bencala, K.E. (1993) The effect of streambed topography on surface-subsurface water exchange in mountain catchments, Water Resource Research, Vol. 29, pp. 89-98

Harvey, J.W., Fuller, C.C. (1998) Effect of enhanced manganese oxidation in hyporheic zone on basin-sccale geochemical mass balance. Water Resour. Res. 34, 623-636

Hatch, C.E., Fisher, A.T., Revenaugh, J.S., Constantz, J., Ruehl, C. (2006) Quantifying surface water-groundwater interactions using time series analysis of streambed thermal records: Method development. Water Resour Res 42:W10410 doi:10.1029/2005WR004787

Hazen, A. (1893) Some physical properties of sands and gravels. Massachusetts State Board, 24th Annual Report

Hem, J.D. (1992) Study and Interpretation of the Chemical Characteristics of Natural Water. U.S. Gov Print Office, Washington, DC

Hill, A.R. and Labadia, C.F. (1998) Hyporheic zone hydrology and nitrogen dynamics in relation to the streambed topography of a N-rich stream, Biogeochemistry, Vol. 42, pp. 285-310

Hill, A.R., Lymburner, D.J. (1998) Hyporheic zone chemistry and stream-subsurface exchange in two groundwater-fed streams. Can. J. Fish. Aquat. Sci. 55, 495-506

Hill, B.H., Herlihy, A.T., Kaufann, P.R. and Sinsabaugh, R.L. (1998) Sediment microbial respiration in a synoptic survey of mid-Atlantic region streams, Freshwater Biology, Vol. 39, pp. 493-501

Hoehn, E., Cirpka, O.A. (2006) Assessing hyporheic zone dynamics in two alluvial flood plains of the Southern Alps using water temperature and tracers. Hydrol. Earth Syst. Sci. Disc. 3, 335-364

Holmes, R.M., Jones, J.B., Fisher, S.G. and Grimm,N.B. (1996) Denitrification in a nitrogen-limited stream ecosystem, Biogeochem., Vol. 33, pp. 125-146

Hunt, B. (1999) Unsteady stream depletion from ground water pumping. Ground Water 37:98-102

Hynes, H.B.N. (1960)The biology of polluted waters. Liverpool University Press, Liverpool, 122 pp

Hyun, Y., Kim, H., Lee, S.S., Lee, K.K. (2011) Characterizing streambed

water fluxes using temperature and head data on multiple spatial scales in Munsan stream, South Korea. J. Hydrol. 402, 377-387

Isiorho, S.A., Matisoff, G., When, K.S. (2005) Seepage relationship between lake Chad and Chad aquifers. Ground Water 34: 819-826

Johnson, L.B., Richards, C., Host, G.E., Arthur, J.W. (1997) Landscape influences on water chemistry in Midwestern stream ecosystems. Freshwater Biol. 37, 193-208

Kalbus, E., Reinstorf, F. and Schirmer, M. (2006) Measuring methods for groundwater, surface water and their interactions; a review, Hydrol. Earth Syst. Sci. Discuss., Vol. 3, pp. 1809-1850

Kaown, D., Kim, H., Moon, H.S., Ko, K.S., Lee, K.K. (2014) Hydrogeochemical and microbial characteristics in aquiferscontaminated with leachate from animal carcass disposal sites. Environ. Earth Sci. DOI 10.1007/s12665-014-3750-3

Kaser, D.H., Binley, A., Heathwaite, A.L., Krause, S. (2009) Spatio-temporal variations of hyporheic flow in a riffle-step-pool sequence. Hydrol Process 23: 2138-2149

Keery, J., Binley, A., Crook, N., Smith, J.W.N. (2007) Temporal and spatial variability of groundwater-surface water fluxes: Development and application of an analytical method using temperature time series. J. Hydrol. 336, 1-16

Kelly, W.E., Frohlich, R.K. (1985) Relations between aquifer electrical and hydraulic properties. Ground Water 23 (2), 182-189

Kendall, C. and Macdonnell, J.J. (1998) Isotope tracers in chatchment hydrology, Elsevier Science, Amsterdam

Kim, B.K., Park, Y.A. (1967) The origin of the so-called Punch Bowl. J Geol Soc Korea 3: 61-66

Kim, H., Hyun, Y., Lee, K.K. (2009) Hydro-ecological characterization in groundwater dependent ecosystem. J. Kor. Wetland Soc. 11 (3), 1-8 (in Korean with English abstract)

Kim, H., Lee, J.Y., Lee, S.S., Hyun, Y., Lee, K.K.(2011) Characterization of vertical temperature distribution in hyporheic zone. J. Kor. Wetland Soc.13(2), 265-273(in Korean with English abstract)

Kim, H., Lee, J.Y., Lee, K.K.(2012) Partial correlation between hydrological, geochemical and microbiological processes in groundwater-stream water mixing zone in a rural area. Kor. Wetland Soc. 14(4), 489-502

Kim, H., Lee, J.Y., Lee, K.K. (2013) Spatial and temporal variations of groundwater-stream water interaction in an agricultural area, case study: Haean basin, Korea. Res. J. Earth Planet. Sci. 2 (2), 71-82

Kim, H., Lee, J.Y., Lee, K.K.(2014a) Thermal characteristics and bacterial diversity of forest soil in the Haean basin of Korea. The Scientific World J. ID 247401

Kim, H., Lee, K.K., Lee, J.Y. (2014b) Numerical verification of hyporheic zone depth estimation using streambed temperature. J. Hydrol. 511, 861-869

Kim, H., Lee, J.Y., Park, Y., Hyun, Y., Lee, K.K. (2014c) Groundwater and

stream water exchange revealed by water chemistry in a hyporheic zone of agricultural area. Paddy Water Environ. 12, 89-101

Kim, H., Kaown, D., Mayer, B., Lee, J.Y., Hyun, Y., Lee, K.K.(2015a) Identifying the sources of nitrate contamination of groundwater in an agricultural area (Haean basin, Korea) using isotope and microbial community analyses. Sci. Total Environ. (accepted)

Kim, H., Lee, J.Y., Lee, K.K. (2015b) Spatial and temporal variations in stream and groundwater chemistry and microbial community in an intensive agricultural area. Hydrol. Process. Major revision

Krupa, S.L., Belanger, T.V., Heck, H.H., Brok, J.T., Jones, B.J. (1998) The next generation seepage meter. J Coastal Res 25: 210-213

Kwon, Y.S., Lee, H.H., Han, U., Kim, W.H. (1990) Terrain analysis of Haean basin in terms of earth science. J Korea Earth Sci Soc 11: 236-241 (in Korean)

LaBaugh, J.W., Winter, T.C., Rosenberry, D.O., Schuster, P.F., Reddy, M.M., Aiken, G.R. (1997) Hydrological and chemical estimates of the water balance of a closed- basin lake in north central Minnesota. Water Resour Res 33: 2799-2812

LaMarche, V.C. (1974) Frequency-dependent relationships between tree-ring series along an ecological gradient and some dendroclimatic implications. Tree-Ring Bulletin 34: 1-20

Langhoff, J.H., Christensen, S., Rasmussen, K.R. (2001) Scale dependent hydraulic variability of streambed on an outwash plain. In: Impact of Human Activity on Groundwater Dynamics, Proceedings of IAHS Symposium

VI.IAHS Publication 269

Lapham, W.W. (1989) Use of temperature profiles beneath streams to determine rates of vertical groundwater flow and vertical hydraulic conductivity, USGS. Water Supply Paper, 2337, 35 pp

Lee, D.R. (1977) A device for measuring seepage flux in lake and estuaries. Am Soc Limnol Oceanol 22: 140-147

Lee, D.R., Cherry, J.A. (1978) A field exercise on groundwater flow using seepage meters and mini-piezometers. J Geol Edu 27: 6-10

Lee, D.R. (1985) Method for locating sediment anomalies in lake beds that can be caused by groundwater flow. J Hydrol 79: 187-193

Lee, J.Y. (2009) Importance of hydrogeological and hydrologic studies for Haean basin in Yanggu. J. Geol. Soc. Korea 45, 405-414 (in Korean with English abstract)

Lee, J.Y., Cheon, J.Y., Lee, K.K., Lee, S.Y., Lee, M.H. (2001) Statistical evaluation of geochemical parameter distribution in a groundwater system contaminated with petroleum hydrocarbons. J Environ Qual 30:1548-1563

Lee, J.Y., Kim, H.S., Yun, S.T., Kwon, J.S. (2009) Factor and cluster analyses of water chemistry in and around a large rockfill dam: Implications for water leakage. J Geotech Geoenviron Eng 135:1254-1263

Lee, J.Y., Lee, K.K. (2000) Use of hydrologic time series data for identification of recharge mechanism in a fractured bedrock aquifer system. J Hydrol 229:190-201

Lee, J.Y.,Lee, K.S.,Park, Y., Choi, H.M., Jo, Y.J. (2012) Chemical and isotopic compositions of groundwater and stream water in a?basin,?Korea: indication of fast circulation. J Geol Soc India (submitted)

Lowry, C.S., Walker, J.F., Hunt, R.J., Anderson, M.P. (2007) Identifying spatial variation of groundwater discharge in a wetland stream using a distributed temperature sensor. Water Resour Res 43: , DOI: 10.1029/2007WR006145

Malcolm, I.A., Soulsby, C., Youngson, A.F., Hannah, D.M., McLaren, I.S., Thorne, A. (2004) Hydrological influences in hyporheic water quality: implications for salmon egg survival. Hydrol Process 18:1543-1560

Malcolm, I.A., Soulsby, C., Youngson, A.F., Petry, J. (2003) Heterogeneity in ground water?surface water interactions in the hyporheic zone of a salmonid spawning stream: towards integrating hydrometric and tracer approaches. Hydrol Process 17:601?617

Marmonier, P., Dole, M.J. (1986) Les Amphipodes des se´diments d'un bras court-circuite´ du Rho?ne: logique de re´partition et re´action aux crues. Sci de l'eau 5:461?486

Martin, P. (1996) The metabolism of organic matter in the hyporheic zone of a mountain stream, and its spatial distribution, Hydorobiologia, Vol. 323, pp. 107-118

McKenna, J.E. (2003) An enhanced cluster analysis program with bootstrap significance testing for ecological community analysis. Environ Model Software 18:205-220

Mengis, M., Schiff, S.L., Harris, M., English, M.C., Aravena, R., Elgood, R.J., MacLean, A. (1999) Multiple geochemical and isotopic approaches for assessing groundwater NO3- elimination in riparian zone. Ground Water 37 (3) 448-457

Molona-Giraldo, N., Bayer, B., Blum, P.(2011) Evaluating the influence of thermal dispersion on temperature plumes from geothermal systems using analytical solutions. Int. J. Thermal Sci. 50 (7), 1223-1231

Munhoven, G. (2002) Glacial-interglacial changes of continental weathering: estimates of the related CO2 and HCO3- flux variations and their uncertainties. Global Planet Change 33:155-176

Murdoch, L.C., Kelly, S.E.(2003) Factors affecting the performance of conventional seepage meters. Water Resour. Res. 39 (6), DOI: 10.1029/2002WR001347

Oberdorfer, J.A. (2003) Hydrologic modeling of submarine groundwater discharge: comparison to other quantitative methods. Biogeochem 66: 159-169

Orghidan, T. (1992) Ein neuer lebenstraum des unterirdischen wassers, der hyporheische biotop, Archivfur Hydrobiologi., 55, 392-414

Panno, S.V., Hackley, K.C., Hwang, H.H., Greenberg, S.E., Krapac, I.G., Landsberger, S., O'Kelly, D.J. (2006) Characterization and identification of Na-Cl sources in ground water. Ground Water 44:176-187

Parker, J.T.C., Fossum, K.D., Ingersoll, T.L.(2000) Chemical characteristics of stormwater sediments and implication for environmental management,

Maricopa County, Arizona. Environ. Manage. 26, 99-115

Peter, J.H. (2002) Human impacts on the stream-groundwater exchange zone, Environmental Management, Vol. 6, pp. 763-781

Rand, M.C., Greenberg, A.E., Taras, M.J. (1992) Standard methods for the examination of water and wastewater. APHA (American Public Health Association), Washington DC

Randall, J.H., Mac Strand and John, F.W. (2006) Measuring groundwater - surface water interaction and its effect on wetland stream benthic productivity, Trout lake watershed, northern Wisconsin, USA, Journal of hydrology, Vol. 320, pp. 370-384

Reghunath, R., Murthy, T.R.S., Raghavan, B.R. (2002) The utility of multivariate statistical techniques in hydrogeochemical studies: an example from Karnataka, India. Water Res 36:2437-2442

Rosenberry, D.O., Morin, R. H.(2004) Use of an electromagnetic seepage meter to investigate temporal variability in lake seepage. Ground Water 42, 68-77

Rosenberry, D.O. (2008) A Seepage meter designed for use in flowing water. J Hydrol 359: 118-130

Rosenberry, D.O., Klos, P.Z., Neal, A. (2012) In situ quantification of spatial and temporal variability of hyporheic exchange in static and mobile gravel-bed rivers. Hydrol Process 26: 604-612

Rosenberry, D.O., Menheer, M.A. (2006) A system for calibrating seepage

meters used to measure flow between groudwater and surface water. USGS Scientific Investigations Rep. 2006-5053. USGS, Washington, DC

Rosenberry, D.O., Morin, R.H. (2004) Use of an electromagnetic seepage meter to investigate temporal variability in lake seepage. Ground Water 42: 68-77

Rosenberry, D.O., Pitlick, J. (2009) Effects of sediment transport and seepage direction on hydraulic properties at the sediment- water interface of hyporheic settings. J Hydrol 359: 118-130

Rosenberry, D.O. (2008) Seepage meter designed for use in flowing water. J. Hydrol. 359, 118-130

Rosenberry, D.O., Klos, P.Z., Neal, A.(2012) In situ quantification of spatial and temporal variability of hyporheic exchange in static and mobile gravel-bed rivers. Hydrol. Proc. 26, 604-612

Rosenberry, D.O., Pitlick, J.(2009) Effects of sediment transport and seepage direction on hydraulic properties at the sediment-water interface of hyporheic settings. J. Hydrol. 373, 377-391

Ruehl, C., Fisher, A.T., Hatch, C., Huertos, M.L., Stemler, G., Shennan, C. (2006) Differential gauging and tracer tests resolve seepage fluxes in a strongly-losing stream. J Hydrol 330: 235-248

Schiff, S.L., Aravena, R.O., Trumbore, S.E., Dillon, P.J.(1990) Dissolved organic carbon cycling in forested watersheds: A carbon isotope approach. Water Resour. Res. 26 (12), 2949-2957

Sebestyen, S.D., Boyer, E.W., Shanley, J.B., Kendall, C., Doctor, D.H., Aiken, G.R., Ohte, N.(2008) Sources, transformations, and hydrological processes that control stream nitrate and dissolved organic matter concentrations during snowmelt in an upland forest. Water Resour. Res. 44, DOI: 10.1029/2008WR006983

Shomar, B., Osenbruck, K., Yahya, A. (2008) Elevated nitrate levels in the groundwater of Gaza strip: Distribution and sources. Sci. Total Environ. 398, 164-174

Shrestha, S., Kazama, F. (2007) Assessment of surface water quality using multivariate statistical techniques: A case study of the Fuji river basin, Japan. Environ. Model Software 22:464-475

Silliman, S.E., Booth, D.F. (1993) Analysis of time-series measurements of sediment temperature for identification of gaining vs. losing portions of Juday Creek, Indiana. J. Hydrol. 146, 1-4

Simeonova, P., Simeonov, V., Andreev, G. (2003) Environmetric analysis of the Struma River water quality. Cent Euro J Chem 2:121-126

Singh, K.P., Malik, A., Mohan, D., Sinha, S. (2004) Multivariate statistical techniques for the evaluation of spatial and temporal variations in water quality of Gomti River (India): a case study. Water Res 38:3980-3992

Smith, J.W.N. (2004) Groundwater-surface water interactions in the hyporheic zone, Environment Agency, Bristol. Science project number SC030155

Sophocleous, M.A., Koelliker, J.K., Govindaraju, R.S., Birdie, T.,

Ramireddygan, S.R., Perkins, S.P. (1999) Integrated numerical modeling for basin-wide water management: The case of the Rattlesnake Creek basin in south-central Kansns. J Hydrol 214: 179-196

Sophocleous, M.A., Koussis, A., Martin, J.L., Perkins, S.P. (1995) Evaluation of simplified stream-aquifer depletion models for water rights administration. Ground Water 33:579-588

Soulsby, C., Malcolm, I.H., Youngson, A.F., Tetzlaff, D., Gibbins, C.N., Hannah, D.M.(2005) Groundwater-surface water interactions in upland Scottish rivers: hydrological, hydrochemical and ecological implications. Scottish J. Geol. 41, 39-49

Stallman, R.W.(1963) Computation of groundwater velocity from temperature data in Methods of Collection and Interpreting Groundwater Data, USGS. Water Supply Paper, 1544-H, 26-46

Stallman, R.W.(1965) Steady one-dimensional fluid flow in a semi-infinite porous medium with sinusoidal surface temperature. J. Geophys. Res. 70 (12), 2821-2827

Stephen, J.R., McCagi, A.E., Smith, Z., Prosser, J.I. and Embley, T.M. (1996) Molecular diversity of soil and marine 16S rRNA gene sequences related to subgroup ammonia-oxidizing bacteria, Appl. Environ. Micribial, Vol. 62, pp. 4147-4157

Sterba, O., Uvira, V., Mathur, P., Rulik, M. (1992) Variations of the hyporheic zone through a riffle in the R. Morava, Czechoslovakia. Regulated Rivers: Res Manage 7:31-43

Stonestrom, D.A., Constantz, J.(2003) Heat as a tool for studying the movement of ground water nears streams. USGS, 1260, 1-96

Stonestrom, D.A., Constantz, J. (2004) Using temperature to study stream-ground water exchanges. USGS; Fact Sheet, 2004-3010, 1-4

Storey, R.G., Howard, K.W.F., Williams, D.D. (2003) Factors controlling riffle scale hyporheic exchange flows and their seasonal exchange in a gaining stream: a three-dimensional groundwater flow model. Water Resour Res 39: 1034

Surridge, B.W.J., Baird, A.J., Heathwaite, A.L. (2005) Evaluating the quality of hydraulic conductivity estimates from piezometer slug tests in peat. Hydrol. Proc. 19 (6), 1227-1244

Taniguchi, M., Fukou, Y. (1993) Continuous measurements of groundwater seepage using an automatic seepage meter. Ground Water 31: 675-679

Taniguchi, M., Turner, J.V., Smith, A.J. (2003) Evaluation of groundwater discharge rates from subsurface temperature in Cockburn Sound, Western Australia. Biogeochem. 66, 111-124

Tarara, J.M., Ham, J.M. (1997) Measuring soil water content in the laboratory and field with dual-probe heat capacity sensors. Agro. J. 89 (4), 535-542

Townsend, C.R., Arbuckle, C.J., Crowl, T.A., Scarscrook, M.R. (1997)The relationship between land use and physicochemistry, food resources and macroinvertebrate communities in tributaries of the Taieri River, New Zealand: A hierarchically scaled approach. Freshwater Biol. 37, 177-191

Triska, F.J., Kennedy, V.C., Avanzino, R.J., Zellweger, G.W., Bencala, K.E. (1989) Retention and transport of nutrients in a third-order stream in northwestern California: Hyporheic processes. Ecol 70:1893-1905

Triska, F.J., Duff, J.H., Avanzino, R.J. (1993)The role of water exchange between a stream channel and its hyporheic zone in nitrogen cycling at the terrestrial-aquatic interface. Hydrobiol. 251, 167-184

Vega, M., Pardo, R., Barrado, E., Deban, L. (1998) Assessment of seasonal and polluting effects on the quality of river water by exploratory data analysis. Water Res 32:3581-3592

Vogt, T., Schneider, P., Hahn-Woermle, L., Cirpka, O.A. (2010) Estimation of seepage rates in a losing stream by means of fiberoptic high resolution vertical temperature profiling. J Hydrol 380: 154-164

Vörösmarty, C.J., Green, P., Salisbury, J., Lammers, R.B. (2000) Global water resources: Vulnerability from climate and population growth. Science 289(5477): 284-288

Vought, L.B.M. (1994) Nutrient retention in riparian ecotones, Ambio, Vol. 23, pp. 342-348

Wakida, F.T., Lerner, D.N.(2005) Non-agricultural sources of groundwater nitrate: a review and case study. Water Res. 39, 3-16

White, D. S. (1993). Perspectives on defining and delineating hyporheic zones. Journal of the North American Benthological Society, 61-69

Wilks, D.S. (1995) Statistical methods in the atmospheric sciences. Academic

Press, 467p

Winter, T.C., Harvey, J.W., Franke, O.L. and Alley, W.M. (1998) Groundwater and surface water, a single resource, USGS Circular 1139

Winto, E.F. (1997) Nitrate in drinking water, Journal of American Water Works Association, Vol. 63, pp. 95-104

Woessner, W.W., Sullivan, K.E. (1984) Results of seepage meter and mini-piezometer study, Lake Mead, Nevada. Ground Water 22(5): 561-568

Yun, S.Y., Jo, Y.J., Lee, J.Y. (2009) Comparison of groundwater recharges estimated by water level fluctuation and hydrograph separation in Haean basin of Yanggu. J Geol Soc Korea 45(4): 391-404 (in Korean)

Zlotnik, V., Huang, H. (1999) Effect of shallow penetration and streambed sediments on aquifer response to stream stage fluctuations (analytical model). Ground Water 37: 599-605

국문 초록

열전달을 통한 지표수 - 지하수 혼합구역의 깊이 추산 및 특성에 관한 연구

김희정

서울대학교 대학원 지구환경과학부

지표수-지하수 혼합구간은 서로 상이한 물리, 화학, 생물학적 에너지를 지닌 두 수체 사이에 존재하면서 이들 사이의 에너지 구배에 의해 활발한 혼합이 일어나는 곳이다. 지표수-지하수 혼합구간은 공간적 특이성에 기반을 두어 오염물의 이동 및 자연저감이 일어난다. 이러한 지표수-지하수 혼합구간에 대한 연구는 다양한 영역(물리, 화학, 생물, 수리적)에서 관심이 지대하다. 지표수-지하수 혼합구간은 하천구간에 걸쳐 하상의 매우 비균질한 특성을 반영하므로 혼합구간의 수리지질학적 상호작용의 공간적 규모를 파악하는 것은 지표수 및 지하수 자원의 통합적 관리를 위해 중요하다.

특히 이 연구에서는 하상을 기준으로 하여 속도의 수직 성분이 0 이 되는 지점을 지하수와 지표수의 혼합이 일어나는 구간으로 정의하였다. 그리고 하상의 깊이별 온도 시계열 자료를 이용하여 지표수-지하수 혼합구간의 깊이를 추정하는 방법을 제시하였다.

제시한 방법을 검증하기 위해 다양한 접근방법을 사용하여 지표수-지하수 혼합구간의 깊이를 정량적으로 평가하였다. 다양한 연구를 통한 지표수-지하수 혼합구간의 정량적 평가를 한 결과는 다음과 같다.

1. 제안한 방법을 이용하여 계산된 지표수-지하수 혼합구간 경계의 깊이는 9-15 cm 이다. 추적자시험을 통해 계산된 지표수-지하수 혼합구간 경계의 깊이는 2-30 cm 였는데, 제안한 방법을 이용하면 보다 정밀성을 높일 수 있다
2. 제안한 방법으로 계산된 지표수-지하수 혼합구간 경계구간에서 서식하는 미생물의 군집구조 및 수질의 특성을 살펴보고, 이를 이용한 지표수-지하수 혼합구간 경계 설정을 시도해 보았다.
3. 혼합구간에서 발생하는 수리적 상태 변화는 현장에 서식하는 토착미생물의 군집구조에 영향을 미친다. 특히, 하나의 수 체 (지하수 또는 지표수)가 지배적인

지점에서는 생물학적 다양성이 감소하였다. 하지만, 지하수 또는 지표수가 동시에 영향을 미치는 지점에서는 생물학적 다양성이 가장 높았다.

4. 지표수-지하수 혼합구간에서 채취한 시료의 이화학적 조성은 지표수와 지하수의 중간적인 특성을 나타내었으며, 지하수 보다는 지표수와의 유사성이 높았다. 그러나 논물과는 이질성을 나타냈다.

주요어 : 지하수-지표수 상호작용;

지표수-지하수 혼합구간 경계설정;

수치해석;

수질;

미생물 군집

학 번 : 2010-30942